Università degli Studi di Napoli Federico II
Ph.D. Program in
Information Technology and Electrical Engineering
XXXV Cycle

Thesis for the Degree of Doctor of Philosophy

The Biomechanical Study of Gait for the Design of Custom Orthoses

by
Armando Coccia

Advisor: Prof. Francesco Amato

Scuola Politecnica e delle Scienze di Base
Dipartimento di Ingegneria Elettrica e delle Tecnologie dell'Informazione

Non vi è emozione come intravedere la legge matematica dietro il disordine delle apparenze.

Galileo Galilei

The Biomechanical Study of Gait for the Design of Custom Orthoses

Ph.D. Thesis presented
for the fulfillment of the Degree of Doctor of Philosophy
in Information and Communication Technology for Health
by

Armando Coccia

October 2022

Approved as to style and content by

____

Prof. Francesco Amato, Advisor

____

Università degli Studi di Napoli Federico II
Ph.D. Program in Information and Communication Technology for Health
XXXV cycle - Chairman: Prof. Daniele Riccio

https://icth.dieti.unina.it/index.php/it/

Candidate's declaration

I hereby declare that this thesis submitted to obtain the academic degree of Philosophiæ Doctor (Ph.D.) in Information and Communication Technology for Healthis my own unaided work, that I have not used other than the sources indicated, and that all direct and indirect sources are acknowledged as references.
Parts of this dissertation have been published in international journals and/or conference articles (see list of the author's publications at the end of the thesis).

Napoli, December 13, 2022

____

Armando Coccia

Abstract

Orthoses are medical devices or, more generally, orthopaedic systems, which are applied externally to the human body in order to influence the structural and functional characteristics of the neuromuscular and skeletal system, supporting the patient in performing a function. Ankle-Foot Orthosis (AFO) are applied on the ankle and provide support to the joint particularly during walking. Foot Drop (FD) syndrome is certainly one of the most common gait abnormalities treated with ankle-foot orthoses. This neuromuscular disorder is characterized by the partial or total inability to raise the foot from the ankle (dorsiflexion). During walking, this is reflected in the dragging on the ground of the toes during the swing phase of the limb, and in the irregular forefoot impact that precedes the usual ground impact of the heel. The use of orthotics can improve the impaired walking mechanics.

Nowadays, thanks to the diffusion and availability of advanced systems for design and production, orthopaedic centres are increasingly adopting the practice of producing custom orthoses on the patient's needs. The present work is focused on this research area, and aims to present functional gait analysis methodologies that can provide support and improve current custom orthosis design and manufacturing processes.

Specifically, a platform has been developed which enables the integration of data from a 3D motion capture system into a customized biomechanical model for the study of lower limb kinematics and dynamics. Anthropometric and biomechanical parameters have been identified that are computed and exported from the platform, and allow, first, the more in-depth customisation of the orthosis on the basis of the functional assessment, and also, the validation of the structure of the device through numerical Finite Element Analysis (FEA), before its actual production. This represents an incremental innovation with respect to the state of the art where the customisation process is only based on morphological information of the body district.

Keywords: Gait Analysis, Ankle-Foot Orthosis, Biomechanical Modelling, Gait Kinematics, Foot Drop.

Sintesi in lingua italiana

Le ortesi sono dispositivi medici o, più in generale, apparecchiature ortopediche, che vengono applicate esternamente al corpo umano al fine di modificare le caratteristiche strutturali o funzionali dell'apparato neuro-muscolo-scheletrico, con conseguente supporto al paziente nell'esecuzione di una funzione. Le ortesi caviglia-piede (*Ankle-Foot Orthosis (AFO)*) agiscono sulla caviglia e forniscono supporto all'articolazione in particolare durante la deambulazione. Tra i deficit del cammino più comunemente trattati con ortesi caviglia-piede vi è certamente la sindrome del piede cadente (*Foot Drop (FD)*). Tale disordine neuromuscolare si caratterizza dall'impossibilità, parziale o totale, di flettere dorsalmente il piede. Nella deambulazione ciò si riflette nel trascinamento al suolo della punta del piede durante la fase di oscillazione dell'arto, e nell'irregolare appoggio dell'avampiede che precede l'usuale impatto del tallone al suolo. L'utilizzo dell'ortesi può migliorare la meccanica del cammino alterata.
Oggi, grazie alla diffusione e disponibilità di sistemi avanzati per la progettazione e produzione, le officine ortopediche adottano sempre di più la pratica di realizzare ortesi personalizzate sulle necessità del paziente. Questo lavoro si colloca in questo ambito di ricerca, ed ha l'obietttivo di presentare metodologie di analisi funzionali del cammino che possano fornire supporto e migliorare gli attuali processi di progettazione e produzione di ortesi personalizzate.
In particolare è stata sviluppata una piattaforma che consente l'integrazione di dati provenienti da un sistema di *3D motion capture* in un modello biomeccanico personalizzato per lo studio della cinematica e dinamica dell'arto inferiore. Sono stati individuati dei parametri antropometrici e biomeccanici che, esportati dalla piattaforma, consentono da un lato la più approfondita personalizzazione dell'ortesi in base al deficit funzionale, e dall'altro la validazione della struttura del dispositivo tramite analisi numerica agli elementi finiti (*Finite Element Analysis (FEA)*), precedentemente la sua realizzazione effettiva. Ciò si configura come un'innovazione incrementale rispetto allo stato dell'arte che vede il processo di personalizzazione basato sulla sola informazione morfologica del distretto corporeo.

Parole chiave: Analisi del Cammino, Ortesi Caviglia-Piede, Modellazione Biomeccanica, Cinematica del Cammino, Piede Cadente.

Contents

Acknowledgements

The author's work has been carried out in the framework of the European Union project of the Horizon program 2014-2020 "APTIS — Advanced Personalized Three-dimensional printed SensorIzed orthosiS", funded by the Italian Ministry of Economic Development. Leading companies: ICS Maugeri SPA SB (Pavia, Italy), Officine Ortopediche Tombolini (Taranto, Italy).

List of Acronyms

The following acronyms are used throughout the thesis.

FO	Foot Orthosis
AFO	Ankle-Foot Orthosis
KAFO	Knee-Ankle-Foot Orthosis
KO	Knee Orthosis
HKAFO	Hip-Knee-Ankle-Foot Orthosis
THKAFO	Trunk-Hip-Knee-Ankle-Foot Orthosis
FD	Foot Drop
AM	Additive Manufacturing
FDM	Fused Deposition Modelling
SLS	Selective Laser Sintering
CAD	Computer Aided Design
OTC	Over-The-Counter
EMG	Electromyography

IR	Infrared
ASIS	Anterior Superior Iliac Spine
GUI	Graphical User Interface
UI	User Interface
API	Application Programming Interface
COP	Center of Pressure
FEA	Finite Element Analysis
HS	Heel Strike
RoM	Range of Motion

List of Figures

List of Tables

Chapter 1

Lower Limb Orthoses

Lower limb orthoses are devices used to improve functions in lower body segments by controlling motion, support foot and leg in correct position during gait, correcting the progression of deformities and reducing pain. One of the proposed classifications for lower limb orthoses is based on the body segments affected by the action of the device [28]:

- Shoes - are the conceptual forefathers of the orthosis, their parts can be customized to correctly redistribute weight and reduce excessive pressures in localized areas.

- Foot Orthosis (FO) - it is a sole or a device acting on foot in order to reach a better foot support phase during gait and static trials.

- Ankle-Foot Orthosis (AFO) - this device extends its action to the ankle, in order to stabilize the joint and restore a more normalized lower limb biomechanics.

- Knee-Ankle-Foot Orthosis (KAFO) - it supports the proper alignment of knee, ankle and foot, and it is often prescribed when quadriceps weakness or dysfunction causes an abnormal walking pattern.

- Knee Orthosis (KO) - a knee orthosis only supplies control of the knee joint but not of the rest of lower limb. KOs can be designed to provide joint support in the sagittal or frontal plane, or to control the axial rotation.

- Hip-Knee-Ankle-Foot Orthosis (HKAFO) - it consists of a KAFO with the addition of a support for hip joint and a pelvic band. This kind of orthotic controls the biomechanics of the entire lower limb.
- Trunk-Hip-Knee-Ankle-Foot Orthosis (THKAFO) - it is a complex system with a spinal orthosis added to a KAFO. A THKAFO is indicated for patients with paraplegia, supporting the static standing and the dynamic ambulation.

The orthotic devices for lower limbs are used in several pathological conditions affecting the normal functionalities of the legs and feet. The prescription of the appropriate device for a patient requires consideration of several factors including diagnosis of disability, Range of Motion (RoM), strength, tone, cognition, dexterity, compliance, sensation, edema, gait pattern, and pain [28].

In the present work the focus is on the common orthopaedic syndrome named Foot Drop (FD). This pathological condition mainly affects the biomechanics of the ankle joints, therefore it is usually treated with AFOs.

1.1 Ankle Foot Orthosis for Foot Drop

Foot Drop (FD), also called drop foot, is a general term indicating the difficulty in performing foot dorsiflexion, causing the front part of the foot to drag along the ground while walking, altering the physiologic biomechanics of the whole body. The abnormal gait pattern is characterised by two major complications: at Heel Strike (HS), the forefoot generally impacts to the ground in an uncontrolled and rapid manner, producing a distinctive slapping noise (foot slap); during foot swing, the inability to lift the front part of the foot causes the toes to drag on the ground with consequent high risk of stumbling and falling (toe drag) [6]. This deficit is caused by partial or complete paralysis of the muscles innervated by the peroneal nerve, which controls active ankle dorsiflexion [48]. The dorsiflexors of the foot and ankle are muscles that help the body to clear the foot during swing phase and control plantar flexion of the foot during HS. The weakness of plantar flexor muscles results in the reduction of push-off power, with consequent increase of energy cost as most of the power during gait is generated during ankle push-off. Dorsal muscles weakness induces an insufficient foot dorsiflexion for lifting the foot adequately in midswing; it results in toe-dragging, lower walking speed, shorter step length, increase in walking metabolism, and high risk of tripping [3]. FD is not properly a disease, rather it is the presentation of lumbar degenerative diseases, with varied aetiology, which can be divided into three broad categories including neurological, muscular or anatomical [46, 5, 9, 48, 35]. In most cases FD is the effect of lesions or disorders affecting directly the peroneal nerve and/or its origins (anterior horn cells, L4 or L5 spinal nerve roots, lumbosacral plexus and sciatic nerve). Nerve conduction examination and Electromyography (EMG), eventually supported by imaging, are effective studies to localise the site of injury, establishing the degree of damage and predicting the degree of recovery. In many other cases, when the diagnosis is less obvious, a peroneal neuropathy remains the likely diagnosis. It can be induced by various causes, including prolonged external compressions, direct traumas, traction injuries, masses and tumours, entrapment, vasculities, diabetes or even leprosy [48].

Regardless of the origin of the motor deficit, patients with FD greatly benefit from the use of a brace to support the foot, aid walking and prevent tripping. Lightweight AFOs are the most adequate solutions [48]. They are applied externally to patient's lower leg and foot in order to support and maintain the foot and ankle in the proper position during movement and to improve the gait pattern. Semi active and Active AFOs contain onboard power source to supply electronic elements such as sensors, actuators and/or control systems. Passive AFOs contain mechanical elements (dampers or springs) to control relative motion between foot and shank, without using electronic components. Passive AFOs are more compact in size and lightweight with respect to active AFOs, which are bulky in size, often uncomfortable to wear and require external power supply. Therefore, passive AFOs are usually preferred by patients for everyday use. Figure 1.1 shows examples of passive, semi-active and active AFOs taken from literature. Another classification of AFOs can be based on relative motion between foot and shank parts of the orthosis: non-articulated (or fixed) AFOs are devices made of a single piece in thermoformable material like polypropylene; articulated AFOs are two-piece (foot part and shank part) devices connected by joints with functional purposes (such as hinges, springs, dampers or flexion stops) [34].

Figure 1.1. Example of AFOs: a. passive AFO; b. semi-active AFO with magnetorheologic fluid brake [24]; c. active AFO with the shank and the foot brace [1]

In the literature review proposed by Kubasad *et al.*, authors underline the lack of a compact, lightweight, untethered, and efficient AFO that could fit for daily life usage. The challenge to deal with in future research is to merge the compactness, ease of use and comfortness of passive AFOs with the effectiveness in rehabilitation provided by the active and semi-active orthoses [34].

1.1.1 The Codivilla Spring AFO

The Codivilla spring was one of the first AFOs developed in history and used to support ambulation in patients with FD. The Codivilla spring is a forerunner of modern AFOs, and some modern versions of the device, with the same structural principles, retain the original name. This orthotic device was firstly conceived at the Rizzoli Orthopaedic Institute in Bologna, Italy. As reported by the historical revision provided by Bardelli *et al.* [8], the orthosis was named after the Professor Alessandro Codivilla, although he never mentioned the spring as we know in his scripts. However, he was a pioneer of the Orthopaedic Italian discipline and developed the Codivilla Rotary spring, which inspired the current model of the orthotics. It was the Professor Francesco Delitala, one of his pupil at the Istituto Rizzoli, to write about an ankle-foot support called "Istituto Rizzoli instrument for sciatic palsy" for the first time in his monography "Gli apparecchi ortopedici" edited in 1921 [18]. Delitala did not hesitate to give rightful credits to his former mentor, prof. Codivilla, whose studies were crucial to the development of lower limb orthoses.

The original version of the Codivilla spring was composed of a steel flat bar covered in leather, which was placed behind the leg, and a sole supporting the foot in the correct position [8]. The structure was able to act as a spring, returning elastically the flexion forces imparted during the terminal stance phase loading of the ankle. Thus, it was conceived to support the foot during the swing phases for patients with dorsiflexion deficit of the foot, caused by neurological or orthopaedic diseases.
Subsequent evolutions in Codivilla spring mainly concerned the materials used, thanks to the introduction in the second half of the last century of thermoplastics materials (in particular polypropylene). The new materials were cheaper and allowed the development of molded orthoses with high level of customization. The plastic spring orthoses, which nowadays are still being produced and used, are usually obtained from a single polypropylene sheet modeled on the morphological and functional needs of patients. The amount of material and its distribution can calibrate the features of the orthosis, in particular providing a certain degree of resistance and rigidity to the structure.

The latest innovations in materials and manufacturing techniques open further new frontiers in customizing the functionalities of passive orthoses. An example is represented by the modern Additive Manufacturing (AM) techniques, which enable the production of very accurate devices, also thanks to the support of digital processing and modelling.

Given the new possibilities in design and production, it would be inappropriate considering the Codivilla spring as a standard universal orthosis. Instead, it should be considered that there are considerable opportunities for customization in order to achieve useful user-specific functionalities. The desirable approach is to tailor a custom AFO with specific mechanical and morphological features, that should compensate the specific mechanical deficiencies of the neuromusculoskeletal function observed in the patient, with the aim to correct or improve static and dynamic function of ankle-foot complex.

Thus the choice of the right orthosis for the right patient, is a key aspect for the professional expertise of orthotists and physiatrists. However, the introduction of computerized gait analysis systems for the biomechanical characterization of gait can revolutionize the process of prescription and

design of orthoses. The kinematic and kinetic analysis of the ankle during gait is useful in defining the deficit the orthosis should limit.
The objective of the project carried out, of which this thesis represents the final summary, was to develop a semi-automated system, based on the biomechanical analysis of gait, to support the design of 3D printed passive orthosis on the model of the Codivilla spring.

1.2 Values and Future Directions of Custom Orthotics

In 2012, in a roundtable about Foot Orthoses [31], the Professor Kevin A. Kirby and other colleagues analysed the advantages and disadvantages of custom orthoses with respect to Over-The-Counter (OTC) devices. The podiatry Simon K. Spooner underlined that OTC orthoses are relatively cheaper and can be dispensed instantly whereas there is usually a time delay between prescription and dispensation of custom devices. These disadvantages can be partially overcome with modern materials and manufacturing technologies. However, as suggested by Kirby, custom orthoses, typically made of polypropylene or other plastics, usually have greater durability (5-15 years) versus the average OTC orthosis (3-9 months). Thermoplastic custom orthoses also experience less alteration in shape over time, thus maintaining relatively constant the prescribed shape and stiffness when compared with OTC orthoses. Moreover, being based on a 3D model, custom orthoses are able to effectively reproduce all of the geometric parameters that constitute the interindividual variation within the plantar surface topography of the human foot, effectively reducing the magnitudes of pressures acting on the plantar foot [37].

Research on effectiveness of orthotics clearly shows that foot orthoses effectively change the kinetics and kinematics of gait. In addition, inverse dynamics studies underline that these devices alter the magnitudes and temporal loading patterns on the internal structural components of the foot and lower extremity, which supports the idea that foot orthoses produce much of their therapeutic effects by altering the forces and moments on internal structures of the foot and lower extremity [31]. This suggests that the design of custom orthoses cannot ignore the study of gait biomechanics in its altered functions, in order to plan the right prescription and achieve corrections through the optimal design of the orthopaedic device.

With regard to the future directions for foot orthosis technologies, Kirby indicated 3D printing or AM technique as the most interesting new technology being developed to produce viable FO products. He also showed confidence in miniature electronic components, which will allow foot orthoses to monitor the condition and the effects of the device, giving instant wireless feedback to the clinician and/or patient. Ten years later, we can affirm that the two technologies can indeed have an impact on orthotic manufacturing.

The former is already gaining success: among the various application fields of AM in medicine, orthopaedics appears to be the sector that benefits the most from this technology. A recent literature review article shows that 53% of the papers published in the scientific literature in recent years refer to the orthopaedic field [50]. It is possible to associate AM with a series of advantages over traditional orthotic manufacturing techniques, such as flexibility in the design phase even with devices of high geometric/functional complexity, differentiation of internal topology and thicknesses, and the possibility of obtaining multi-material and multi-part objects. All this translates into the possibility of guaranteeing the patient a much higher degree of compliance, shorter delivery times while ensuring the provider company reduced waste and lower costs for complex devices (complexity for free).
AM technologies mainly used for prototypes design and fabrication in the medical field (e.g., orthotics) are based on extrusion of thermoplastic polymer filaments Fused Deposition Modelling (FDM) or Selective Laser Sintering (SLS) of thermoplastic powders. FDM technology generates 3D prototypes by heating and extruding a filament of plastic material that is deposed on the printing platform in X and Y directions following a controlled scheme, while SLS technology enables 3D generation of an object by selectively sintering (i.e., forming a solid mass of material by heating it avoiding liquefaction) successive layers of powder, placed on a powder bed. SLS machines are capable of producing higher resolution objects and are more accurate than their FDM counterparts, since the resolution is mainly determined by the size of the laser's optical dot, but at the same time they are more costly and there is a need for more attention by operators working with powders.

Another promising tool identified as potentially relevant in the process of design of custom orthoses is the finite element modelling and analysis. With such modelling the orthoses superior surface geometry, the load/deformation characteristics and the frictional characteristics can be manipulated. Within the safety of the virtual environment the analysis can assess the influence of various orthoses designs and the effect that these designs have on the "virtual" tissue stress and strain. Through this approach a better knowledge on the most effective design variables in providing the best effects on the target tissue can be achieved [31].

The aim of the work is to explore the biomechanics of gait of FD patients, in order to develop a semi-automated system supporting the functional design of custom AFOs. Chapter 2 presents the study of gait biomechanics, with an overview of principles and systems for gait analysis and a focus on biomechanical modelling and simulation of gait. In Chapter 3 the novel process of design and production of custom AFO is shown, underlining the innovative methods developed in a user-interface platform. Chapter 4 summarizes the achievements of this product, analyzing the innovative elements but also the limitations found in this scientific research and technology transfer work.

Chapter 2

Biomechanical Modelling of Human Gait

This chapter introduces the basic concepts of the biomechanical modelling, investigating its use for the study of human gait, aimed at supporting the custom fabrication of orthoses for lower limbs. An introduction on the history, general principles and system for gait analysis opens the chapter. Then a discussion about the biomechanical modelling of gait is provided, with specific focuses on the gait models and on the methods (hardware, software platform, *etc*) exploited to achieve the purposes of this work.

2.1 Gait Analysis

Gait Analysis represents nowadays a tool of great interest in the clinical practice for the quantitative study of locomotion. Clinical gait analysis refers to the assessment of gait disorder or gait abnormalities, using clinical approach and techniques. Most of the physical problems are caused by an abnormal gait, i.e. back pain, joint pain at the lower limbs, muscle strain, etc.[51]. Since gait and, in general, movement are the results of the interaction of three main physiological systems: nervous, musculoskeletal and sensory, gait analysis can provide information not only on the patient's level of functional limitation resulting from pathology, but also useful information regarding the pathologies of the aforementioned systems allowing the planning of possible medical, surgical or rehabilitation therapies to be adopted as appropriate.

In the past, gait was recorded by camera systems providing qualitative measures of subject's locomotion, which was interpreted very subjectively by the clinician. Very often this type of detection, which is qualitative, proved to be incomplete and susceptible to errors of interpretation; in fact, video analysis does not provide information related to the exchange of forces to the ground (dynamics) and muscle activity (EMG) during the analyzed movement. These limitations can be overcome through the use of modern gait analysis, which allows two-dimensional qualitative assessments to be combined with three-dimensional quantitative assessments related to both kinematics and dynamics of movement and muscle activation.

Movement analysis represents a computerized, multifactorial, three dimensional gait assessment method that aims to collect quantitative information related to the mechanics of the musculoskeletal system during the execution of a motor act, with the aim of objectively characterizing it. The clinical gait analysis is aimed to study the loads distribution over body structures in quiet standing and symmetry of motion pattern, cadence, and forces sharing during walking or dynamic tasks [55].

In particular, systems for gait analysis process the following information:

- the absolute motion of the center of mass of the whole body or a portion of it;
- the absolute motion of bones or body segments;
- the relative motion between adjacent body segments (joint kinematics);
- the forces and torques exchanged with the environment;
- the resultant loads transmitted through sections of body segments or carried through joints (inter-segmental loads);
- the forces and torques transmitted by internal structures (muscles, tendons, ligaments, bones);
- changes in energy of body segments, muscle work and power.

As a great advantage, gait analysis is a non-invasive technique, and therefore usable even in minimally cooperative patients or those with peculiar gait. It is also easily repeatable making it possible to easily and effectively monitor the patient over time.

2.1.1 Basis of Human Gait Analysis

Gait is characterized by a cyclic pattern of motor activity of the lower limbs and trunk to transfer body weight onto the supporting limb and to advance the contralateral limb forward. Since each motor sequence is characterized by the interaction between the two lower limbs and the entire body mass, the identification of the events that occur, during such sequences, requires the observation and analysis of gait from different points of view. To this end, it is essential to describe and divide the gait cycle, which is the functional reference unit in gait analysis, into a series of basic phases.

Gait Cycle

The movement of the human body can be described along three main planes: sagittal, frontal and transverse Figure 2.1:

- the sagittal plane divides the human body into two symmetrical parts: right and left;
- the frontal plane divides the body into two asymmetrical parts: anterior and posterior;
- the transverse plane divides the body into two asymmetrical parts: upper and lower.

The movements of the human body occur along an axis perpendicular to each of the planes and are:

- Flexion and extension movements along an axis perpendicular to the sagittal plane;
- Movements of abduction and adduction around a sagittal axis perpendicular to the frontal plane;

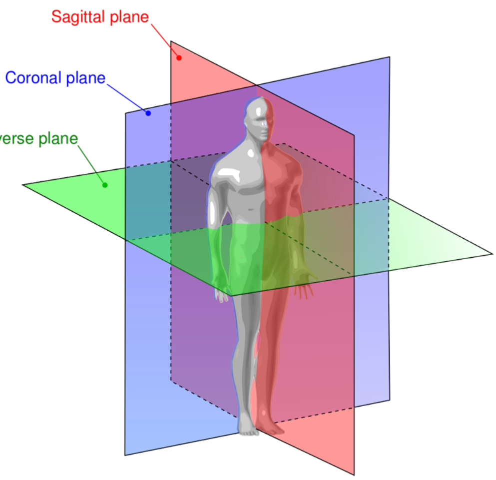

Figure 2.1. Anatomical planes of human body.

- Intra- and extra-rotational movements along a vertical axis perpendicular to the transverse plane.

Through the loss of balance and its subsequent recovery, a cyclic sequence of movement can be enacted that involves phases of support and swinging of the lower limb. As the body moves forward, one limb acts as a moving support on the ground while the other moves forward to the next stance; subsequently, the limbs switch their roles and both feet are in contact with the ground during the transfer of body weight from one limb to the other. This sequence of events is repeated by each limb at reciprocal times, and a single sequence of these functions, per limb, is called gait cycle.

The gait cycle represents the functional unit in gait analysis: it is the interval between two successive analogous gait events of the same foot. By convention, the gait cycle begins with a HS of a foot on the ground and ends when the same heel hits again on the ground, starting the foot support. The schematic representation of the phases of gait cycle is reported in Figure 2.2.

The gait cycle can be distinguished into two complementary periods:

- Stance phase: identifies the entire period during which the foot is in

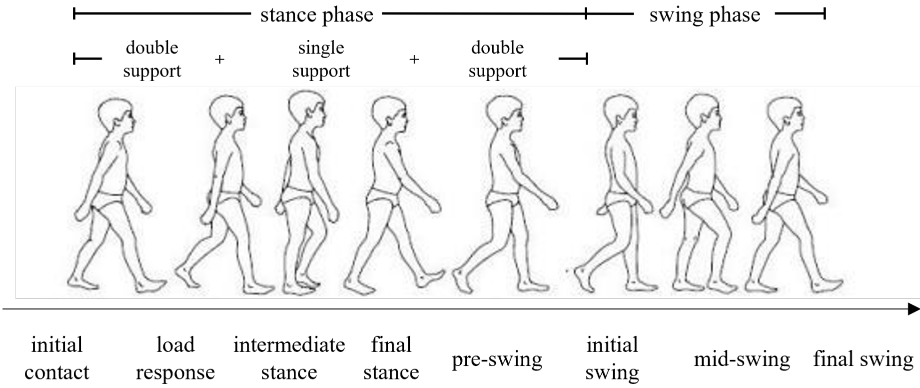

Figure 2.2. Schematic representation of gait cycle phases.

contact with the ground;

- Swing phase: refers to the time during which the foot is elevated from the ground for the progression of the limb.

The duration of the two phases varies from subject to subject: in a normal gait, the stance phase comprises about 60 percent of the gait cycle, while the swing phase accounts for about 40 percent. The stance phase begins with the initial contact of heel with the ground and ends with the toe-off, namely, the separation from the ground of the same foot. Simultaneously, the swing phase of the contralateral limb occurs, which is the interval within which the limb is elevated from the ground. It begins with toe-off and ends with initial contact.
The stance phase is divided into three separate sub-phases:

- initial double support: both feet are in contact with the ground;
- single support: during which a foot is in contact with the ground and the contralateral foot is swinging;
- terminal double support: in which both feet are again in contact with the ground, following the end of the swing phase of the contralateral foot.

Two basic concepts should also be distinguished (Figure 2.3):

- Stride: it is the equivalent of the gait cycle. It is defined as the interval between two successive initial contacts of the same foot and represents the time reference in which all other biomechanical events and muscle activity are described;

- Step: it is the interval between the HS of a foot and the strike of the same part of the contralateral foot.

The basic spatio-temporal parameters characterising the gait cycle are the following:

- Stride length: the sum of foot length and the distance covered during the swing phase;

- Step width: the distance, in the frontal plane, between the heel and the line of progression;

- Cadence: the number of steps in the unit of time (second or minute);

- Mean walking speed.

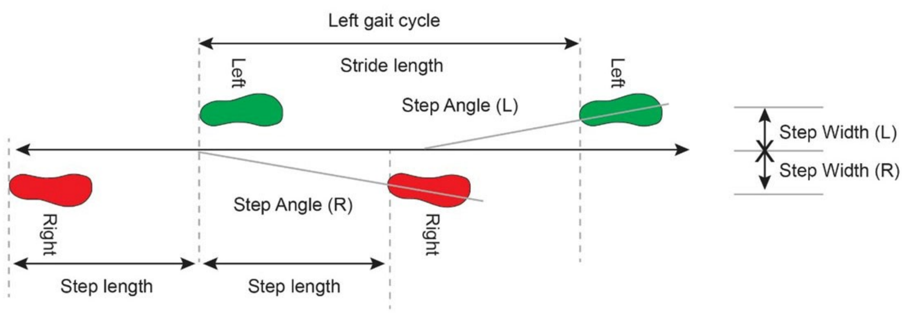

Figure 2.3. Distinction between step and stride.

Walking Phases

The gait cycle is divided into eight functional phases. The combination of the phases allows the limb to perform three basic tasks:

- Load acceptance, that characterises the beginning of the stance period and uses the first two phases of the stride (initial contact and load response);
- Single stance, includes the next two phases (intermediate stance and terminal stance);
- Advancement of the limb, begins in the final phase of stance (pre-swing) and continues through the three phases of swing (initial swing, mid-swing and terminal swing).

The single phases are here deeper detailed (Figure 2.2).

1. **Initial Contact**
   Range: 0-2 % of the gait cycle. This phase includes the initial contact of heel with the ground. During the initial contact, the hip is flexed, the knee is extended, the foot is dorsiflexed, and the tibia is positioned at 90° (neutral position). In terms of muscle activity, both the quadriceps and the pretibial and ischiocrural muscles (i.e., semimembranosus, semitendinosus, and long head of the biceps femoris) are active in this phase.

2. **Load Response**
   Range: 2%-10% of the gait cycle. This phase is the beginning of the double support, starting with initial ground contact and continuing until the other foot is lifted for the swing. During the load response phase, body weight is transferred to the advancing limb. The heel is used as a fulcrum, while the knee is flexed to absorb the contact shock. The flexion of the tibia limits the rolling of the heel by forefoot contact with the ground. The contralateral limb is in the pre-swing phase. The end of this phase is determined by the lifting of the contralateral limb from the ground. During this interval, the gluteus and quadriceps muscles are active.

3. **Mid-Stance**
   Range: 10-30% of the gait cycle. This phase begins at contralateral toe-off and continues until the weight of the body is aligned on the forefoot; with simultaneous progression on the supporting foot. In the first half of the single support phase, the limb advances beyond

the foot, resulting in dorsiflexion of the ankle while the knee and hip extend. The contralateral limb is approaching the swing phase. In this phase the soleus and gastrocnemius are the only active plantarflexor muscles.

4. **Terminal Stance (Heel Off)**
   Range: 30-50% of the gait cycle. In this phase the body passes over the supporting foot. The terminal stance begins when the heel is lifted from ground (heel off) and continues until the contralateral limb touches the ground. During this phase, body weight is transferred beyond the forefoot, the heel lifts and the limb advances. The knee continues to extend and then flexes slightly. Increased hip tension causes the limb to move forward, transferring the weight to the forefoot. The contralateral limb is in the terminal swing phase.

5. **Pre-Swing (Toe-Off)**
   Range: 50-60% of the gait cycle. This phase, also called weight transfer or weight release, is the terminal phase of the double support period of the gait cycle. This phase ranges from the initial contact of the contralateral limb to the ipsilateral toe-off. The limb reacts with an increase in plantar flexion of the foot, an increase in knee flexion, and a decrease in hip extension. The opposite limb is in the load response phase. In terms of muscle activity, the adductor longus and rectus femoris act. There is weight transfer from the limb of interest to the contralateral limb.

6. **Initial Swing**
   Range: 60-73% of the gait cycle. This phase begins with the toe-off and ends with the foot swinging over the contralateral limb. The foot is lifted and the limb advances by hip flexion and knee flexion. The ankle is in partial dorsi-flexion. The opposite limb is in the initial phase of mid-stance.

7. **Mid-Swing**
   Range: 73-87% of the gait cycle. This phase begins when the swinging limb passes over the opposite supporting limb, and ends when the swinging limb advances and the tibia is vertical. The advancing of the limb let the weight of the body move forward for hip flexion.

The knee may extend as a response to gravity while the ankle reduces the dorsiflexion to neutral angle. The contralateral limb is in the terminal phase of the mid-stance. The hip flexors and the dorsal tibial flexors muscles are active during this phase.

8. **Late Swing**
   Range: 87-100% of the gait cycle. This is the final phase of the swing, that ends when the foot hits the ground (HS). The knee is in extension, while the hip maintains its initial flexion and the ankle returns to neutral angle. The other limb is in the terminal stance phase. The pretibial, ischiocrural (i.e., semimembranosus, semitendinosus and long head of the biceps femoris) and quadriceps muscles are active.

2.1.2 Systems for Gait Analysis

There are two macro-categories in which the gait analysis can be divided: qualitative (visual analysis and video-recorded analysis) and quantitative (instrumented analysis). In visual analysis, movement is assessed by direct observation by a clinician: this technique requires knowledge of the correct dynamics of the movement being analyzed, perfect anatomical and physiological knowledge to register any changes from normality [45, 44, 63, 36]. The advantage is that it is a simple and inexpensive technique, requiring no special technological nor expensive equipment. However, this analysis is biased and conditioned by the experience of the clinician who performs the observation [39]. The assessment is global and limited to macro-movements, since the human eye perceives only some movements, omitting the particulars. The impossibility of reviewing the movement and comparing it with other movements or different subjects makes this technique hardly objective and verifiable, with consequent excessive inter- and intra-subject variability.

In video-recorded analysis, motion is recorded with video tools and it is later analyzed. This technique allows assessment of movement in the three planes (sagittal-frontal-transverse) and the possibility of reviewing the movement for further analysis. The advantage is the possibility of a retrospective study: data can be analyzed and compared with other data taken at different times, to evaluate, for example, the achievements carried out in a rehabilitation treatment [39]. However, this technique is still a qualitative assessment, especially if it is done with a single video shot from a single angle that limits the view of the gesture. The assessment, therefore, remains global and generic, being limited to the macro-movements.

In contrast to this background, in recent years the progress and advances in new technologies in the field of electronics, optoelectronics and computing, have given fresh impetus to the development of devices and techniques for the objective analysis of gait. The amount of gait analysis instrumentation that has been developed is extensive, allowing the evaluation of different gait parameters [2]. This current evolution results in more efficient measurement, providing clinicians with more informative and reliable information on patients' gait. This reduces the inaccuracy caused by subjective techniques [41].

The instrumented gait analysis provides quantitative information on body kinematics (accelerations, velocities, and displacements) and on spatio-temporal evaluation of walking. Some integrated gait analysis systems also combine these information with studies of kinetic (i.e., forces and moments that cause or restrict movements), muscle activity (EMG, i.e., electrical signals of muscle activation measured with electrodes), and other information such as balance and plantar pressures [2, 39].

The instrumented analysis can be performed by means of different technological devices, which can be classified according to two different approaches: those based on non-wearable sensors or on wearable sensors [21, 10, 41]. Non-wearable sensors are located in dedicated laboratories, and capture data on the gait while the subject walks on a clearly marked walkway. In contrast, systems based on wearable sensors allow to capture data outside the laboratory and analyse human gait also during everyday activities. There are also hybrid systems based on a combination of both sensors.

A large part of instrumented gait analysis systems are based on optical principles. A set of cameras captures the field where the subject moves, the movement of the body's segments are recognized thanks to the use of passive or active markers positioned on specific landmarks of body [26, 32]. Passive markers react to external sources (i.e. Infrared (IR) cameras), while active markers are the source of signal themselves. There are also systems which recognize movements without the use of markers.

Marker-less systems automatically recognize the different body segments in the acquired images, and then calculate their position and orientation in three-dimensional space. Other systems recognize the entire figure of the subject acquired by the cameras, and calculate the volume occupied by the subject in space at each instant of time. Several technologies can be applied in marker-less system, such as camera triangulation (stereoscopic vision), laser range scanner [43], and Time-of-Flight methods [29], structured light [25, 16], and IR thermography [57].

Non-optical systems include systems based on floor sensors and systems based on wearable devices. Floor sensors include force platforms or instrumented walkways where spatio-temporal and kinetic gait data are extracted by the analysis of pressure or force signals, collected when the subject walks on them.

Gait analysis using wearable sensors is now widely used in the clinical field, with the advantage that it is often easier to perform without the need for a fully equipped laboratory. In these applications motion sensors are worn or attached to various parts of the patient's body, such as the foot, waist, trunk or arms, in order to measure various characteristics of the human gait. The most used wearable sensors for gait analysis are accelerometers, gyroscopes, and magnetoresistive sensors, which can be also embedded within a single inertial measurement unit. The miniaturization of inertial sensors allows to simply attach them on different body parts, to directly collect kinematic information about movements, such as linear and angular velocities, accelerations and orientations in the space. The pressure and force sensors can also be used as wearable device to collect useful information about gait. These sensors are usually integrated into instrumented shoes or insoles [7, 47, 22], detecting the foot contacts with the ground and assessing the distribution of plantar pressures. EMG allows the study of muscles activation and has relevance in the study of gait. The EMG signal can be non-invasively measured on the subject with surface electrodes, therefore wearable devices have been developed to add this kind of assessment in gait analysis.

Other wearable solution in the field of gait analysis are represented by flexible goniometer, electromagnetic tracking system, sensing fabric, and ultrasonic sensors. Based on these technologies, a single device or a combined sensors system may be used for various gait analysis applications.

The number and categories of wearable sensors for gait analysis will certainly increase in the future, thanks to evolution of micro-electronics and motion-sensing technology [52].

Many companies have developed integrated systems for gait analysis exploiting one or more of the above mentioned technologies. In the following section it is described the gait analysis laboratory SMART-DX by BTS Bioengineering (Garbagnate Milanese, Milan, Italy). The focus on this opto-electronic system is provided since it was used to collect data regarding patient's gait, that were then exploited to support the custom design of the orthotic devices.

The Opto-Electronic System SMART-DX

SMART-DX is an opto-electronic motion capture system for gait analysis developed by BTS Bioengineering[1]. It is based on the SMART technology, that combines the use of a set of digital cameras equipped with IR illuminators and passive markers which are identified with high accuracy in the three-dimensional space. Attaching the markers on specific reference points of the body, specified on the basis of the selected protocol, the software is able to reconstruct the movement of the person and analyse the kinematics and kinetics of gait. The combination of these elements ensures a very accurate and relatively non-invasive analysis. The SMART System, as all optoelectronic systems, needs to be calibrated before the use in order to capture accurate information. This procedure allows the system to correctly combine the two-dimensional data captured by each camera, in order to reconstruct the three-dimensional sequence of points, referred to a single point in space, identified as the origin of the laboratory reference system. In Figure 2.4 the organization of a gait analysis laboratory using SMART-DX is proposed: the IR cameras surround the laboratory to have the stereoscopic vision of the walkway where the gait trials are performed; other normal video-cameras can be used to visually record the test execution; all the electronic components are connected to a workstation where specific software controls and analyses the collected data.

The system can also integrate signals from EMG probes and force plat-

[1] https://www.btsbioengineering.com/products/smart-dx-motion-capture/

Figure 2.4. Schematic representation of SMART-DX system for motion analysis.

forms in order to provide more specific analysis. In the scenario of the work presented these tools were not used, as the interest was limited to the collection of the 3D trajectories of the markers, in order to perform the digital modelling of gait. Following, the hardware and software tools exploited in this study are further detailed.

Hardware

The hardware parts making up the system are: IR cameras, passive markers and video cameras.

The IR cameras (Figure 2.5) allow the detection of the 3D position of the markers during the test. The system is equipped with eight IR cameras, positioned within the laboratory in order to cover the entire acquisition volume and ensure visibility of each marker. The cameras generate IR illumination and then collect the reflected signal returned by the passive markers positioned on the body of the subject. The signal is transduced and sent to the workstation for digital processing. IR cameras record the IR signals above a certain intensity and a two-dimensional image of the marker. It is sufficient, therefore, that at least two cameras have the marker in their field of view to determine its 3D coordinates (x, y, z). The IR cameras of the system used (SMART DX-700) have the following technical characteristics: resolution of 1.5 Mpixel, acquisition frequency at maximum resolution 250 fps, maximum acquisition frequency 1000 fps, accuracy lower than 0.1 mm on a 4x3x3 m acquisition volume.

Figure 2.5. IR cameras of the SMART-DX system by BTS Bioengineering.

Passive markers are small spheres with a diameter ranging from 3 to 20 mm covered with a film of reflective material (aluminum powder) and supported by plastic supports (Figure 2.6a). Their spherical geometry allows the complete and correct visualization, as they produce an isotropic reflection of the IR rays emitted by camera illuminators. These markers are placed on the bare surface of the subject's body, by means of double-sided tape or elastic belts (Figure 2.6b), at points that coincide with anatomical landmarks detectable by palpation (Figure 2.6c). The detection of passive markers requires a pre-processing stage by a human expert, in order to verify the correct identification and to classify the marker relating to its body position.

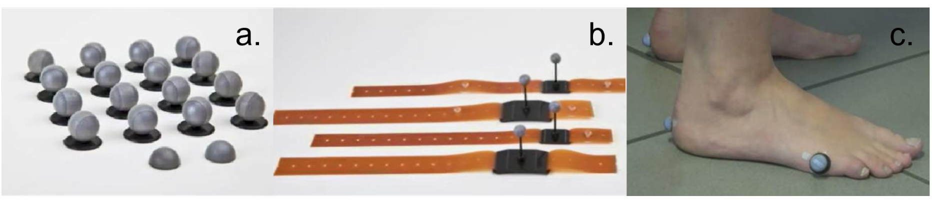

Figure 2.6. a. Reflective passive markers; b. elastic belt to attach markers on body; c. example of marker positioning on the foot.

The system is also equipped with a video recording system consisting of two video cameras (Figure 2.7) synchronized to the optoelectronic system. The cameras record movements during the test in the frontal and sagittal directions, providing qualitative information to support the clinical investigation and the interpretation of data.

Figure 2.7. Video cameras used to record the walking trial, in order to support the clinical investigation.

Software

The software used by Smart System is the SMART-SUITE package. This package consists of three tools:

- SMART Capture;
- SMART Tracker;
- SMART Analyzer.

The SMART Capture component is a tool used to perform system calibration and acquire kinematic data. It enables complete control of the capture system, real-time display of acquired data, identification of marker position in 2D images, and control of camera sensitivity via software. The rendering of the markers' positions identified in the 3D volume of acquisition is performed by combining the two-dimensional data acquired from the cameras during the trial, and those obtained during calibration.

The SMART Tracker component is an interactive graphical environment that allows the identification of markers in order to obtain a three-dimensional image of the movement and path of each marker with the creation of the "stick figure" (Figure 2.8). The stick figure approximates the skeleton of the test subject and it is realized by assigning a label to each marker (labeling), on the basis of its position on subject's body. The algorithm connects contiguous markers to reproduce the stick figure. The tracking operation is the first stage of data processing: it represents the logical linking of two successive frames in order to identify the time course of each marker. This is a very complex operation that requires high accuracy in order to avoid errors that would later compromise data processing. At this point of processing, the markers trajectories over time can be exported and used for the biomechanical modelling. To be torough the last software tool is also described, although it was not used in the workflow presented in this work.

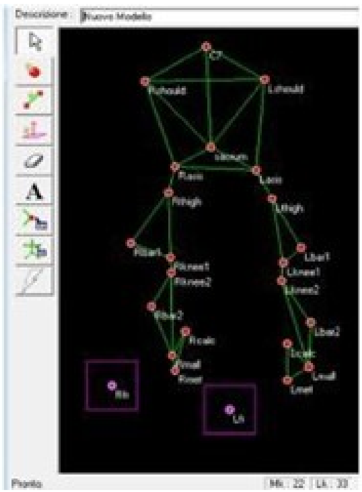

Figure 2.8. The SMART Tracker tool is needed to assign the correct label to the markers.

The SMART Analyzer tool is an interactive graphical environment designed to process data acquired from BTS SMART system. Starting from the spatio-temporal data acquired by the opto-electronic components, the SMART Analyzer uses biomechanical resources to calculate a set of kinematic and kinetic parameter regarding the dynamic trial under analysis. Moreover, this tool enables for the creation of new analysis protocols; import and export of raw and processed data acquired with other systems or software ; visualization of the displacements of each marker along the three dimensions of the laboratory reference system and creation of custom clinical reports, in which all the processed data are summarised with graphs and tables.

Davis Heel Protocol

A protocol is the scheme that controls the acquisition and processing of the kinematic gait data using a given marker-set and mathematical conventions. It also ensures that the acquisition method is standardized and the measurement is repeatable. In general, a gait analysis protocol for optical systems includes the placement of markers according to a predefined pattern, the set of anthropometric measurements to be taken on the subject, as well as the algorithm that allows the calculation of various spatial, temporal, kinematic and kinetic parameters.

The Davis protocol [17] was developed by Davis Roy B. III at Newington Children's Hospital in New York and is the most widely used gait analysis protocol. It represents a gold standard, particularly in applications related to infant cerebral palsy.

The first phase of the protocol involves physical assessment of the subject and measurement of some anthropometric variables including body weight, height, leg length, femur length, knee and ankle widths, distance between right and left pelvic Anterior Superior Iliac Spine (ASIS) and vertical distance in the sagittal plane between the ASIS and the greater trochanter.

The next phase regards the application of the passive reflective markers on subject's body. The marker-set consists of 22 markers summarized in Table 2.1. Markers are positioned in specific landmarks indicated in Figure 2.9. Part of the markers are applied directly on the skin using tape, while others are spaced from the body using little wands, ranging in length from 5 to 10 cm. Specifically, one wand is placed on the central part of each femur (Femur wand) and one on the central part of each leg (Fibula wand).

As shown in the Table 2.1 and Figure 2.9, markers placement can be summarized as follows:

- Trunk: two markers placed on the right and left acromioclavicular joints and one at the same height at the level of the spinous process;

- Pelvis: two markers placed at the level of the right and left ASIS,

Table 2.1. Marker Set in Davis Protocol.

Body Segment	Marker Acronym	Marker Name
Trunk	RS	Right acromioclavicular joint
	LS	Left acromioclavicular joint
	N	Spinous process C7
Pelvis	R	Right ASIS
	B	Left ASIS
	H	Sacrum
Thigh	RH (LH)	Right Greater trochanter (Left)
	RF (LF)	Right femur wand (Left)
	RK (LK)	Lateral epicondyle of the right femur (Left)
Shank	RP (LP)	Head of the right fibula (Left)
	RB (LB)	Right fibula wand (Left)
	RA (LA)	Right lateral malleolus (Left)
Foot	RT (LT)	Fifth metatarsal head of right foot (Left)
	RQ (LQ)	Right heel (Left)

and one at the level of the sacrum so that the three points are in the same plane containing the ASIS and posterior superior iliac spines;

- Thigh: a marker placed on the greater trochanter, one on the lateral epicondyle of the femur and one on a wand placed at 1/3 of the length of the thigh so that the plane containing the three markers is parallel to the frontal plane;
- Shank: a marker placed on the lateral malleolus, one on the head of the fibula and another on a wand placed at 1/3 of the length of the leg;
- Foot: a marker on the heel and one on the lateral aspect of the foot at the fifth metatarsal head. The heel-toe marker vector is parallel to the sole of the foot.

The described marker placement scheme ensures visibility, because all markers are placed on the external sides of the body segments.
The protocol then requires a static acquisition of the subject, which consists of acquiring, for a few seconds, the subject in a standing position. During this acquisition the motion camera system collects marker data in

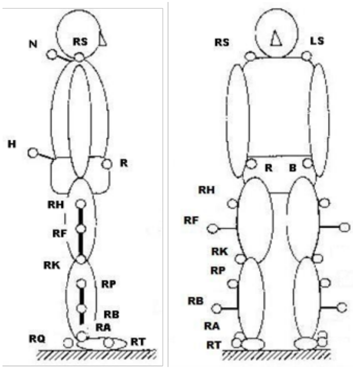

Figure 2.9. Placement of the markers following the Davis heel protocol (Figure from [17]).

order to establish the location(s) of each joint center, with reference to the associated segment-fixed coordinate system.

After the static acquisition, the subject is asked to walk, at comfortable speed on the walkway placed in the field of view of IR cameras. The session includes at least three walking trials. In the consequent processing phase, the two-dimensional coordinates of the centroid of each marker is identified in each frame of camera data. Three dimensional marker coordinates are then computed stereometrically from the two dimensional cameras data. Basing on markers coordinates, an embedded reference system for each body segment is determined. The location of joints centers are calculated relative to the associated embedded coordinate system origin. This is done for hip, knee and ankle, which represent the joints around which the segments rotate. Starting from this, it is possible to calculate the joint rotation angles (trunk and pelvic obliquity tilt and rotation, hip ad/abduction flexion/extension and rotation, knee flexion/extension, ankle plantar/dorsiflexion, and foot rotation). The angular initial offset values are computed from the standing data collected prior to the motion test.

For the kinetic analysis, in the first phase the segments masses and moments of inertia are obtained from anthropometric measurements. Then the net 3D joint moments are computed via Newtonian mechanics through the application of Newton's Second Law and Euler's equations of motion, exploiting the kinematic data previously described.

As mentioned before, the kinematic and kinetic assessment has been treated just for sake of completeness. However the proposed workflow exploits just data relating the 3D coordinates of markers, that can be exported from the SMART Tracker software and used for further custom analysis.

2.2 Biomechanical Modelling of Gait

One of the principal aims of this work is to provide a novel custom and user-friendly tool able to perform the biomechanical modelling of subject's gait in order to deeply analyse some fundamental aspects of walking, which can represent useful information to support and improve the mechanical design of an orthosis. The platform will be described in Chapter 3, however it is useful to provide a general description of the biomechanical modelling, with particular reference to the study of human gait. This section does not provide a broad didactic presentation of the topic, while the basic concepts required for the intended purpose are described. To support and facilitate the dissertation, the software platform OpenSim (Copyright (c) 2005-2012 Stanford University and the Authors), where the biomechanical models and simulations were initially developed, is also presented. The user platform was then developed in MATLAB exploiting OpenSim API.

2.2.1 OpenSim Platform

Thanks to the rapid development in software engineering of the recent years, it has been possible to create an open-source simulation environment, called OpenSim, which allows researchers to share and integrate multiple different dynamic simulations. The following section will describe the software, its capabilities, the types of data it accepts as input, and the various tools, which will then exploited for advanced gait analysis.

In the early 1990s, Delp and Loan, at the National Center for Simulation in Rehabilitation Research (NCSRR Stanford University), introduced a musculoskeletal modelling software, called SIMM (Software for Interactive Muskuloskeletal Modelling), which allows users to create, modify, and evaluate models of various structures of the musculoskeletal system. In these years many reasearchers, using SIMM, have developed lower and upper limb models with which it has been possible to simulate many human movements, to examine the biomechanical consequences of surgical interventions such as osteotomies and joint replacement grafting, to estimate the length of the muscle-tendon complex, the moment arms of individual muscles with respect to a joint, to calculate the velocity and accelerations induced and the forces present on the joints during a movement, and many other applications. All these studies have underlined the utility of biomechanical modelling and simulation. However SIMM platform do not provide tools to compute and analyse the muscle excitation and the results of dynamic simulations.

In 2007 Delp with other co-workers presented OpenSim, as a development of SIMM platform, that complements and augments the functionalities of SIMM by providing advanced simulation and control capabilities [20]. OpenSim is an open-source platform (https://opensim.stanford.edu/) hosted on Simtk.org by a group of researchers and is used for modelling, simulation and analysis of the neuromusculoskeletal system. It includes a Java-based Graphical User Interface (GUI) to run the key functionalities of the main application, that invokes low-level computational tools. The GUI allows users to extend functionality by developing their own biomechanical models, controllers and analysis. The open source nature has been chosen to encourage users to accelerate the development and share their simulation, allowing other rersearchers to reproduce results produced by other laboratories, make improvements and adapt code to meet their needs.

An OpenSim model constitutes the basis of simulation, and represents a system of rigid bodies and joints on which forces act to produce motion. The *.osim* file, which describes the model in OpenSim, consists of bodies connected by joints and exchanging mutual forces. Also muscles can be added in a model, they extend over joints and generate forces and motion. Most of the properties of an OpenSim model can be defined and modified in the GUI. Once the musculoskeletal model is created, OpenSim allows users to study the effects of musculoskeletal geometry, joint kinematics, and muscle-tendon properties on the joint forces and moments that muscles can produce. The analysis can be run using the several tools offered by the software, such as inverse kinematic and dynamic, direct dynamic, muscle control and others.

The principal tools offered by OpenSim are the following:

- Resizing the dimensions of the muscoloskeletal model;
- Performing Inverse Kinematics analysis to calculate joint angles from marker positions;
- Performing Inverse Dynamics analysis to calculate joint moments, using both joint angles and external forces;
- Solve a Direct Dynamics problem and generate simulations of the motion;
- Analyze and plot the results;
- Create videos or take snapshots of model motion.

The software tools allow biomechanical simulation of the musculoskeletal system during motion, followed by the accurate analysis of the results, also made through the comparison with experimental data, in order to validate the developed model. The major application of the software involves the analysis of experimental data from a Motion Capture system; these data usually include marker trajectories, generalized coordinate values obtained from the laboratory acquisition system (joint angles), supports reaction forces, centers of pressure, and EMG measurements.

In the following subsection examples of biomechanical models available in OpenSim repository are described. They have been specifically developed to study the lower limbs mechanics during gait tasks, and they have been used as the basis for the development of the custom model used in this study, which will be described in Chapter 3.

2.2.2 Biomechanical Models

A model has several components:

- Reference frames, to which the positions of bodies and markers are referred;
- Bodies, the rigid segments representing the bones (e.g., femur, pelvis);
- Joints, express the relationship between the rigid bodies they connect (e.g., hip joint);

- Forces, can be passive (springs, contact forces) or active when subject to external control (from the user or actuators or muscles);
- Constraints, determine the movements allowed by the model;
- Contact geometries, define the interaction with external systems (ground or other objects);
- Markers, define a set of reference points placed on the model, which can be matched with real markers placed on subject's body;
- Controllers, can be used to control an active force.

Bodies are the major components of a model, they are interconnected by joints, which define the allowed mutual movements between parent and child bodies. A constraint can also be applied to limit the motion of bodies. The muscles are force elements connected to rigid bodies, that act at the insertion point. The structure of the muscle fibers and tendon in the model, the rate of stretch of the fiber, and the level of muscle activation determine the force of a muscle.

The body is the primary building block of the model, and the system dynamics is based on the structure of the body set. Each body is connected to a parent body through a joint. The relative motion is controlled by the coordinates and kinematic transforms defined by the modeled joint. The single body is defined through its name, a geometry and a set of mass properties (mass, mass center and inertia). In OpenSim the geometry can be specified using .vtp, .stl or .obj files. Alternatively a set of common analytical shapes are available in the repository (brick, sphere, cylinder, cone, ellipsoid).

The kinematic relationship between two bodies is defined by a joint. The parent body defines the fixed reference frame, while the child body is a moving reference frame. In each body a joint frame is also defined. The typical joints are: weld joint (no kinematic, fused bodies), pin joint, slider joint (one translational coordinate), ball joint (three rotational coordinates), ellipsoid joint (three rotational coordinates with coupled translations), free joint (six degrees of freedom). It is also possible to define a custom joint to model more complex biomechanical joints. To define the behavior of a custom joint the spatial transform matrix must be modeled.

It comprises six transform axes (three rotations and three translations), that define the spatial position of the child body with reference to te parent body frame reference, as a function of coordinates. Each transform axis enables a function of joint coordinates to operate about or along its axis.

The motion of a rigid body can be limited through a constraint, which are useful elements to reproduce the limitation of human body joints (e.g. hyperextensions). Three types of constraints are avalable in OpenSim models: point constraint (no relative translations), weld constraint (no translations nor rotations), and coordinate coupler constraint (user function that controls the coordinate of a given joint basing on any other coordinates in the model).

The force set defines the applied forces that actuate the model. Forces and torques act between bodies, while generalized forces are custom applications that can be applied along the axis of a generalized coordinate. Passive forces are related to element such as springs, dampers or contact geometries. Active forces are controlled by an input supplied by the user or by a controller. Active forces are called actuators, and the major actuators in a human body model are the muscles. The muscle is defined through a geometry, muscle points and properties. The set of muscle points indicate where the muscle is connected to bones (bodies), defining the force application point. Muscle properties, e.g. fiber lengths or activation rate, are used to determine muscle activation and contraction dynamics.

Markers are elements specifically introduced to integrate the experimental information collected using motion capture systems. Through the definition of a set of virtual markers that matches the positions of the experimental markers, an inverse kinematics can be performed to reproduce the motion of the subject studied in gait analysis laboratory.

Gait Models

As can be argued, the definition of the appropriate model is the first step to perform an accurate study of motion, as required in this work. OpenSim software offers several pre-developed musculoskeletal models. They can be used as the starting point for the development of a custom model. The choice of which model to use should be made based on what the users want to study in their project. Among them, there are two models specifically developed to describe in full detail the lower limbs of the human body: the Gait2392 and Gait2354.

The names of the two models are related to the number of degrees-of-freedom and muscle-tendon actuators. Both models present 23 degrees-of-freedom. In Gait2392 model, 92 muscle-tendon actuators are used to model the activity of 76 muscles in the lower limbs and torso. In Gait2354 model, the number of muscles was reduced to improve simulation speed. In Figure 2.10 the models are shown in OpenSim visualizer window.

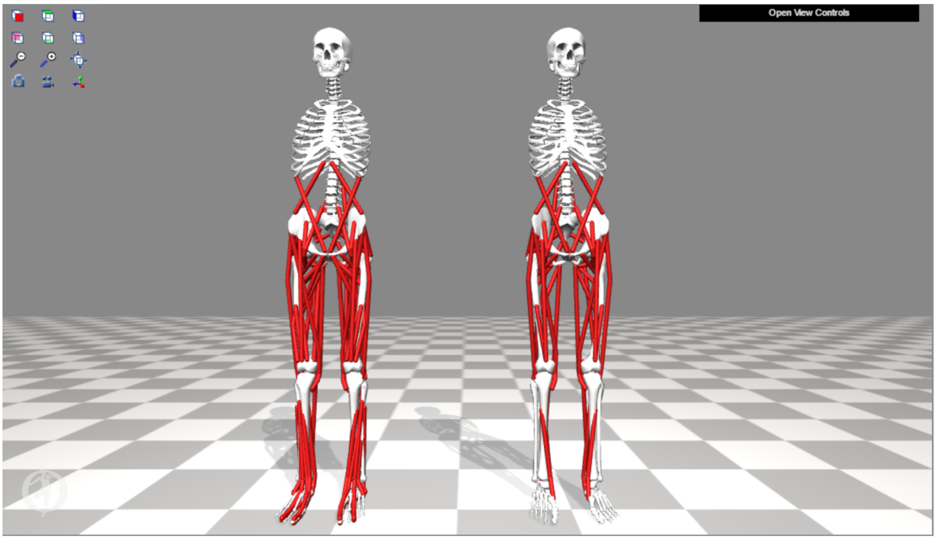

Figure 2.10. Models Gait2392 (left) and Gait 2354 (right) in OpenSim.

The models were developed by Darryl Thelen, Ajay Seth, Frank C. Anderson, and Scott L. Delp, exploiting the lower extremity joint definitions proposed by Delp *et al.* [19], low back joint and anthropometry adopted from Anderson and Pandy [4], and a planar knee model adopted from Yamaguchi and Zajac [58].

The geometry of bodies is defined with meshes of polygons describing the surfaces of the bones. They are created basing on data provided by Stredney *et al.* [49]. Seven rigid bodies compose the lower extremity: pelvis, femur, patella, tibia/fibula, talus, foot (which includes the calcaneus, navicular, cuboid, cuneiforms, metatarsals), and toes. Reference frames are fixed in each segment, they are shown in Figure 2.11.

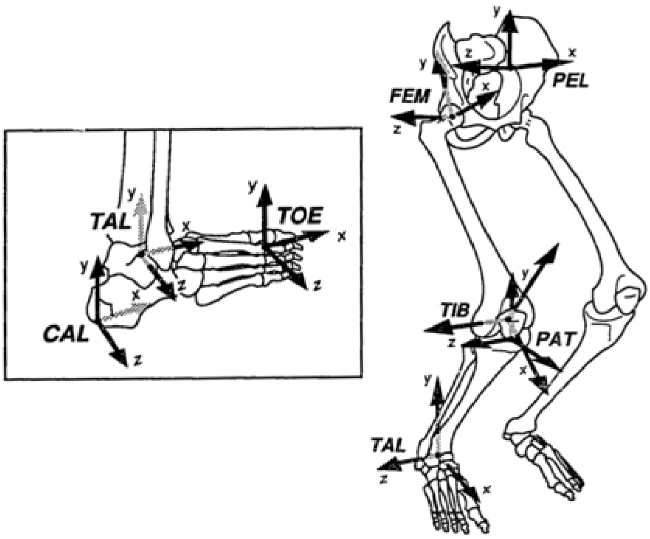

Figure 2.11. Placement of the body segments reference frames (Figure from [19]).

The relative motions between the bodies are defined by the following joints: hip, knee, ankle, subtalar, and metatarsophalangeal. The hip joint connects pelvis (parent body) and femur (child body). It is modeled as a ball joint, allowing the rotations around the three axes of the space, fixed in the femoral head.

The complexity of knee joint is represented using the simplified model proposed by Delp [19], represented in Figure 2.12. The joint model presents a single degree-of-freedom: the femur condyles, represented as ellipses, remain in contact with the tibial plateau, represented as a line segment, through the entire RoM. The contact points are specified basing on data provided by Nisell *et al.* [42], as function of the knee angle.

The foot model comprises three joints: ankle, subtalar and metatarphalangeal. They are modeled as frictionless revolute joints, with the axis oriented as shown in Figure 2.13.

Muscles and tendons are represented as line segments in the model. Their geometry and insertion points are defined basing on anatomy. Muscle

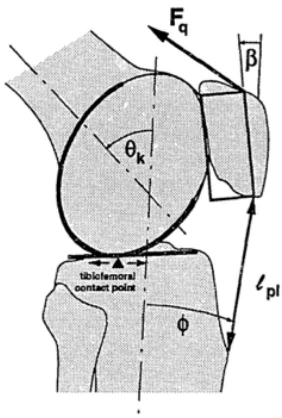

Figure 2.12. Geometry of knee joint in the sagittal plane (Figure from [19]).

forces are actuated at the insertion points, where the muscle is connected to bodies. The number of activated points depends on the type of muscle and on the position, with reference to anatomical concepts. The muscle physiological cross-sectional area, which controls the peak isometric force, is calculated as a combination of values provided by Friederich *et al.* [23] and Wickiewicz [54]. Fiber lengths and pennation angles are taken from Wickiewicz *et al.* [54].

To completely define the body set, masses and inertial properties have to be associated to the bodies. These properties are gathered from the model proposed by Frank C. Anderson and Marcus G. Pandy [4], based on averaged anthropometric data obtained from a cohort of five subjects, and then scaled by a factor of 1.05626, to reach a total mass of about 75 kg. The scale factor is uniformly applied to all bodies, thus not affecting the relative distribution of masses and the general anthropometry of the model. Body segments' geometry and lengths are taken from the Delp model [19]. The masses and moments of inertia for each body segment in the Gait 2392 Model are summarized in Table 2.2. These quantities are referred to a model representing a subject with height 1.80 m and a mass of 75.16 kg.

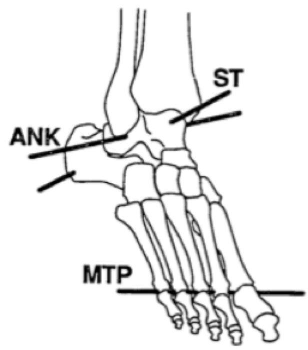

Figure 2.13. The three revolute joints of the foot model: ankle (ANK), subtalar (ST), and metatarphalangeal (MTP) joints (Figure from [19]).

2.2.3 Basics of Biomechanical Modelling of Gait

Starting from a muscolo-skeletal model, a dynamic simulation of gait can be obtained exploiting data gathered with motion capture system in gait analysis laboratory. The steps needed are the following:

1. The first step is to scale the model basing on subject's anthropometric measurements.

2. In the next step, the coordinate values of the experimental markers are exploited to solve an inverse kinematics problem. The output describes the kinematics of the body segments during gait.

3. In the third step, using the kinematics results, an inverse dynamics problem is solved to determine the forces and torques acting on a system.

In the following the three phases are detailed.

Scaling

The scaling procedure alters the anthropometry of the model to match the characteristics of the subject. The procedure is based on the comparison of the experimental markers data and virtual markers placed on the

Table 2.2. Masses and inertial parameters for the body segments of the model.

Body segment	Mass (kg)	Moments of Inertia		
		xx	yy	zz
Torso	34.2366	1.4745	0.7555	1.4314
Pelvis	11.777	0.1028	0.0871	0.0579
Right femur	9.3014	0.1339	0.0351	0.1412
Right tibia	3.7075	0.0504	0.0051	0.0511
Right patella	0.0862	0.00000287	0.00001311	0.00001311
Right talus	0.1000	0.0010	0.0010	0.0010
Right calcaneus	1.250	0.0014	0.0039	0.0041
Right toe	0.2166	0.0001	0.0002	0.0010
Left femur	9.3014	0.1339	0.0351	0.1412
Left tibia	3.7075	0.0504	0.0051	0.0511
Left patella	0.0862	0.00000287	0.00001311	0.00001311
Left talus	0.1000	0.0010	0.0010	0.0010
Left calcaneus	1.250	0.0014	0.0039	0.0041
Left toe	0.2166	0.0001	0.0002	0.0010

model. A static trial can be used to collect the trajectories of experimental markers to be used in scaling procedure. In the static trial the subject must stand in a static pose for several seconds. The virtual markers are placed on the model in positions that reflect the experimental positions of the markers. It is therefore recommended to place markers in specific body landmarks, easy to identify and replicate. In Figure 2.14 it is shown an example of correspondence.

The first task in scaling is the determination of the scale factors for each body segments. The scale factor for a segment is computed by comparing the experimental and virtual distances between two markers that identify the segment dimension. With reference to Figure 2.14, e_1 represents the distance between the markers at the two ends of the femur, while m_1 the correspondent length in the virtual model. Therefore the scaling factor for the femur is defined as the ratio between the experimental and the virtual lengths. The overall scale factor is then the average of the scale factors computed on the two femurs.

After the scale factors are computed for all bodies, the model's geometry is scaled accordingly. In particular, in this phase, the joint frame locations, mass center location, force application points and muscle attach-

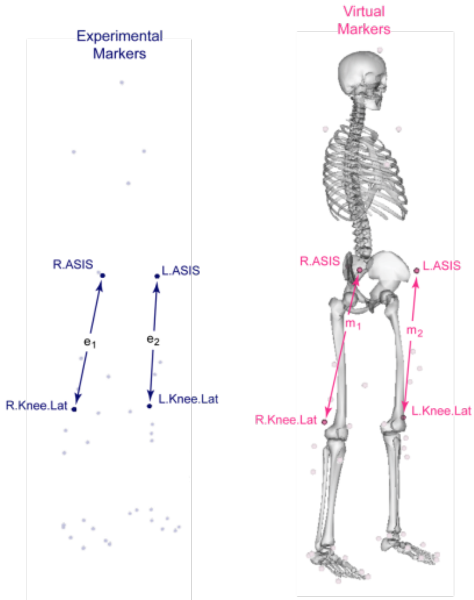

Figure 2.14. Experimental markers (on the left in blue) and virtual markers placed on the model (on the right in red).

ment points are rearranged.

Then new segments' masses are calculated. If the mass distribution of the initial model has to be preserved, then each body mass is scaled by its own scale factor. Moreover, if an input target mass is specified (the mass of the subject experimentally measured), then each body segment is scaled by the ratio of the target mass to the mass of the entire model.

In the following task all the remaining component are scaled. As an example, in this phase, ligaments and muscles are updated according the new dimensions of the segments they are connected to.

Finally the markers placement is also updated in order to match the experimental positions, obtained as the average of the markers coordinates over the several frames composing the static acquisition.

Inverse Kinematics

The Inverse Kinematics procedure is intended to simulate the motion of the body according to the experimental data collected in gait analysis laboratory. It is still based on the coordinates of the experimental markers, and their evolution through the volume of acquisition. In particular, the inverse kinematics tool tries to set the virtual model in a pose that best matches the experimental markers coordinates, for each time frame of the acquisition. It is accomplished by minimizing the sum of squared errors between experimental and virtual markers' coordinates. The change in the virtual markers' position over time leads to the variations of the joints angles, that represent the kinematic output of the procedure.

From a mathematical point of view it is configured as a least squares problem, that aims to minimize two types of errors: marker errors and coordinate errors. The first one represents the spatial distance between the analogous experimental and virtual markers. A weight can be associated to each marker to specify how strongly that marker's error term should affect the minimization procedure.

The latter is the error between experimental kinematic values and those computed by the inverse kinematics. The experimental data can be represented by joint angles gathered from the motion capture system, or with other systems (e.g. goniometers, inertial units) or exploiting specific algorithms. If the kinematic data of a certain coordinate are experimentally computed with high confidence, then it will not be considered in the inverse kinematic problem and will not be changed. Usually the coordinate error is not considered because of the lack of experimental data, and the inverse kinematics is only based on marker errors.

Therefore, for each frame obtained from motion capture, the quantity to be minimized is the sum of squared errors shown in the following equation:

$$error = \sum_{i \in markers} w_i \| x_i^{exp} - x_i(q) \|^2 + \sum_{j \in coordinates} w_j (q_j^{exp} - q_j)^2$$

Where x_i^{exp} is the experimental position of marker i, $x_i(q)$ is the position of the corresponding model marker (which depends on the coordinate values), q_j^{exp} is the experimental value for coordinate j. The weights w_i

and w_j determine the impact of the specific marker/coordinate error on the solution of the problem.

The problem solved by the inverse kinematics tool is the definition of the coordinates vector q that minimizes this quantity. The problem is defined as follows:

$$\min_q [\sum_{i \in markers} w_i \|x_i^{exp} - x_i(q)\|^2 + \sum_{j \in coordinates} w_j (q_j^{exp} - q_j)^2]$$

Where q is the vector of generalized coordinates being solved for, and represents the output of the procedure.

Inverse Dynamics

Given the motions determined with the kinematic analysis, an inverse dynamics problem can be solved to establish the generalized forces (net forces and torques) acting on the joint and responsible for movement.

The procedure is based on the classical mechanics expression that links kinematics and dynamics $F = ma$. Expanding the relation in three dimensions and adding all the relevant forces, the equation of motions may be written as follows:

$$M(q)\ddot{q} + C(q, \dot{q}) + G(q) = \tau$$

where (said N the degrees of freedom):

- $q, \dot{q}, \ddot{q} \in R^N$ are the vectors of positions, velocities and accelerations respectively, that are computed in the inverse kinematics problem;
- $M(q) \in R^{N \times N}$ is the system mass matrix;
- $C(q, \dot{q}) \in R^N$ is the vector of Coriolis centrifugal forces;
- $G(q) \in R^N$ is the vector of gravitational forces;
- $\tau \in R^N$ is the unknown vector of generalized forces.

All the terms on the left side of the equations are known. The inverse dynamics tool solves these equations, in the inverse dynamics sense, to yield the net forces and torques at each joint which produce the movement.

Chapter 3

A Novel Platform for the Analysis of Gait Biomechanics

This chapter shows the development of the platform for the biomechanical analysis of human gait, with the general aim to offer the users all the features to perform a custom analysis of kinematics and dynamics of movement. The platform also provides a specific tool for the extraction of selected parameters which can improve the process of design of custom AFOs. This Biomechanical platform was developed in the MATLAB development environment and involved the implementation of algorithms to perform the biomechanical modelling and simulation tasks explored in the previous Chapter. In order to develop a practical user interface the MATLAB App Designer was used, since the platform is intended to be used also by a non-expert user. The open source OpenSim Application Programming Interface (API) was exploited for the implementation of the major functionalities, regarding biomechanical modelling and simulation.

This chapter opens with the description of the development environment. Then the external resources required for the correct use of the platform are presented. The main section describes the implementation of the algorithms, while the last section shows the main application in the field of orthopaedics, but also the general use for the biomechanical analysis of gait. The user manual is reported in Appendix A.

3.1 Integrated Development Environment

MATLAB was selected as the environment for the development of the platform. MATLAB provides the App designer tool in order to develop interactive GUIs, which represent a convenient solution when a user application has to be deployed. Unlike other GUI development tools, MATLAB has the advantage of combining the app designer with the well-known computing and processing capabilities, based on matrices and linear algebra, in the area of numerical analysis, for data processing, image processing, and model development. In this regard, MATLAB allowed the integration of biomechanical modelling and analysis procedures into the user platform, also exploiting libraries distributed by OpenSim, which can be easily integrated in the development environment.

3.1.1 MATLAB App Designer

The Biomechanical platform was developed in the form of an application, using, for the graphical design of the interface, the App designer tool, a MATLAB development environment dedicated to the implementation of interactive applications. App Designer enables the combined visualization of the application layout and of the associated code, assisting the developer in the coherent editing of both features. Graphical interfaces are a useful tool for developing applications for less experienced users, as they guide the user through the process, thus reducing errors.

Application development in MATLAB app designer is based on event and object-oriented programming. Objects are represented by the graphical elements (User Interface (UI) components) added to the interface, or by other elements directly defined by the developer. Events are typically associated with objects, they are triggered by user actions, and activate the set of commands associated with them by the developer. The Design VieW workspace is available for building the graphical interface of the application. Here the developer can add elements from the extended UI components library, so that various interactive functionalities can be created. The changes made in Design View are automatically reflected in the code section, referred to as Code View. In this way, many aspects of the application can be configured without writing any code. Conversely, the properties and functionalities of UI components can also be modified by code.

Figure 3.1 shows the UI components library available in MATLAB App Designer (ver. R2022a). Components are divided in four macro-categories: common, containers, figure tools e instrumentation. The following list provides a brief description of the principal components; part of them have been used in the development of the application.

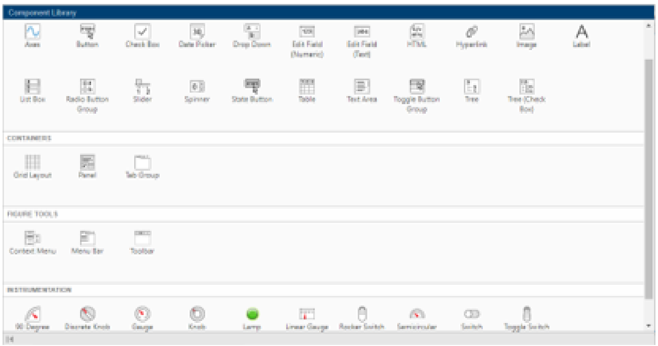

Figure 3.1. UI Component Library in MATLAB App Designer.

The common components are the basic elements, depending on the type they have a different use:

- Axes: a section where a plot, a chart, a diagram or a figure can be visualized;
- Button: element generating an event when pushed;
- Check Box: a graphical widget that allows the user to make a binary choice (ticked or not);
- Drop Down Menu: allows the selection of a single option from a list;
- Edit Field (Text/Numeric): a field where the user can add text/numbers;
- HTML: display simple markup or embedded HTML file;
- Hyperlink: open a webpage or execute MATLAB code;
- Image: used to add a static image;

- Slider: horizontal or vertical track bar;
- Label: non-editable text;
- List Box: a list of items where the user can select one or more options;
- Radio Button Group: allows the selection of only one option of the group;
- Spinner: enter numeric data and adjust value with increment or decrement buttons;
- State Button: toggle button with two states (pushed or not);
- Table: shows tabular data;
- Text Area: used to enter multi-line text;
- Toggle Button Group: allows the selection of a single toggle button in the group;
- Tree: displays hierarchical list of items;
- Check Box Tree: hierarchical list of items with the opportunity to check one or more options.

The containers components are elements that can handle the simultaneous use of multiple common elements:

- Grid: arranges components in grid with specified resizing behaviour;
- Panel: groups many components in a single panel container;
- Tab Group: groups and manages components in different tabs.

Figure tools are aimed at managing the application tools and the search for their properties:

- Context Menu: displays context menu when the associated component is right-clicked;
- Menu Bar: groups and displays application commands and options by functionalities;

- Toolbar: groups and displays tools at the top of the application.

Instrumentation components enable a more elaborate and pleasing visualization of variables and data:

- 90 Degree Gauge: displays values on 90 degree radial scale;
- Discrete Knob: adjusts value to one of several distinct states;
- Gauge (Semicircular Gauge): displays value on complete (180 degree) radial scale;
- Knob: adjusts value within a specified range;
- Lamp: illuminates to indicate status;
- Linear Gauge: displays value on linear scale;
- Switch (Rocker/Toggle Switch): toggles between two exclusive states.

Other UI components can be included, by adding new toolboxes to the MATLAB environment.

The components added to the interface can be organized, resized, aligned, grouped and customized throw the definition of their properties, directly in the Design View workplace. Component properties can be also modified by code, especially when the change has to occur during the use of the application.

The code editor presents editable and uneditable sections. The latter are managed by App Designer for the execution of the application. The editable sections allow the developer to define custom properties and elements and implement functions associated with objects and events, exploiting all MATLAB functionalities.

3.1.2 OpenSim API

In order to implement the biomechanical modelling functionalities described in Chapter 2, the API provided by SimTK OpenSim was exploited. The API can be used in MATLAB or Python: it allows the usage of already embedded components, properties or models, but it is also opened for customization and extension of the libraries, for example, writing plugins or creating new Components. OpenSim libraries are written using object-oriented programming, consisting of a large set of classes that are divided into subclasses: as an example, the Model class contains all the components of a model such as Body, Joint, and Force classes. The organization of classes is hierarchical. The major classes are organized with the structure shown in Figure 3.2. Each class of OpenSim API is built on top of (i.e., requires) the components underneath.

The development of the biomechanical platform required operation on the Model Components class and on higher level classes (dynamics engine, manager, optmizer, analyzer). The specific use of classes and related properties are discussed in Section 3.3, where the implementation of the platform is deeply discussed.

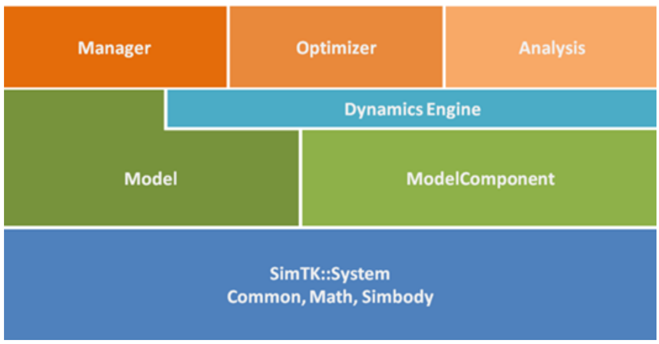

Figure 3.2. The hierarchical structure of OpenSim API classes: each class is built on the components underneath.

3.2 External Resources

The biomechanical platform is structured as a standalone application, in order to give the opportunity to be used by heterogeneous users. However a set of external resources are required to achieve the proper functioning. In particular the following resources are required:

- Biomechanical Model: it is the starting model on which the processing is executed. This model has to be customized to be properly processed and reach the intended goals of the analysis.

- Anthropometric Measures: these are the metrics characterizing the subject, and used for the scaling of the model. They are collected in the experimental phase by an expert clinical technician, so they have to be imported in the platform using a semi-automatic method.
- Experimental Marker Data: these represent the 3D trajectories of the markers placed on the subject, gathered during the static and dynamic trials. They are collected using other external systems, so they have to be imported in the platform as an external resource.
- Setup Scale File: this file contains all the useful information to run the scaling procedure, including the path of the other external resources.

The following sections analyze individually the external resources required, showing how they are prepared to be imported in the platform.

3.2.1 Biomechanical Model

The models presented in Section 2.2.2 represent the basic models on which a customized analysis can be run for each patient under study. Their importance is in providing an already complete set of body segments and joints connecting them, which are the basis of the biomechanical analysis. However, in order to scale the model and track the subject posture and movements, the starting model needs to be equipped with a set of virtual markers that are then used to match the trajectories of the experimental markers. Therefore, it is convenient to develop a general model equipped with a set of virtual markers, placed at specific landmarks in the model, corresponding to the anatomical points where the experimental markers are applied during the acquisitions on the study subjects.

The first step is to select a model on which the markers will be placed: the Gait2392 model was selected because it is the most complete in describing the kinematics and kinetics of the lower limbs during walking. A new marker added to the model is defined through its properties. The main identifying properties are the following:

- Marker Label: it represents the name identifying the marker. For convenience and to automate subsequent processing steps, it is convenient to use the same name used by the 3D tracking system to indicate the experimental markers placed on patient's body.

- Parent Frame: it represents the virtual body of the model the marker is associated to. It also identifies the reference point in the space for the definition of the relative coordinates of the marker. Another important aspect is the 'fixed' parameter. It is a Boolean parameter that indicates whether the marker should be fixed with respect to its reference point during the scaling procedures. When it is set as false, the marker can be translated with respect to its reference during the scaling operation in order to reach a better match with its experimental counterpart.

- Location: it is expressed with the 3 coordinates of the space with reference to the parent frame.

In the experimental procedures examined in this work, the markers are placed on the subject following the Davis protocol (see Section 2.1.2). This protocol includes the use of 22 markers placed in specific landmarks of the body. Therefore, the corresponding 22 virtual markers were added to the Gait2392 model, generating the starting biomechanical model for the study of gait through the novel application.

Table 3.1 defines the properties of the 22 markers added. In addition, the physical landmark on body, indicated by the Davis protocol to guide the proper placement, is also specified.

Figure 3.3 shows the developed model, with the 22 virtual markers represented as pink dots in the Visualizer Window and listed in the Navigator window on the left side of the figure.

3.2.2 Anthropometric Measures

The anthropometric measures are a set of quantitative metrics regarding the body of the subject under test. They are collected by a clinician before the starting of the experimental procedures of walking trials. These metrics are relevant as they support the development of the specific biomechanical model of the subject. In particular the anthropometric measures are used during the scaling of the model, leading to a more accurate scal-

Table 3.1. Properties of the markers added to the model.

Marker Label	Parent Frame	Relative Location (x,y,z)	Body Landmark
c7	Torso	$(-0.08, 0.44, 0)$	Spinous Process c7
r.should	Torso	$(0.03, 0.44, 0.15)$	Right acromioclavicular joint
l.should	Torso	$(-0.03, 0.44, -0.15)$	Left acromioclavicular joint
r.asis	Pelvis	$(0.02, 0.03, 0.128)$	Right ASIS
l.asis	Pelvis	$(0.02, 0.03, -0.128)$	Left ASIS
sacrum	Pelvis	$(0.16, 0.04, 0)$	Second sacral vertebra
r.thigh	Right Femur (*femur_r*)	$(0.02, -0.024, 0.09)$	Right greater trochanter
r.bar1	Right Femur (*femur_r*)	$(0.008, -0.21, 0.13)$	Femur wand between markers r.thigh and r.knee1
r.knee1	Right Femur (*femur_r*)	$(0, -0.404, 0.05)$	Lateral epicondyle of the right femur
r.knee2	Right Tibia (*tibia_r*)	$(0.005, -0.065, 0.05)$	Head of the right fibula
r.bar2	Right Tibia (*tibia_r*)	$(0.0003, -0.25, 0.09)$	Fibula wand between markers r.knee2 and r.mall
r.mall	Right Tibia (*tibia_r*)	$(0.005, -0.41, 0.053)$	Lateral malleolus right
r.heel	Right Calcaneus (*calcn_r*)	$(0.02, 0.02, 0)$	Fifth metatarsal head on right foot
r.met	Right Calcaneus (*calcn_r*)	$(0.14, 0.026, 0.036)$	Right heel
l.thigh	Left Femur (*femur_l*)	$(0.02, -0.024, -0.09)$	Left greater trochanter
l.bar1	Left Femur (*femur_l*)	$(0.008, -0.21, -0.13)$	Femur wand between markers l.thigh and l.knee1
l.knee1	Left Femur (*femur_l*)	$(0, -0.404, -0.05)$	Lateral epicondyle of the left femur
l.knee2	Left Tibia (*tibia_l*)	$(0.005, -0.065, -0.05)$	Head of the left fibula
l.bar2	Left Tibia (*tibia_l*)	$(0.0003, -0.25, -0.09)$	Fibula wand between markers l.knee2 and l.mall
l.mall	Left Tibia (*tibia_l*)	$(0.005, -0.41, -0.053)$	Lateral malleolus right
l.heel	Left Calcaneus (*calcn_l*)	$(0.02, 0.02, 0)$	Fifth metatarsal head on left foot
l.met	Left Calcaneus (*calcn_l*)	$(0.14, 0.026, -0.036)$	Left heel

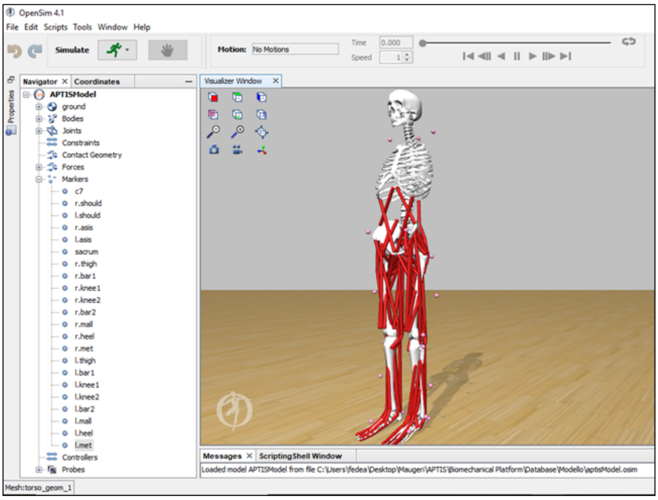

Figure 3.3. The starting model Gait2392 equipped with the set of virtual markers represented as pink dots. On the left, the list of markers is reported.

ing procedure. In order to have reliable measurements, a set of detailed instructions for collecting the values is provided to the clinician.

First, the weight [kg] and height [cm] of the subject have to be collected. The following guidelines describe how the other anthropometric parameters are measured.

- Pelvis width [cm]: with the patient lying on a couch in supine position, identify the location of the ASISs by palpation. Mark the points and measure their distance using a martin pelvimeter.

- Pelvis height [cm]: locate the gran trochanter, moving the hip into maximum flexion and intra-rotation. Then, bringing the limb back into axis, consider a plane parallel to the couch passing through the greater trochanter, and measure the perpendicular distance between the ASIS and this plane.

- Total leg length [cm]: with the knees in full extension, measure the linear distance between the ASIS and the medial malleolus.

- Knee diameter [cm]: with the knee flexed, measure the distance between the medial and lateral femoral condyles using a martin pelvimeter.

- Ankle diameter [cm]: measure the distance between the medial and lateral malleolus using a martin pelvimeter.

The anthropometric measurements are saved in a text file with a standard structure shown in Figure 3.4, in which the first three rows provide information about the patient, while the following lines report the anthropometric measurements. This standard structure allows the automatic import of this information into the platform.

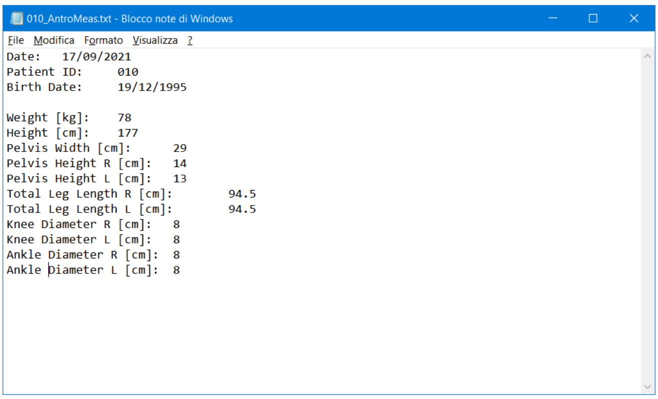

010_AntroMeas.txt - Blocco note di Windows
File Modifica Formato Visualizza ?

```
Date:	17/09/2021
Patient ID:	010
Birth Date:	19/12/1995

Weight [kg]:	78
Height [cm]:	177
Pelvis Width [cm]:	29
Pelvis Height R [cm]:	14
Pelvis Height L [cm]:	13
Total Leg Length R [cm]:	94.5
Total Leg Length L [cm]:	94.5
Knee Diameter R [cm]:	8
Knee Diameter L [cm]:	8
Ankle Diameter R [cm]:	8
Ankle Diameter L [cm]:	8
```

Figure 3.4. The standard file used to store the anthropometric measurements collected on a subject before the experimental session. The standard structure allows the automatic import of data in the platform.

3.2.3 Experimental Marker Data

Marker trajectories collected during the experimental sessions are essential data needed to perform the biomechanical modelling and the analysis of gait. For the scaling procedure it is required the collection of the experimental marker trajectories during a static trial in which the subject stands in orthostatic position, with aligned feet and arms along the body, for a period during at least ten seconds. The standing trial is performed once per session.

After the static trial, the subject performs the dynamic trials, consisting in walking at self-selected cadence, on a path placed in the range of view of the motion tracking system. Walking trials are usually performed several times per session, in order to enhance the reliability of results.

During the entire session the subject is equipped with the markers placed on body following the Davis protocol (see Section 2.1.2). Markers trajectories gathered by the motion capture system are used in the processing performed on platform: the static trial is needed for the scaling and to get the posture of the subject, while the walking trials are used to perform the inverse kinematics.

Markers traces have to be exported from the motion capture system in order to be imported and processed by the biomechanical platform. Each system may have different procedures for data export. The following discussion is about the export procedures of markers traces from the 3D tracker System SMART-DX by BTS Bioengineering shown in Section 2.1.2, which represents the system used for the described activity.

Data acquired by the IR cameras are processed using the software SMART Tracker. The first step is the labeling, namely the assignment of each trace to the correct marker. This phase is automatically managed by the software, however user intervention is usually required to correct labeling errors. Then the software performs the tracking procedure, connecting markers to form a stick model representing the subject.

At this point the markers traces can be exported. They are organized in a text file with extension *'.trc'*. Figure 3.5 shows the structure of the file. The first three rows constitute the header, with information about the file path and technical information about the system used for acquisition. The header is followed by two rows labeling the columns. After a blank line, data are reported. The first column reports the frame number, with a progressive integer value. The second column reports the acquisition time, expressed in seconds. The next columns represent the 3 coordinates (x, y, z) of each of the markers used in the experimental session and correctly tracked. Then each row contains the position of all markers in space in a single time frame. Data are delimited by *TAB* characters. The *.trc* files are automatically imported in the biomechanical platform and used for the analysis of gait kinematics.

```
PathFileType	4	(X/Y/Z)	C:\Documents and Settings\BTSUser\Desktop\Lionetti Michele\Senza AFO\0023~aa~Standing.trc
DataRate	CameraRate	NumFrames	NumMarkers	Units	OrigDataRate	OrigDataStartFrame	OrigNumFrames
70.00	70.00	732	22	mm	70.00	1	735
Frame#	Time	sacrum			r.asis			r.thigh			r.bar1			r.knee1			r.knee2			r.bar2
		X1	Y1	Z1	X2	Y2	Z2	X3	Y3	Z3	X4	Y4	Z4	X5	Y5	Z5	X6	Y6	Z6	X7	Y7

0	0.000000	-217.681110	1036.870956	43.715876	-11.092847	984.605134	177.557603	-57.182748	945.905745	233.982220	-33.
1	0.014286	-217.702150	1036.881447	43.743115	-11.110704	984.605312	177.609786	-57.330620	945.911527	234.006703	-33.
2	0.028571	-217.672110	1036.881924	43.759316	-11.141406	984.579623	177.656695	-57.395730	945.901632	234.029427	-33.
3	0.042857	-217.700869	1036.910534	43.787543	-11.183764	984.556675	177.675873	-57.371743	945.871234	234.041765	-33.
4	0.057143	-217.712387	1036.918521	43.824766	-11.216376	984.556794	177.674428	-57.331339	945.869127	234.048843	-33.
5	0.071429	-217.690170	1036.904931	43.848354	-11.211256	984.549880	177.654728	-57.263035	945.875466	234.054744	-33.
6	0.085714	-217.699856	1036.896944	43.865658	-11.137327	984.559774	177.635998	-57.217367	945.882320	234.051973	-33.
7	0.100000	-217.704356	1036.907911	43.895047	-11.128166	984.571218	177.630782	-57.229977	945.885181	234.062895	-33.
8	0.114286	-217.764452	1036.919713	43.915723	-11.144508	984.581053	177.645579	-57.276092	945.871174	234.095454	-33.
9	0.128571	-217.764750	1036.912918	43.912124	-11.161745	984.583199	177.697286	-57.330966	945.852757	234.131724	-33.
10	0.142857	-217.715025	1036.906838	43.895725	-11.161918	984.575391	177.756712	-57.414208	945.838630	234.184340	-33.
11	0.157143	-217.702478	1036.912084	43.883510	-11.224830	984.535992	177.818745	-57.529010	945.824146	234.228879	-33.
12	0.171429	-217.716917	1036.906719	43.893412	-11.276032	984.494030	177.879050	-57.622820	945.817888	234.286040	-33.
13	0.185714	-217.750624	1036.919355	43.910429	-11.311697	984.480023	177.926779	-57.693660	945.817351	234.332278	-33.
14	0.200000	-217.790201	1036.951542	43.955989	-11.317134	984.495521	177.958429	-57.752766	945.812285	234.367624	-33.
15	0.214286	-217.807546	1036.978602	44.011381	-11.319304	984.513998	177.950025	-57.782985	945.825815	234.411031	-33.
16	0.228571	-217.811704	1037.004113	44.044480	-11.330602	984.509587	177.942529	-57.779841	945.836186	234.425277	-33.
17	0.242857	-217.859909	1037.032366	44.074513	-11.328089	984.493375	177.943751	-57.806235	945.828438	234.426156	-33.
18	0.257143	-217.844054	1037.053585	44.083934	-11.384141	984.440625	177.929252	-57.790082	945.823967	234.424368	-33.
19	0.271429	-217.827186	1037.069321	44.100113	-11.360134	984.411716	177.921012	-57.807986	945.816994	234.436750	-33.
20	0.285714	-217.851669	1037.087679	44.146873	-11.355621	984.399676	177.920923	-57.816051	945.795119	234.456182	-33.
21	0.300000	-217.864886	1037.097812	44.181529	-11.383889	984.370887	177.918196	-57.840757	945.762992	234.478801	-33.
22	0.314286	-217.888325	1037.112117	44.185415	-11.388004	984.360218	177.946582	-57.854734	945.733368	234.489948	-33.
23	0.328571	-217.900395	1037.111282	44.176508	-11.452484	984.341025	177.960336	-57.862498	945.724964	234.494805	-33.
```

Figure 3.5. The .trc file used to store the markers traces exported from BTS tracking system.

3.2.4 Setup Scale File

The Setup Scale file is used to collect and provide the information and parameters needed to perform model scaling. The file is textual with *.xml* extension, and consists of 5 sections: execution parameters; subject parameters (e.g., mass, height, age); model parameters; scaling properties; and marker placement properties. An example of a Setup file is shown in Figure 3.6.

The properties for the scaling operation are enclosed in the opening and closing tags *<ScaleTool>* and *</ScaleTool>*. Subject measurements are the *<mass>*, *<height>* and *<age>* properties, respectively expressed in kg, mm, and years. The age is specified for informational purposes only, and does not affect the scaling result. Height and mass are gathered from the anthropometric measurements and are used to improve the scaling of the model. The scaled model can be set to have a total mass equal to the mass value specified in the file (setting as true the *<preserve_mass_distribution>* property).

The property *<GenericModelMaker>* points to the starting model to be scaled, described in Section 3.2.1, while the virtual marker set is referenced with the property *<marker_set_file>*. The referenced file contains all the information about the virtual markers arranged to match the experimental markers of the Davis protocol.

The scaling properties are enclosed in the *<ModelScaler>* tag. As de-

```xml
<?xml version="1.0" encoding="UTF-8" ?>
<OpenSimDocument Version="40000">
    <ScaleTool>
        <!--Mass of the subject in kg.  Subject-specific model generated by scaling step will have this total mass.-->
        <mass>75</mass>
        <!--Height of the subject in mm.  For informational purposes only (not used by scaling).-->
        <height>-1</height>
        <!--Age of the subject in years.  For informational purposes only (not used by scaling).-->
        <age>-1</age>
        <!--Notes for the subject.-->
        <notes>Unassigned</notes>
        <!--Specifies the name of the unscaled model (.osim) and the marker set.-->
        <GenericModelMaker>
            <!--Model file (.osim) for the unscaled model.-->
            <model_file>aptisModel.osim</model_file>
            <!--Set of model markers used to scale the model. Scaling is done based on distances between model markers compared to the same distances between the corresponding experim
            <marker_set_file>BTSmarkers.xml</marker_set_file>
        </GenericModelMaker>
        <!--Specifies parameters for scaling the model.-->
        <ModelScaler>
            <!--Whether or not to use the model scaler during scale-->
            <apply>true</apply>
            <!--Specifies the scaling method and order. Valid options are 'measurements', 'manualScale', singly or both in any sequence.-->
            <scaling_order> measurements</scaling_order>
            <!--Specifies the measurements by which body segments are to be scaled.-->
            <MeasurementSet>
                <objects>
                    <Measurement name="femur">
                    <Measurement name="femurLeft">
                    <Measurement name="tibiaRight">
                    <Measurement name="tibiaLeft">
                    <Measurement name="pelvis">
                    <Measurement name="calcnRight">
                    <Measurement name="calcnLeft">
                    <Measurement name="femurRight">
                    <Measurement name="tibia">
                    <Measurement name="calcn">
                </objects>
                <groups />
            </MeasurementSet>
            <!--Scale factors to be used for manual scaling.-->
            <ScaleSet>
                <objects />
                <groups />
            </ScaleSet>
            <!--TRC file (.trc) containing the marker positions used for measurement-based scaling. This is usually a static trial, but doesn't need to be.  The marker-pair distances
            <marker_file>Unassigned</marker_file>
            <!--Time range over which to average marker-pair distances in the marker file (.trc) for measurement-based scaling.-->
            <time_range> 0 9.62857</time_range>
            <!--Flag (true or false) indicating whether or not to preserve relative mass between segments.-->
            <preserve_mass_distribution>true</preserve_mass_distribution>
            <!--Name of OpenSim model file (.osim) to write when done scaling.-->
            <output_model_file>Unassigned</output_model_file>
            <!--Name of file to write containing the scale factors that were applied to the unscaled model (optional).-->
            <output_scale_file>Unassigned</output_scale_file>
        </ModelScaler>
        <!--Specifies parameters for placing markers on the model once a model is scaled. -->
        <MarkerPlacer>
    </ScaleTool>
</OpenSimDocument>
```

Figure 3.6. The .xml file used to store all the properties needed to perform the scaling of the biomechanical model.

scribed in Section 2.2.3, scaling can be performed based on measurements or manually. The *<scaling_order>* property specifies which of the two methods is used (using the *measurements* and *manualScale* keywords, respectively).

The *<marker_file>* property is used to specify the file containing experimental data about marker trajectories during the standing trial. This information is automatically set by the platform once the patient and acquisition session are selected. Similarly, the *<time_range>* tag is filled after the *.trc* file is loaded.

Finally, once the scaling operation has been completed, the scaled model will be saved in the file specified in the property *<output_model_file>*, while the *<output_scale_file>* property specify where to store the setup file used for the processing.

3.3 Platform Implementation

The biomechanical platform is structured as shown in Figure 3.7. In the schematic, the platform is represented by the light blue block. It is built on a database containing the information to be processed and structured in a standard way as described in Section 3.3.1. The platform is made up of four macro-blocks, reflecting four MATLAB functions called when needed by the main application, as will be seen in the detailed description of the structure.

The application opens with an initial interface that first requires the selection of the database to be referenced for further processing. Once the database is selected, the user is prompted to select the patient. From there the several functions presented in the diagram can be accessed. The singular building blocks constituting the platform will be discussed in detail below. A focus is also provided about the database, whose structure is of central importance as it also determines the proper functioning of the entire platform.

At this stage of development the platform does not take into account the possibility of different users with separate privileges in terms of data accessibility, modification and types of analysis. Future developments will consider the use of an authentication stage for the user, allowing, for instance, different functionalities for a physician or a technical user, or the visualisation of only their respective list of patients for different physicians. This could also help to better manage privacy issues.

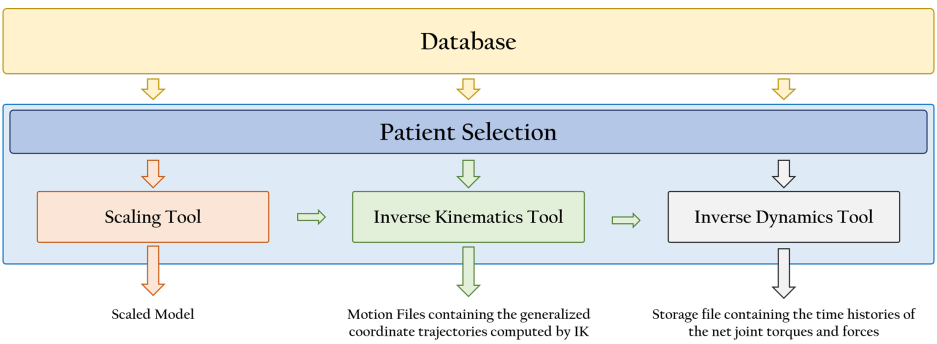

Figure 3.7. Design diagram of the Biomechanical Platform.

3.3.1 Database

The resources accessible to the biomechanical platform are structured within a database in a schematic and rigorous arrangement, such that the platform can automatically manage them. Inside the database, files are grouped first by subject, then by system used for acquisition, and finally by acquisition session. The nested structure of the folders is presented in Figure 3.8. The outer folder is related to the individual subject identified by a progressive three-digit numeric ID. The name of the folder has a rigid structure: the three-digit ID is followed by an underscore "_", then by the subject's surname with the initial capitalized letter, separated from the first name by an additional underscore (e.g.: 001_Smith_John). In the case of a surname or name consisting of several words, they will not be separated but each will have a capitalized initial (e.g.: 001_Wright-Phillips_JohnPeter).

Figure 3.8. Nested structure of the folders in the database.

The subject's folder contains a folder for each acquisition system used to collect data. The system folder name repeats the subject ID, followed by the identification of the system expressed with four capitalized characters. The code used for the tracking system SMART-DX by BTS Bioengineering is *BTSX*. For instance, the folder named *020_BTSX* contains all data gathered using the SMART-DX system on subject identified with the ID *020*.

Inside the system folder there are as many sub-folders as the number of experimental sessions taken on the selected subject. The session folder is again identified by the three-digit subject ID, followed by the system's four-letter identification code, which is followed by information about the use of the AFO during acquisitions and the date on which the measurement session was conducted. All information are separated by an underscore in the folder name. The information about the use of the AFO is needed as the experimental session can be conducted in three different conditions, which are encoded with a single integer:

- 0 - the subject did not use an AFO in the experimental trials;

- 1 - the subject used a commercial AFO to perform the experimental trials;
- 2 - the subject used a custom 3D-printed orthosis to perform the experimental trials.

The date is reported with structure *ddmmyyyy*. For instance, the folder named *005_BTSX_1_31032022* contains all the data acquired on the patient identified by code 005 with BTS SMART-DX system using a commercial AFO on March 31, 2022.

Data in this folder are structured in several folders and files containing the input and output of the processing tasks carried out by the platform. In particular, the structure is shown in Figure 3.9.

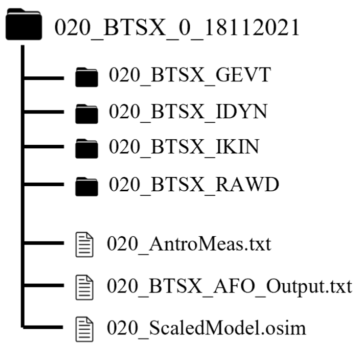

Figure 3.9. Organization of data contained in the folder related to a single experimental session.

The folders *020_BTSX_RAWD* and *020_BTSX_GEVT* are populated with the experimental data acquired using the motion capture system BTS SMART-DX. In detail, the folder name *020_BTSX_RAWD* keeps the information related to the subject ID and the acquisition system, adding the information related to the type of data, in this case *RAWD* stand for *Raw Data*, i.e. the raw data output from the system. In particular, two files for each trial (standing or walking) are exported from the motion capture system: a *.trc* file containing the experimental trajectories of the markers, and a *.mot* file containing the forces and torques registered by the force platforms (this information is not used in this version of the platform). Therefore, the raw data folder contains two file for the single standing trial and two files for each of the walking trials performed during the session, as shown in Figure 3.10.

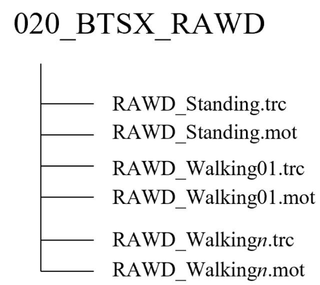

Figure 3.10. Files organization in the raw data folder.

The folder *020_BTSX_GEVT*, contains a series of text files with information about the timing of gait events occurred in the walking trials. These information are eventually useful to frame the signals and analyze the single step or the gait phases within a step. One text file is stored for each walking trial.

The folders identified by the codes *IKIN* and *IDYN* contain the results of the inverse kinematics and inverse dynamics respectively. They are automatically populated by the platform after the processes are run. The inverse kinematics processing produces *.mot* files containing the information about the evolution of the joints angles during the walking trials. The inverse dynamics processing produces *.sto* files regarding the forces and torques calculated on the joints. In both folders, a file for each walking trial is produced.

In the example folder shown in Figure 3.9, the text file *020_AntroMeas.txt* contains the anthropometric measurements collected on the subject, as described in Section3.2.2.

The file *020_BTSX_0_Output.txt* reports parameters from data processing selected to support the custom design of the AFO, a topic that will be further discussed in the following.

Finally, the file *020_ScaledModel.osim* represents the scaled model obtained from the scaling procedure run by the platform.

In future developments the strict structure of folders and subfolders will be transformed in a SQL relationship database, providing major enhancement to the proposed platform.

3.3.2 Selection of Database and Patient

The opening interface of the platform is designed as shown in Figure 3.11. The elements introduced in this interface are numerous and have both functional and aesthetic purposes.

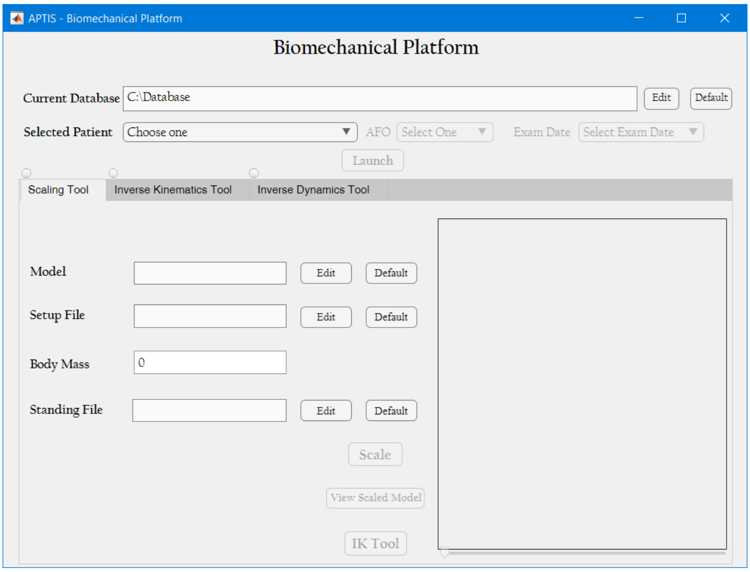

Figure 3.11. Design of the opening interface.

At the top of the interface the title is presented along with other elements for database and subject selection. The database path is specified in a static string, non-editable by the user. Two push buttons have been included to change the database path or to restore the default one. The user is then prompted to select the subject to study using a drop down menu. After the subject is selected, the platform load all data available from the corresponding folder of the database. If more than one session is available, the user selects the one of interest using the other drop down menus.

The first functionality of the platform then concerns the selection of the reference database and, subsequently, the subject on which the processing is run. When the platform opens, a default database is selected that is located within the same directory in which the platform execution files are. The database path is therefore built from the application reference path, so that there are no absolute references that would not allow compatibility of the platform between different users. The database path is then shown in the static textbox located at the top of the interface. These operation are run when the platform is launched, so the corresponding code is placed in the *startupFcn* function.

```
    function startupFcn(app)
        app.databaseText.Value = strcat(cd,'\Database');
        changeDB(app);
    end
```

The first command creates the database path from the current directory path and displays it in the string on the interface. The actual database change is performed by the *changeDB(app)* function that is called in the second line. The function code below shows how this function reads the database path and inserts it into a variable created as an application property (app.dbPath), so it can be used in any function.

```
    function changeDB(app)
        % Load and update database path
        value = app.databaseText.Value{:};
        app.dbPath = value;
        % Read and fill the dropdown menus with available patients
        list = struct2cell(dir(value));
        list = list(1,cell2mat(list(5,:)));
        app.selectPatient.Items = [{'Choose one'},list(1,3:end)];
        % Prompt the user to the starting Scaling Tab
        app.TabGroup.SelectedTab = app.ScalingToolTab;
    end
```

This function also automatically checks within the database for the presence of subject folders and inserts their names as items of the drop down menu for subject selection.
To conclude the discussion about database selection, there are two more buttons in the platform for its management, whose associated code is reported below.

```
    function editDBButtonPushed(app, event)
        app.databaseText.Value = uigetdir();
        changeDB(app);
    end
```

```

    function defaultDBButtonPushed(app, event)
        app.databaseText.Value = strcat(cd,'\Database');
        changeDB(app);
    end
```

The buttons and related functions have intuitive names: the *Edit DB* button allows the user to select an alternative database path, exploiting the *uigetdir* function that opens a dialog box for selecting a folder from file system. The *DefaultDB* button returns to the selection of the default database, repeating the operations performed in the *startupFcn*.

The choice of the database path enables the selection of a subject from the drop down menu. After the subject is selected by the user, the *selectPatientValueChanged* function is called to enable selection of the available biomedical data. In the first part of the function (see code below), the path pointing to the subject folder is built using the item selected from the drop down menu. Within the subject folder, the folder related to the acquisition system of interest for this scenario is then identified, if present. The system identifier described in Section 3.3.1 is used to locate the folders.

```
function selectPatientValueChanged(app, event)
    % Reset platform for new configuration
    cleanScaleTab(app);
    cleanIKTab(app);
    cleanIDTab(app);
    app.afo.Value = app.afo.Items(1);
    app.sessionDate.Value = app.sessionDate.Items(1);
    app.TabGroup.SelectedTab = app.ScalingToolTab;

    % Read available data in the selected patient folder
    value = app.selectPatient.Value;
    patientPath = strcat(app.dbPath,'\',value);
    folders = struct2cell((dir(patientPath)))';
    availableData = folders(cell2mat(folders(:,5)),1);
    availableData = availableData(3:end);

    % Fill dropdown menus with available data
    btsfolder = contains(availableData,'BTSX');
    if any(btsfolder)
        app.afo.Enable = 'on';
        app.btsPath = strcat(patientPath,'\',...
            availableData{btsfolder});
        app.btsTestFolders = struct2cell((dir(app.btsPath)))';
        app.btsAvailableTest = app.btsTestFolders(...
            cell2mat(app.btsTestFolders(:,5)),1);
        app.btsAvailableTest= cell2mat(app.btsAvailableTest(3:end));
        app.btsAfoTest = str2num(app.btsAvailableTest(:,10));
```

```
        app.btsDatesTest = datestr(datevec(...
            app.btsAvailableTest(:,12:end),'ddmmyyyy'));
        app.afo.Items = [{'Select One'}, ...
            app.afoCondition(unique(app.btsAfoTest)+1)];
    end

end
```

In the next part of the function, basing on data available in the subject folder, the second drop down menu is activated allowing the selection of the walking condition (without AFO, with commercial AFO, or with custom AFO). When the desired walking condition is selected, the *afoValueChanged* function is called to enable the drop down menu for the selection of the session to analyse, identified by the date. The drop down menu only shows the available session date for the walking condition selected. The available dates are derived from the name of the folders that identify the experimental sessions.

Once the session is selected, the *LaunchButton* is enabled. The push button event is associated with the *LaunchButtonPushed* function, whose main objective is to perform a check on the files contained in the database for the selected patient and session. In order to perform this check, the database paths are created and updated, using the *createAndUploadPath* function. After that, the available files contained in the folders of each acquisition session are actually counted. The analysis of available data is a drop-down search: first data needed for the scaling phase are checked by the function *scalingControl*; if available, the same function calls the *ikControl* to check data for inverse kinematics; which in turn evokes the *idControl* function to search for data on which the inverse dynamics analysis can be performed. On the basis of the accessible data, the platform is set up by enabling the available functionalities. In particular, the application proposes a light for each processing panel that indicates whether that analysis has already been performed (green), whether it has been partially performed only for a subset of trials (yellow), whether it has not yet been performed on any subject data (red), or whether that tool cannot be performed because it requires preliminary actions (inactive). The user will be automatically taken to the panel of the processing phase to be performed, and all the commands related to it will be activated and, if provided, filled with the available data.

```
function LaunchButtonPushed(app, event)
```

```
    createAndUploadPath(app);
    scalingControl(app);
    % Selection of the model in the 'Resource' folder
    app.modelLoc = strcat(cd,'\Resources','\aptisModel.osim');
    app.model.Value = app.modelLoc(end-14:end);
    % Selection of the setup scale file in the 'Resource' folder
    app.setupScaleLoc=strcat(cd,'\Resources','\aptisSetupScale.xml')
    app.setupScaleFile.Value = app.setupScaleLoc(end-18:end);
```

The last lines load the general model and the setup scale file required in the scaling phase.
A subsequent check is made for the presence of the text file containing the subject's anthropometric measurements. If the file is available in the folder, it is read and the information about the subject's mass is saved for automatic use in subsequent processing.

```
if any(contains(app.sessionAvailableData,'AntroMeas.txt'))
        % Load the anthropometric data from file selected by user
        antroMeasLoc = char(strcat(app.sessionFolders(1,2),'\',...
            app.sessionAvailableData(...
            endsWith(app.sessionAvailableData,'AntroMeas.txt'))));
        antroMeas = antroMeasImport(antroMeasLoc);
        app.bodyMass.Value = str2double(antroMeas(...
            contains(antroMeas(:,1),'Peso'),2));
end
```

Thus, this function is useful in setting up the interface to the following processing stages for the selected subject. The functionalities of the platform will be discussed in more detail below. The discussion will be done following the logical order of its operation, grouping the elements of the platform by macro-functions.

3.3.3 Scaling

The scaling operation is performed by clicking the *scaleButton* button, associated with the *scaleButtonPushed* function, which in turn calls the function *aptisScaling*. This function is reported below.

```
function [scaledModelLoc] = aptisScaling(setupScaleLoc,modelLoc,...
    trcStandingLoc,sessionFolders,bodyMass)
    % Import OpenSim API
    import org.opensim.modeling.*
    % Initialize Model
    model1 = Model(modelLoc);
    model1.initSystem;
    aptisModel = Model(model1);
    aptisModel.initSystem;
```

```
    idPatient = sessionFolders(end-18:end-16);

    % Setup of Scaling procedure
    scTool = ScaleTool(setupScaleLoc);
    scTool.setName(idPatient);
    scTool.setSubjectMass(bodyMass);
    scTool.setPathToSubject('');

    scTool.getGenericModelMaker().setModelFileName(modelLoc);
    scTool.getGenericModelMaker().setMarkerSetFileName(...
        setupScaleLoc);
    scTool.getGenericModelMaker().processModel();

    scTool.getModelScaler().setMarkerFileName(trcStandingLoc);
    scTool.getModelScaler().processModel(aptisModel,'',bodyMass);

    % Load marker traces in Standing acquisition
    motStandingLoc = regexprep(trcStandingLoc,'.trc','.mot');
    scTool.getMarkerPlacer().setCoordinateFileName(motStandingLoc);
    scTool.getMarkerPlacer().setMarkerFileName(trcStandingLoc);
    scTool.getMarkerPlacer().processModel(aptisModel);

    % Set location of the output scaled model
    aptisModel.setName(idPatient);
    scaledModelLoc = strcat(sessionFolders,'\',...
        sessionFolders(end-18:end-8),'ScaledModel.osim');
    scTool.getModelScaler().setOutputModelFileName(scaledModelLoc);

    outfile = ['Setup_IK_',idPatient, '.xml'];
    scaleSetup = fullfile(sessionFolders, outfile);
    scTool.print(scaleSetup);

    % Run scaling tool
    scTool.run();
end
```

The first command, *import org.opensim.modeling**, is needed to import OpenSim API. In the first part of the script, the *aptisModel* object is created, on which the scaling operation is then performed. The *scTool* object is then created, which has as input the generic setup file loaded into the platform and passed as input to the MATLAB function. The generic setup for scaling is uploaded with subject-related information, such as the total mass, the subject ID and marker traces collected during the standing trial. The last lines of code allow the scaling of the model and the saving, in '.osim' format, in the designed path inside the database.

Once the scaling has been performed and the subject-specific scaled model is obtained, clicking the *ViewScaledModelButton* the scaled model is shown in the axes element present in the Scaling tab of the platform. The button is associated to the *ViewScaledModelButtonPushed* function.

```
function ViewScaledModelButtonPushed(app, event)
    %Set up the plot and slider for visualization
    app.FrameSlider.Enable = 'on';
    % Read trc marker trajectories in standing trial
    [app.RAWD_Standing,app.marker] = trcReading(app.trcStandingLoc);
    app.FrameSlider.Limits = [1 size(app.RAWD_Standing,3)];
    frame = round(app.FrameSlider.Value);
    % Build the MATLAB matrix to plot markers and visualize model
    [plotMatrix] = matrixToPlot(app.RAWD_Standing,app.marker,frame);
    plot3(app.plotScaledModel,plotMatrix(:,3),plotMatrix(:,2),...
        plotMatrix(:,1),'o-','MarkerFaceColor','r','Color','k')
    axis (app.plotScaledModel,'equal')
end
```

The slider element is first activated, allowing the user to move along the time frames that make up the entire duration of the acquisition. Then, the *trcReading* function is called. This function was generated by exploiting the *Import Data MATLAB toolbox* and allows the file produced by the BTS system to be read automatically. That file has extension *.trc* and presents the structure discussed in Section 3.2.3. In order to display the markers and the stick model, the *matrixToPlot* function was used, which performs a substantial rearrangement of the markers so that they can be plotted in the correct order and with the right mutual links. The last aspect of the visualisation concerns the slider that allows switching between frames of the acquisition. This is done with a call to the function *FrameSliderValueChanged*, reported below. When the user changes the position of the slider, the plot is updated showing the corresponding time frame.

```
function FrameSliderValueChanged(app, event)
    % Refresh plot when the slider is moved
    frame = round(app.FrameSlider.Value);
    [plotMatrix] = matrixToPlot(app.RAWD_Standing,app.marker,frame);
    plot3(app.plotScaledModel,plotMatrix(:,1),plotMatrix(:,2),...
        plotMatrix(:,3),'o-','MarkerFaceColor','r','Color','k');
    axis (app.plotScaledModel,'equal')
end
```

3.3.4 Inverse Kinematics

The second processing phase implemented in the application is the inverse kinematics. The design of the tab dedicated to this operation is shown in Figure 3.12.

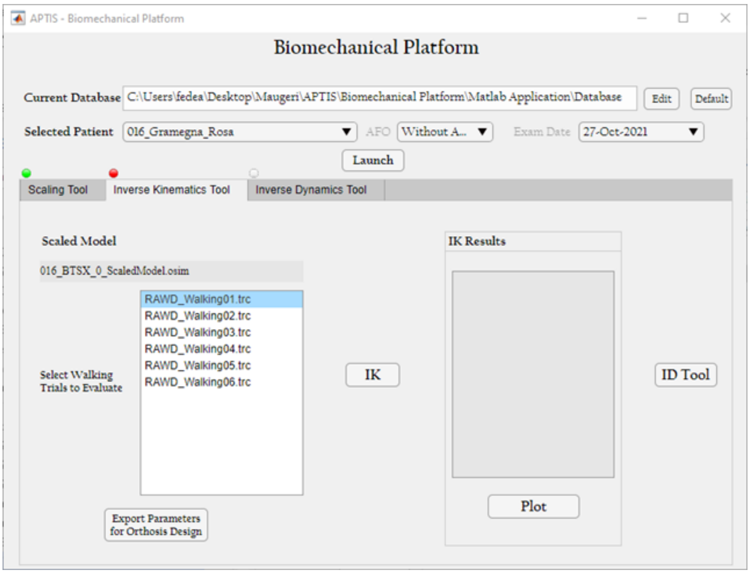

Figure 3.12. Design of the inverse kinematics tab.

A first label-type element reports the scaled model of the subject on which the inverse kinematics is performed. Below this, a dedicated box lists the '.trc' files related to the walking trials performed by the subject, available in the Raw Data folder, and thus ready for the inverse kinematics operation. The user has the possibility to make a multiselection of items in order to simultaneously perform the inverse kinematics operation on all available files. Once the items in the list have been selected, clicking the *IK* button, the *aptisInverseKinematic* function is called. The code of the function is reported below. The function allows the inverse kinematics operation to be performed on the walking trials selected by the user from the list presented in the application. This operation is performed starting from the scaled model, which is passed as input, along with the path to the marker data of the selected walking trials. The last two inputs are necessary for the construction of the path in which to save the '.mot' files generated by the processing.

The first line of code imports the libraries that exploit the OpenSim classes. The *ikTool* object is then created, which, with its associated methods, allows all the necessary operations to be performed. In the next line of code, the scaled model to be taken as a reference is set and initialized.

An iterative loop is then implemented in the function to repeat the inverse kinematics operations for each of the walking trials selected. Within the for loop, the marker data file related to the selected trial is selected, the start and end times of the trial are extracted, and the path for saving the output file is defined. The *for* loop closes with the execution of the inverse kinematics for the single walking trial.

```
function [ikModelLoc,initialTime,finalTime]=aptisInverseKinematic...
    (setupScaleLoc,scaledModelLoc,walkingTrials,ikFolder,rawFolder)
    % Include OpenSim API
    import org.opensim.modeling.*
    % Set up Inverse Kinematic Tool
    ikTool = InverseKinematicsTool(setupScaleLoc);
    model = Model(scaledModelLoc);
    model.initSystem();
    % Load dynamic trials
    idPatient = ikFolder(end-12:end-10);
    ikTool.setModel(model);
    nTrials = length(walkingTrials);
    % Run Inverse kinematic for each dynamic trial
      for trial = 1:nTrials
        markerFile = walkingTrials{trial};
        walkingPath = strcat(rawFolder,'\',markerFile);
        markerData = MarkerData(walkingPath);
        initialTime = markerData.getStartFrameTime();
        finalTime = markerData.getLastFrameTime();
        ikTool.setName(strcat(idPatient,'_',markerFile(6:end-4)));
        ikTool.setMarkerDataFileName(walkingPath);
        ikTool.setStartTime(initialTime);
        ikTool.setEndTime(finalTime);
        ikModelLoc = strcat(ikFolder, '\IKIN_',...
        markerFile(6:end-4),'.mot');
        ikTool.setOutputMotionFileName(ikModelLoc);
        ikTool.run();
    end
end
```

The paths of the results file are passed as output of the function so that they can then be listed in the second component list, on the right part of the application tab (see Figure 3.12. The user can now proceed in two ways: perform the inverse dynamics operation on these outputs, or visualize and analyze the inverse kinematics results graphically. The latter possibility can be accessed by selecting one of the listed resulting files and clicking the *Plot* button. This button opens a new window, where the plotting tool is implemented. The design of this application tool is shown in Figure 3.13.

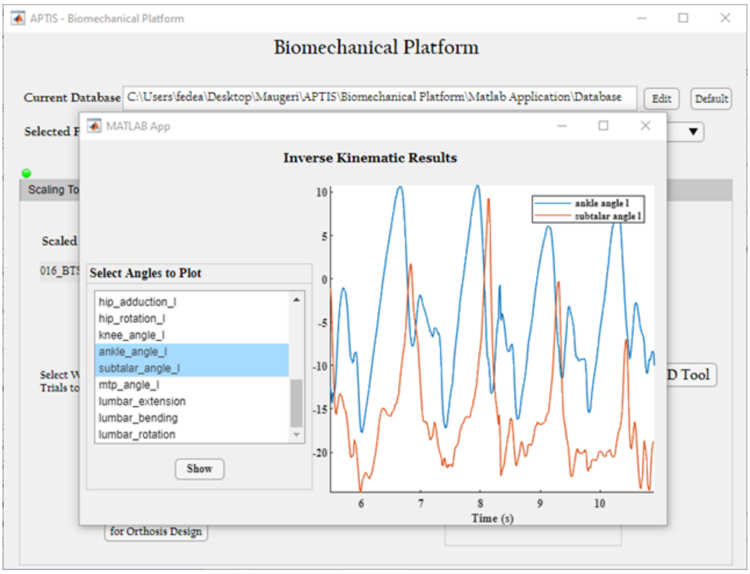

Figure 3.13. Design of the plot tool for Inverse Kinematics results.

The window presents a box that lists all the lower limb joints angles resulting from the inverse kinematics. The values are read from the *.mot* files created as output of the inverse kinematics and stored in the corresponding folder. The tool is implemented as a separate Matlab application, so the set up operation are run in the *startup* function.

```
function startupFcn(app, mainapp, selectedMotFile)
    app.CallingApp = mainapp;
    % Load the selected results file
    app.selectedMotFile = selectedMotFile;
    app.anglesData = dataReading(app.selectedMotFile);
    app.anglesList.Items =...
        app.anglesData.Properties.VariableNames(2:end);
    app.anglesList.Multiselect = 'on';
end
```

The user can select one or more angles of interest, and clicking the *Show* button, associated with the *ShowButtonPushed* function, the data are plotted with the corresponding legend.

```
function ShowButtonPushed(app, event)
    plot(app.plotFigure,app.anglesData{:,1},...
        app.anglesData{:,app.anglesList.Value});
    legend(app.plotFigure,strrep(app.anglesList.Value,'_',' '));
    axis(app.plotFigure,"tight")
end
```

Closing the app the user is reported to the main application to continue the analysis. Here, by clicking the *IDTool* button, the next tab is opened allowing the Inverse Dynamics operation.

3.3.5 Inverse Dynamics

The third tool implemented is the inverse dynamics tool, developed in a dedicated tab with the design presented in Figure 3.14.

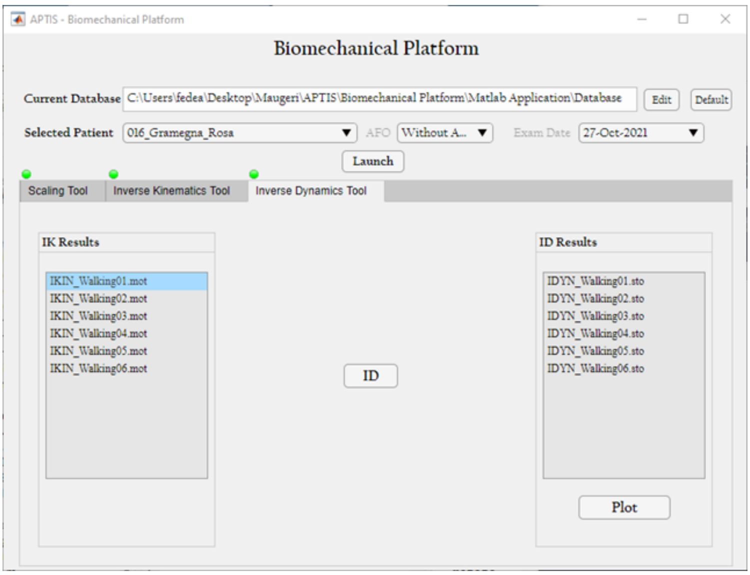

Figure 3.14. Design of the inverse dynamics tab.

The structure is simple, an initial list component reports the kinematic data files resulting from the previous analysis. The user can make a single or multi-selection of the available data on which performing the inverse dynamics. Once the items in the list have been selected, clicking the *ID* button the *aptisInverseDynamic* function is called.

```matlab
function [idModelLoc] = aptisInverseDynamic(scaledModelLoc,...
    selectedMotFile,idFolder,ikFolder,rawFolder,...
    initialTime,finalTime)
    % Include OpenSim API
    import org.opensim.modeling.*
    % Set up model and inverse dynamics tool
    scaledModel = Model(scaledModelLoc);
    idTool = InverseDynamicsTool();
    idTool.setModel(scaledModel);
    nTrials = length(selectedMotFile);
    idPatient = idFolder(end-12:end-10);
    % Load and process each single dynamic trial selected
    for trial = 1:nTrials
        motFile = selectedMotFile{trial};
        idTool.setCoordinatesFileName(strcat(ikFolder,'\',motFile));
        kinematicFilterFrequency = 6;
        idTool.setLowpassCutoffFrequency(kinematicFilterFrequency);
        % Build the output path
        idModelLoc = strcat(idFolder, '\IDYN_',...
            motFile(6:end-4),'.sto');
        idTool.setResultsDir(idFolder);
        idTool.setOutputGenForceFileName(strcat('\IDYN_',...
            motFile(6:end-4),'.sto'));
        if nargin <6
            walkingPath = strcat(rawFolder,'\',...
                regexprep(motFile,{'IKIN','.mot'},{'RAWD','.trc'}));
            markerData = MarkerData(walkingPath);
            % Load the time series
            initialTime = markerData.getStartFrameTime();
            finalTime = markerData.getLastFrameTime();
        end
        idTool.setStartTime(initialTime);
        idTool.setEndTime(finalTime);
        excludedForces = ArrayStr();
        excludedForces.append('Muscles');
        idTool.setExcludedForces(excludedForces);
        % Run inverse dynamics
        idTool.run();
    end
end
```

The function performs the inverse dynamics operation on the kinematic data selected by the user in the list presented in the application. Again, the operation must be performed on the basis of a model, so the inputs of the function are represented by the selected *'.mot'* files and also by the path to the reference scaled model. The other inputs are the paths to the subject's folders in the database.

The first line of code imports the libraries that exploit the OpenSim classes. The *idTool* object is then created, which, with its associated methods, allows all the necessary operations to be performed. In the next line of code, the scaled model to be taken as a reference is set and initialized.

An iterative loop is then implemented in the function to repeat the inverse dynamics operations for each of the kinematic data file selected. Within the for loop, the kinematic data are loaded and filtered with a 6 Hz lowpass filter. The start and end times of the trials are extracted, and the path for saving the output file is defined. It is then defined that no external force is acting on the subject. The *for* loop closes with the execution of the inverse kinematics for each single walking trial.

The results of the inverse dynamics represent the forces and torques calculated on the lower limbs joint. The list of the analyzed walking trials is reported in the second component list, on the right part of the application tab (see Figure 3.14. Also in this case the user can exploit the visualization tool to plot and analyze the inverse dynamics results (the description of the tool is reported at the end of the Section 3.3.4).

3.3.6 Export Tool

An additional feature of the platform involves the option of exporting a set of biomechanical-anthropometric information that may be of interest in supporting the design of custom orthoses. The Export Tool is is available in the Inverse Kinematics panel, because it acts on the kinematic data resulting from this operation. It is launched by clicking the 'Export Parameters for Orthosis Design' button. The tool was developed as a stand-alone application, which is called in the function related to the button just mentioned. The design scheme of the Export Tool is shown in Figure 3.15.

The structure of the interface is very simple: on the left side there is a list-box that displays the processed walking trials, on which the processing steps to calculate the exportable parameters can be performed. A central button (*Evaluate*) launches the processing, while in the right part a set of check-boxes allows the user to select the parameters to export. In the same panel the *Launch* button allows the finalization of the export.
When the export tool is launched, the list of available kinematic data is filled with the trials actually processed. This information is obtained from the main application calling the export tool. In order to transfer the MATLAB variables to the new interface, these information are passed

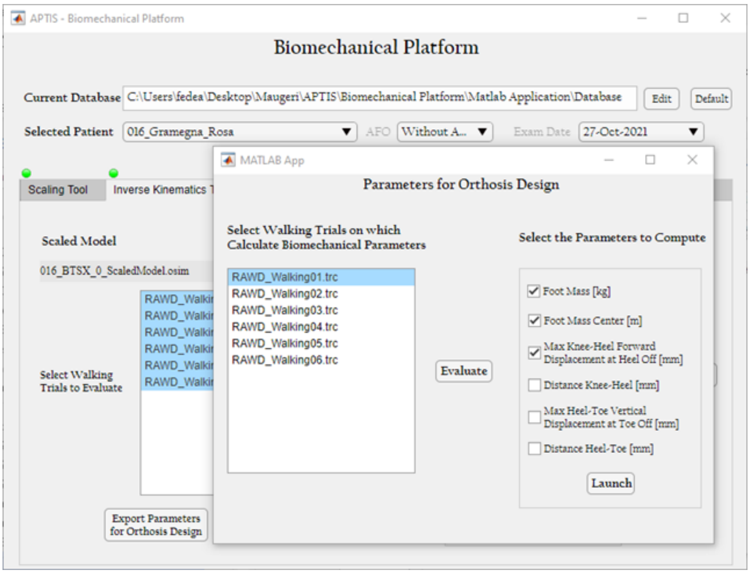

Figure 3.15. Design of the export tool.

as inputs of the start-up function of the export tool application. In this function all the elements of the window are configured for the use.

```
function startupFcn(app, mainapp, scaledModelLoc, rawFolder,...
    rawFolderContents, afoConditionExp)
    app.CallingApp = mainapp;
    % Disable check-box if no trial is selected
    app.FootMasskgCheckBox.Enable = 'off';
    app.FootMassCentermCheckBox.Enable = 'off';
    app.MaxKneeHeelForwardDisplacementatHeelOffmmCheckBox.Enable...
        = 'off';
    app.DistanceKneeHeelmmCheckBox.Enable = 'off';
    app.MaxHeelToeVerticalDisplacementatToeOffmmCheckBox.Enable =...
        'off';
    app.DistanceHeelToemmCheckBox.Enable = 'off';

    % Load folders location and user selection
    app.scaledModelLoc = scaledModelLoc;
    app.rawFolder = rawFolder;
    app.rawFolderContents = rawFolderContents;
    app.afoConditionExp = afoConditionExp;
    % Load walking trials
    app.walkingTrials.Items = app.rawFolderContents(...
        contains(app.rawFolderContents(:,1),'.trc') &...
        contains(app.rawFolderContents(:,1),'Walk'));
```

```
    % Allow selection of the walking trials
    app.walkingTrials.Multiselect = 'on';
end
```

The check-boxes are disabled: they will be enabled just after a walking trial is selected and processed. The listbox is filled with the available kinematic data trials. The last command enables multiple choice of items in the listbox, since, as will be seen below, it will also be possible to select multiple trials on which to launch the processing and export tasks.
The *Evaluate* button has no real processing purpose. It only confirms the selection of trials by activating the check-boxes useful for the export phase, as can be argued from the code expressed in the associated callback *EvaluateButtonPushed*.

```
function EvaluateButtonPushed(app, event)
    cleanCheckBox(app)
    % Enable selection of check boxes
    app.FootMasskgCheckBox.Enable = 'on';
    app.FootMassCentermCheckBox.Enable = 'on';
    app.MaxKneeHeelForwardDisplacementatHeelOffmmCheckBox.Enable...
        = 'on';
    app.DistanceKneeHeelmmCheckBox.Enable = 'on';
    app.MaxHeelToeVerticalDisplacementatToeOffmmCheckBox.Enable =...
        'on';
    app.DistanceHeelToemmCheckBox.Enable = 'on';
end
```

After the user has selected the check-boxes of interest, the *Launch* button runs the processing of the kinematic data and creates the export text file. The function *LaunchButtonPushed* is the callback associated with the button: the information selected by the user in the interface (trials to be analyzed and parameters to be exported) are obtained and then transferred to the *parametersForModelling* function that develops all the processing and export tools.

```
function LaunchButtonPushed(app, event)
    % Read the selected items by user
    parametersSelected.footMass = app.FootMasskgCheckBox.Value;
    parametersSelected.footMassCenter =...
        app.FootMassCentermCheckBox.Value;
    parametersSelected.maxKneeHeelForwardDisplacementHO =...
        app.MaxKneeHeelForwardDisplacementatHeelOffmmCheckBox.Value;
    parametersSelected.distanceKneeHeel =...
        app.DistanceKneeHeelmmCheckBox.Value;
    parametersSelected.maxHeelToeVerticalDisplacementTO =...
        app.MaxHeelToeVerticalDisplacementatToeOffmmCheckBox.Value;
    parametersSelected.distanceHeelToe =...
```

```
            app.DistanceHeelToemmCheckBox.Value;
        rowNames = {'footMass','footMassCenter',...
            'maxKneeHeelForwardDisplacementHO',...
            'distanceKneeHeel','maxHeelToeVerticalDisplacementTO',...
            'distanceHeelToe'};

        %Call function to calculate and export parameters
        parametersForModelling(app.scaledModelLoc,...
            app.walkingTrials.Value,app.rawFolder,...
            app.afoConditionExp,parametersSelected);
        % Close window
        delete(app)
    end
```

In the *parametersForModelling* function, the biomechanical scaled model of the subject and the files containing the coordinates of the markers related to the selected walking trials are first imported. From the model, the anthropometric information are obtained: the mass and position of the center of gravity of the foot. Since in the model the foot is the combination of the bodies calcaneus (*calcn*) and toes (*toes*), the total mass will be determined as the sum of the masses while the center of gravity as a combination of the centers of mass of the two bodies. The code that implements the processing is the following.

```
% Calculate foot mass and center of mass as combination of single
    components
footMass_L = calcnMass_L + toesMass_L;
footMass_R = calcnMass_R + toesMass_R;
footBarTot_L = (calcnMass_L*calnBar_L+toesMass_L*toesBarGlob_L)./...
    footMass_L;
footBarTot_R = (calcnMass_R*calnBar_R+toesMass_R*toesBarGlob_R)./...
    footMass_R;
```

Biomechanical and kinematic parameters are then calculated, which are determined from the relative positions of the markers at specific events of the gait cycle, such as heel-off or toe-off. In particular, it was found interesting to focus on the displacement between the knee and heel at the heel-off event, in order to estimate the maximum advancement of the tibia with respect to the heel when the heel is still in contact with the ground. The other parameter is the vertical displacement between the heel and metatarsal bones at the toe-off event, in order to estimate the maximum vertical deformation of the orthosis when the metatarsal bones are in contact with the ground. These two events are considered because they represent the phases when the orthosis would be most stressed. Therefore, as will be seen below, the measured displacements will be used to test whether the designed orthosis can tolerate these deformations.

These parameters are calculated for all walking trials considered and for all steps detected in the walking trial. This is implemented with a double for loop (see code below). Among all the values calculated, the maximum value is selected and exported, as the data will be used as stresses for validation of the static structure of the orthosis, which will be obviously done in the worst case of maximum deformation.

```
for trial = 1:nTrials
    % Load folder paths and import markers traces
    walkingTrial = walkingTrials{trial};
    walkingTrcLoc = strcat(rawFolder,'\',walkingTrial);
    walkingTrc = importFileData(walkingTrcLoc);
    emtLoc = strcat(regexprep(rawFolder,'RAWD','GEVT'),...
        '\GEVT_',walkingTrial(6:end-4),'.emt');
    [gaitEvents,HeelStrikeR,HeelStrikeL,ToeOffTimeL,ToeOffTimeR]...
        = importFileEmt(emtLoc,walkingTrc);
    % Filter marker traces
    banda=70/2;
    cutoff=5;
    [b,a] = butter(5,cutoff/banda);
    rheel_y_filt = filtfilt(b,a,walkingTrc.rheel_y);
    rmet_y_filt = filtfilt(b,a,walkingTrc.rmet_y);
    lheel_y_filt = filtfilt(b,a,walkingTrc.rheel_y);
    lmet_y_filt = filtfilt(b,a,walkingTrc.rmet_y);

    % Find distances between markers
    tibiaDisplacement_R = walkingTrc.rknee2_x - walkingTrc.rheel_x;
    tibiaDisplacementHO_R = tibiaDisplacement_R(idxHeelOff_R);
    rkneePos = [walkingTrc.rknee2_x,walkingTrc.rknee2_y,...
        walkingTrc.rknee2_z];
    rheelPos = [walkingTrc.rheel_x,walkingTrc.rheel_y,...
        walkingTrc.rheel_z];
    dist_R = mean(vecnorm(rkneePos-rheelPos,2,2));
    tibiaDisplacement_L = walkingTrc.lknee2_x - walkingTrc.lheel_x;
    tibiaDisplacementHO_L = tibiaDisplacement_L(idxHeelOff_L);

    lkneePos = [walkingTrc.lknee2_x,walkingTrc.lknee2_y,...
        walkingTrc.lknee2_z];
    lheelPos = [walkingTrc.lheel_x,walkingTrc.lheel_y,...
        walkingTrc.lheel_z];
    dist_L = mean(vecnorm(lkneePos-lheelPos,2,2));
    toeDisplacement_R = walkingTrc.rheel_y - walkingTrc.rmet_y;
    toeDisplacementTO_R = toeDisplacement_R(idxToeOff_R);
    rToePos = [walkingTrc.rmet_x,walkingTrc.rmet_y,...
        walkingTrc.rmet_z];
    distHeelToe_R = mean(vecnorm(rheelPos-rToePos,2,2));
    toeDisplacement_L = walkingTrc.lheel_y - walkingTrc.lmet_y;
```

```
    toeDisplacementTO_L = toeDisplacement_L(idxToeOff_L);
    lToePos = [walkingTrc.lmet_x,walkingTrc.lmet_y,...
        walkingTrc.lmet_z];
    distHeelToe_L = mean(vecnorm(lheelPos-lToePos,2,2));
end
```

Finally, the function writes the parameters thus determined into a text file that will be automatically saved inside the folder related to the analyzed session, with the name *ID_BTSX_AFO_Output.txt* according to the database structure (e.g. *020_BTSX_0_Output.txt*). The output file will report only the parameters selected by the user. The code that implements this functionality is reported below.

```
% Build structure to write output file
parametersName = {'Mass'; 'Mass Center';...
    'Max Knee-Heel Forward Displacement at Heel Off';...
    'Distance Knee-Heel';...
    'Max Heel-Toe Vertical Displacement at Toe Off';...
    'Distance Heel-Toe'};
right = {footMass_R; footBarTot_R; tibiaDisplacementHO_R; dist_R;...
    toeDisplacementTO_R; distHeelToe_R};
left = {footMass_L; footBarTot_L; tibiaDisplacementHO_L; dist_L;...
    toeDisplacementTO_L; distHeelToe_L};
% Build header of the output textual file
header_R = ['Right Foot \nMass [kg]:\t%5.3f\n',...
    'Mass Center [m]:\t%5.3f\t%5.3f\t%5.3f\n',...
    'Max Knee-Heel Forward Displacement at Heel Off [mm]:\t%i\n',...
    'Distance Knee-Heel[mm]:\t%i\n',...
    'Max Heel-Toe Vertical Displacement at Toe Off [mm]:\t%i\n',...
    'Distance Heel-Toe[mm]:\t%i\n\n'];
header_L = ['Left Foot \nMass [kg]:\t%5.3f\n',...
    'Mass Center [m]:\t%5.3f\t%5.3f\t%5.3f\n',...
    'Max Knee-Heel Forward Displacement at Heel Off [mm]:\t%i\n',...
    'Distance Knee-Heel[mm]:\t%i\n',...
    'Max Heel-Toe Vertical Displacement at Toe Off [mm]:\t%i\n',...
    'Distance Heel-Toe[mm]:\t%i\n\n'];
% Open File with writing permission
fileID = fopen(strcat(scaledModelLoc(1:end-28),...
    '\',idPatient,'_BTSX_',indAfo,'_Output.txt'),'w');
% Print file contents
fprintf(fileID,header_R,footMass_R*parametersSelected.footMass,...
    footBarTot_R*parametersSelected.footMassCenter,...
    round(max(tibiaDisplacementHO_R))*...
    parametersSelected.maxKneeHeelForwardDisplacementHO,...
    round(dist_R)*parametersSelected.distanceKneeHeel,...
    round(max(toeDisplacementTO_R))*...
    parametersSelected.maxHeelToeVerticalDisplacementTO,...
    round(distHeelToe_R)*parametersSelected.distanceHeelToe);
fprintf(fileID,header_L,footMass_L*parametersSelected.footMass,...
    footBarTot_L*parametersSelected.footMassCenter,...
```

```
    round(max(tibiaDisplacementHO_L))*...
    parametersSelected.maxKneeHeelForwardDisplacementHO,...
    round(dist_L)*parametersSelected.distanceKneeHeel,...
    round(max(toeDisplacementTO_L))*...
    parametersSelected.maxHeelToeVerticalDisplacementTO,...
    round(distHeelToe_L)*parametersSelected.distanceHeelToe);
% Close file
fclose(fileID);
```

In Figure 3.16 an example of the output of the export tool is shown. It reports all the parameters selected to support the design of custom AFO.

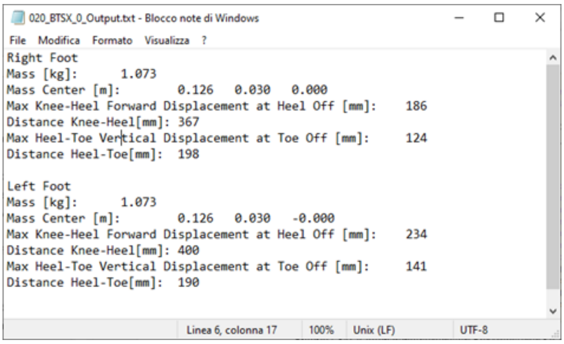

020_BTSX_0_Output.txt - Blocco note di Windows

File Modifica Formato Visualizza ?

```
Right Foot
Mass [kg]:      1.073
Mass Center [m]:        0.126   0.030   0.000
Max Knee-Heel Forward Displacement at Heel Off [mm]:    186
Distance Knee-Heel[mm]: 367
Max Heel-Toe Vertical Displacement at Toe Off [mm]:     124
Distance Heel-Toe[mm]:  198

Left Foot
Mass [kg]:      1.073
Mass Center [m]:        0.126   0.030   -0.000
Max Knee-Heel Forward Displacement at Heel Off [mm]:    234
Distance Knee-Heel[mm]: 400
Max Heel-Toe Vertical Displacement at Toe Off [mm]:     141
Distance Heel-Toe[mm]:  190
```

Linea 6, colonna 17 | 100% | Unix (LF) | UTF-8

Figure 3.16. Output file of the export tool reporting the parameters used to support the design of custom AFO.

3.4 Applications

The major application of the developed platform is to support the orthopaedic technician in the design of a patient-specific orthosis, with information that can improve the standard designing and realization processes. However another application is represented by the biomechanical analysis of gait. The platform offers the user all the tools to specifically analyse the kinematics and dynamics of the single body districts constituting the lower limbs. In this perspective, it can be used as a gait analysis tool to investigate interesting aspects of the lower limbs biomechanics. In this section, examples and more details on possible applications are provided, starting with the main focus of this research and continuing with alternative implementation used for clinical and scientific purposes.

3.4.1 Support to Ankle-Foot-Orthosis Design

The biomechanical platform described in the previous Section is part of wider project aimed at improving the processes of design and realization of custom orthosis. The Figure 3.17 shows a simplified scheme explaining how the platform is integrated in the development process of the orthosis.

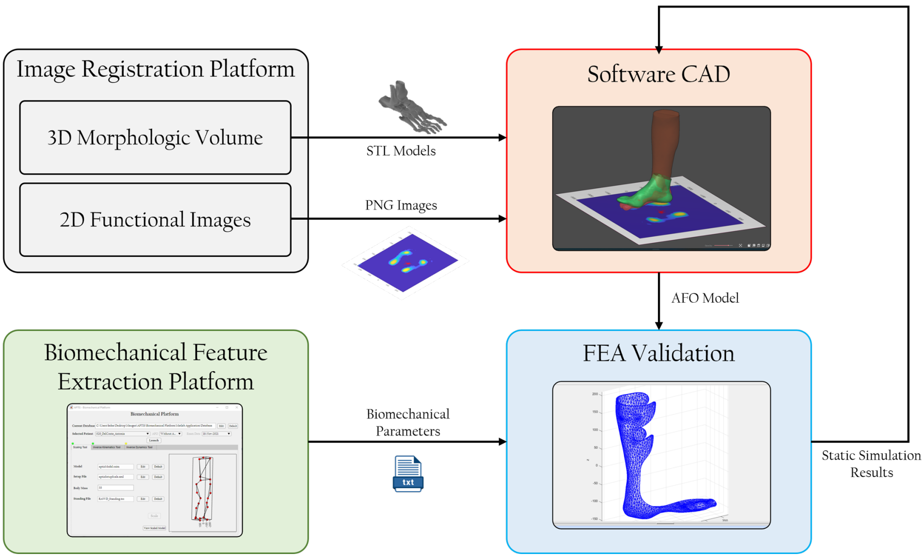

Figure 3.17. Schematic process diagram showing the relationships between the tools used to design and develop a custom AFO.

The Image Registration platform is an application that allows to merge morphological and functional information about the patient. These information are provided as three-dimensional structures, bi-dimensional images and graphs, in order to be imported in the Computer Aided Design (CAD) environment to support and improve the modelling of the custom orthosis.

In particular the Image Registration platform can produce 3D models (*.stl*) representing the internal structure and/or the external surface of the analysed limb, exploiting data from imaging techniques, such as Computed Tomography or Magnetic Resonance Imaging. Models developed with this techniques are more accurate than those obtained by 3D scanning, which is the technique usually used to create a 3D model of the body segment. Moreover the Image Registration platform provides, through clinical imaging techniques, information about internal bone structures that 3D scanning cannot give. This is useful as can highlight any deformity to be taken into account in the development of the orthotic device.

The Image Registration platform also enables the processing of diagnostic-functional biomedical images and data. In particular the platform allows to combine data gathered from a sensorized baropodometric platform and a stabilometric-proprioceptive system. The combined information reports the plantar map that details the pressures at each point of foot plant, along with a trace of the body's Center of Pressure (COP) at the ground during the execution of static or dynamic trials. The functional data are also imported in the CAD environment and help the designer in developing a structure that compensate for incorrect pressure distributions identified in the orthostatic position or in specific gait cycle events.

In Figure 3.18 an example of 3D model of the foot internal structure and a 2D representation of plantar pressures and COP exported from the Image Registration Platform are reported. It is also shown how they are imported in the CAD environment to support the design of the orthosis.

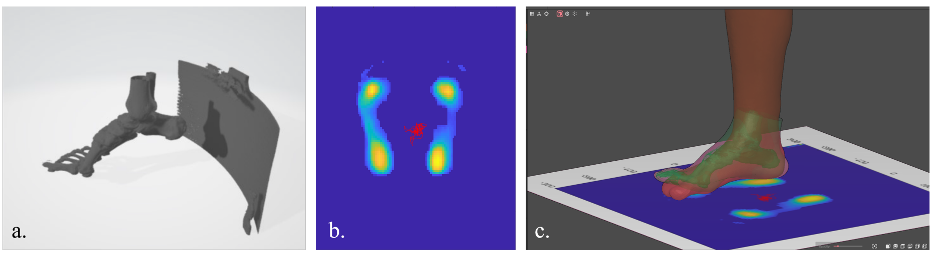

Figure 3.18. Morphological and functional data to support AFO design: a. 3D model of the internal foot structure; b. plantar pressure map and COP evolution in orthostatic trial; c. integration of data in CAD environment for AFO design.

In parallel, the Biomechanical platform, operating on the customized models and gait analysis data, produces biomechanical and anthropometric data used to validate the CAD mechanical design of the orthosis, to verify its stability under the loading and deformation applied during normal use by the subject. This operation, which can be performed using

Finite Element Analysis (FEA), represents an innovative step to verify the load capacity of the designed structure before its actual fabrication. The results of the analysis, in an iterative manner, will be useful in identifying corrective actions to be achieved in the design of the orthotic device.

The workflow briefly described can be of much broader significance than the single case of AFO design, as it can be a support in the production of any type of orthosis, brace or prosthesis.

In the following section the application of the biomechanical platform will be detailed, exploring the chosen parameters and how they are used in the process of validation of the device structure.

Biomechanical Parameters from Gait Analysis

The Biomechanical platform is based on biomechanical models customised for individual patients to evaluate kinematics and dynamics starting from data acquired during walking trials. The kinematic gait analysis, in conjunction with anthropometric and biomechanical information, can be relevant to identify the stresses and deformations that the orthosis may experience during the use. These data, therefore, can be the starting boundary conditions for the FEA of orthosis structure.
In the numerical analysis, it is considered significant to analyse the distribution of stresses over the orthosis at two separate moments that are considered most critical for specific areas of the brace:

- Heel-Off: it is the gait event at which the heel area of the orthosis is assumed to be more affected by bending moment than in the other phases of gait, since at the instant just before heel-off, the tibia is moved to the maximum displacement in forward direction with respect to the heel itself, which remains in contact with the ground.

- Toe-Off: it is the gait event at which the metatarsal area of the brace is assumed to be more affected by bending moment than in the other phases of gait, because at the moment just before the toe-off, the heel is moved to the maximum displacement in the vertical direction with respect to the metatarsals, which remain in contact to the ground.

These values represent the deformations the orthosis undergoes during the walking phases, therefore they have particular relevance for improving the design process. As seen in previous Section, a tool for the export of these information has been developed within the Biomechanical platform. The processing of data is automatic and can involve a single walking trial or a set of multiple trials. In the first case the exported data represent the maximum values of displacement recorded among the different steps taken within the walking test. In the second case, the maximum value is extracted from all steps of all selected walking trials.

The displacement values are determined as the difference in position on the reference axes of markers proximal to the landmarks of interest. The first value of interest concerns the displacement in the direction of gait between the marker positioned on the side of the knee and the one positioned on the back of the heel at the instant when the heel leaves the ground (heel-off). Figure 3.19 shows the positions of the two considered markers.

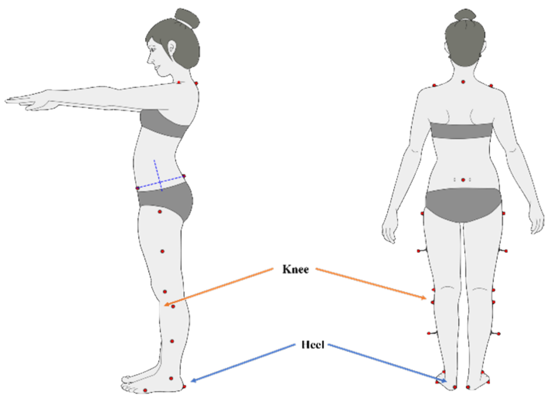

Figure 3.19. Position of the markers used to calculate the forward displacement of the knee with respect to the heel in walking trials.

The second value of interest is determined as the displacement in the vertical direction, between the marker positioned on the back of the heel and the one positioned on the lateral side of the fifth metatarsal bone at the gait phase in which the metatarsals leave the ground (toe-off). Figure 3.20 shows the positions of the two markers considered for the calculation.

Another anthropometric-biomechanical information considered of interest in the design of the orthosis is the weight of the body segment of

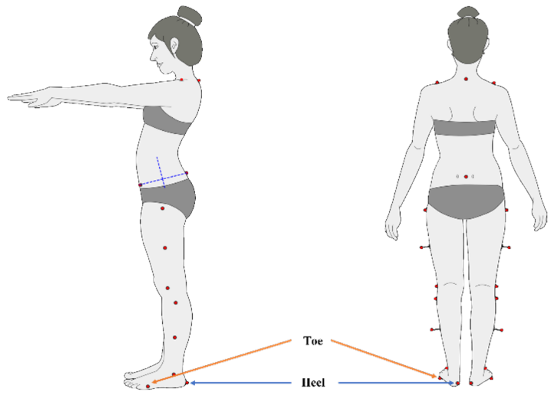

Figure 3.20. Position of the markers used to calculate the vertical displacement of the heel with respect to the metatarsal bones in walking trials.

the foot and the position of the center of gravity. These data can allow an initial estimate of the bending moment on the ankle, thus identifying, as a first approximation, the most suitable material and thickness to be used to produce the orthosis in order to provide the mechanical strength to support the weight of the foot during the flight phase. These data can also be exported from the Biomechanical platform through simple processing. Specifically, the foot body segment, in the biomechanical model considered, is composed of two bodies, calcaneus (calcn) and toes (toes). Therefore, the mass of the foot is determined as the sum of the masses of the two bodies in the subject-specific scaled model. The center of mass is obtained by combining the centers of mass of the two bodies. The parameters are exported in a text file, with the structure shown in Figure 3.16, in order to be used in the FEA.

Finite Element Analysis for AFO Structure Validation

The MATLAB software tool FEATool Multiphysics was used to perform the FEA on the orthosis structure.

As a first step, three areas are defined in the MeshMixer environment on the orthosis, where the constraining conditions will be set during the FEA. The areas are: proximal soleus, heel, and metatarsal area (Figure 3.21).

The *.stl* model of the AFO is then imported in MATLAB and the mesh

Figure 3.21. The three areas defined to apply the constraints in FEA.

grid for the analysis is created. The grid size value is chosen to generate a sufficiently accurate grid without excessively increasing the computational cost of the process (Figure 3.22 an example of the generated grid mesh).

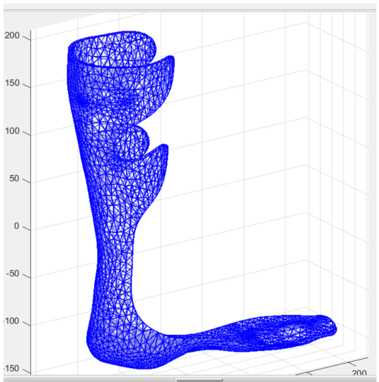

Figure 3.22. Grid generated on the model to perform FEA.

Then the values characterizing the material to be used are set. The values of interest are the elastic modulus, the density and the Poisson's ratio, which are retrieved from data sheets and mechanical tests performed on the materials.

The areas previously defined are now exploited to set the displacement constraints on the edge. These conditions are those obtained from the Biomechanical platform described above. To determine the correct offset value to be set on the brace edges, basic trigonometric formulas were used, specifically concerning similar triangles identified between the gait markers and the brace edges.

The FEA is then run in stationary conditions. In Figure 3.23 an example of results is shown. Results are plot in terms of Von-Mises Stress, used to identify the stress combinations that cause yielding [38]. The visualization shows the range map of the parameter values displayed using a colorimetric scale. In order to verify the structure, it is necessary to control that the maximum Von-Mises stress value from FEA is lower than the Tensile Strength value of the material.

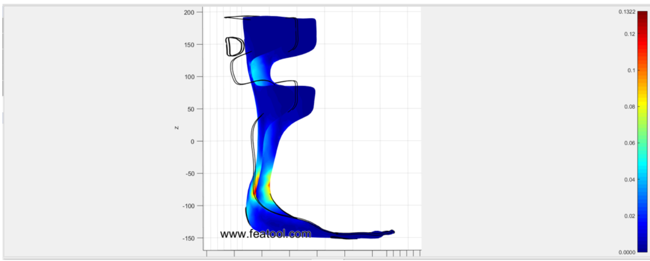

Figure 3.23. An example of the results of FEA simulation, obtained with displacement constraints gathered from the biomechanical analysis. Results are shown in terms of Von-Mises stress.

3.5 Other Applications in Gait Analysis

In this section it is reported another application of the methods previously described. It is about the biomechanical study of gait, in particular the aim was to determine the impact of the use of a commercial AFO on a group of patients suffering the FD syndrome. The procedures deployed provided a detailed analysis of the joint angles of greatest interest for the considered disease.

3.5.1 Background

Gait analysis is a powerful tool to study the level of the impairment and quantify the improvements in walking abilities related to rehabilitation treatments or a specific factor under analysis. The usual spatio-temporal gait analysis performed with the widespread clinical systems allows to describe the general walking pattern of subjects, usually enabling to discover specific features or deviations from the physiological gait in group of patients with homogeneous disease, which can have a potential diagnostic value. The reviews by Choo & Chang [15] and Tyson & Kent [53] identified several works exploring the effects of the AFO in FD patients, which are mainly focused on spatio-temporal gait parameters, such as gait speed, cadence, stride length and others. However a further characterization of gait can be obtained using biomechanical modelling and simulation, which allows to explore the kinematics of body joints during walking pattern. The kinematic analysis describes the relative motion of body's segments, and it is therefore particularly used in clinical practice to explore and analyse limb movement in specific tasks. Wiszomirska *et al.* [56] underlined the effective impact that the FD syndrome has on the kinematics of the impaired ankle joint. Zollo *et al.* quantified the impairment, proposing specific metrics extracted from the signal of ankle joint, broadening the focus also on other joints of the lower limbs [62]. Other works underlined the improvements brought by the AFO on the kinematics of the paretic limb [60, 59] which allows to limit the RoM and improve the angle of impact with the ground of the affected foot.

In this application the proposed methods are used, thus integrating data from markers of the motion capture system with a custom biomechanical model to simulate and analyse the walking biomechanics of the patient in order to further explore his gait features and evaluate the AFO performances during walking. The focus is on the ankle joint angle, but also on the subtalar joint. The latter was not analysed in previous literature about FD, while here it is considered as a relevant question to deepen in order to understand the altered biomechanics of walking. The subtalar joint plays a major role in ankle stability, and the alteration of its regular biomechanics has been linked to the FD syndrome [33]. Moreover, the forced inversion or eversion of this joint is a common cause of pain or injuries [61]. For these reasons it is useful to better analyse the mechanics of the subtalar joint during walking. On this topic the following analysis pointed out interesting results.

3.5.2 Methods and Materials

Study Population

Nineteen patients (7 women, 12 men) with FD syndrome, admitted for rehabilitation treatment in the Neurology and Functional Recovery and Rehabilitation Units of ICS Maugeri Institute of Care and Scientific Research in Bari (Italy) were involved in the experimental protocol. In Table 3.2 the anamnestic data of the study population are reported.

The first inclusion criterium was the ability to walk independently. Patients with bilateral impairment, who walk with AFO on both feet, were exluded from the analysis. None of the subjects was affected by other pathologies involving gait. All subjects gave their informed consent to participate in the study.

Test Protocol

Experimental data needed for the biomechanical analysis were collected following the protocols described in the previous chapters of this work. The motion capture system SMART-DX 700 by BTS Bioengineering was used to collect the trajectories of 22 markers placed on subject's body according to the Davis protocol (see Section 2.1.2 for further details), as shown in Figure 3.24. The experimental session consisted of a static and a walking trial. In the static trial the subject stands quietly, with aligned feet and arms along the body, for ten seconds. The walking trials were performed with and without the orthosis on the affected limb, at self-selected walking speed, over the 10-meters walkway placed in the range of view of the IR cameras. If needed, the subject performed several trials to get comfortable with the situation and then the walking test used for the analysis was acquired.

The orthosis used in the analysis is a commercial Codivilla spring, prescribed to the patient for rehabilitation during their hospital stay.

Data Processing

Data relating the 3D coordinates of the markers, recorded in the experimental sessions, were used in the custom biomechanical platform to

Table 3.2. Anamnestic data of the study population.

Subject	Age (yr)	Gender	Weigth (kg)	Heigth (m)	BMI (kg/m2)	Drop Foot
001	47	M	58	1.65	21.3	R
002	66	M	58	1.76	18.7	R
003	69	M	75	1.78	23.7	R
004	68	M	74	1.73	24.7	R
005	69	F	73	1.65	26.8	L
006	35	M	65	1.70	22.5	R
007	72	M	65	1.70	22.5	L
008	37	M	125	1.88	35.4	L
009	65	M	77	1.86	22.3	R
010	55	M	88	1.84	26.0	R
011	64	F	67	1.66	24.3	L
012	47	F	56	1.75	18.3	R
013	75	M	80	1.68	28.3	R
014	50	M	68	1.83	20.3	L
015	36	F	45	1.60	17.6	L
016	36	F	55	1.65	20.2	L
017	78	F	63	1.68	22.3	R
018	53	F	52	1.68	18.4	L
019	62	M	91	1.75	29.7	L
Mean	57.1		70.3	1.73	23.3	
Std	14		18	0.080	4.5	

scale the ‘Gait2392’ model and to perform the inverse kinematics analysis. Then the study was focused on the analysis of kinematics of the foot, specifically analysing the ankle and the subtalar angles. The first refers to the dorsi-plantar flexion, which is the movement of the ankle joint in the sagittal plane, while the latter regards the inversion and eversion of the subtalar joint. Joints angles signals were exported from the platform and further processed using MATLAB.

The signals of each walking trial were segmented into successive steps ranging between two subsequent HSs. HS events for each limb were manually found basing on videos recorded during walking trials and markers

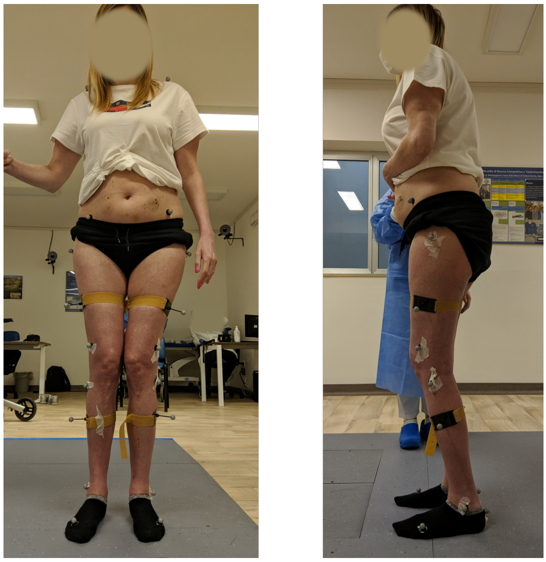

Figure 3.24. Markers position according to Davis protocol.

3D coordinates signals. The step segments of each walking trial were re-sampled on a common number of samples (the minimum among different steps) and then averaged. By doing so, a dataset was produced containing signals representing the evolution of the ankle and subtalar angles over a gait cycle, for each limb, for each condition of walking (with or without AFO) and for each subject. Finally a set of quantitative measures were extracted from the signals. For each of the two angles the following values were considered: the mean value over the entire gait cycle, the RoM and the angle value at HS.

Statistical Analysis

The statistical analysis was conducted by means of a two-way repeated measures ANOVA. The test was conducted to analyse the effects of the two factors: walking condition (with versus without AFO) and limb (affected versus contralateral). Also the combination of the two (condition*limb) was analysed in order to explore the effects of the interaction between the two factors. Since the variability between subjects has a considerable impact on the data, as it can be argued by the values of standard deviation shown in Table 3.3, it has been taken into account by considering the subject as a blocking factor in the analysis. All statistical procedures were performed on R version 4.0.3 (R Foundation, Vienna, Austria).

3.5.3 Results

Figure 3.25 shows the evolution of the ankle angle and subtalar angle over a complete gait cycle in the two walking conditions. The plots represent the mean signals obtained averaging the data of all the subjects, resampled on a common number of samples. In Figure 3.25a and 3.25b, positive values represent dorsiflexion, while negative values are related to plantar flexion angles. In Figure 3.25c and 3.25d, positive values represent the inversion, while negative values are related to the eversion of the subtalar joint. The variability of data among subjects is represented by shaded areas covering two standard deviations around the mean values. The average Toe-Off time is represented by vertical dashed lines for both conditions. Table 3.3 summarises the values obtained for the considered kinematic parameters for each walking condition and each foot. Data are reported as mean ± standard deviation, and all values are expressed in degrees.

Table 3.4 reports the results of the statistical analysis conducted by means of ANOVA test. The p-values are only reported if significant ($p - value < 0.5$), otherwise it is reported the absence of statistical significance (ns). Four different α values were considered to assess the level of statistical significance ($p < 0.05, p < 0.01, p < 0.001, p < 0.0001$).

The statistical analysis of the kinematic parameter related to ankle dorsi-plantar flexion highlights that the mean angle over a gait cycle and the angle registered at foot contact don't change significantly when the AFO is used. An increase in the mean values is registered for both parameters on the affected limb (the mean ankle angle increases from 6.00 without AFO to 8.50 with AFO, the ankle angle increases from -0.875 to 0.952 using AFO), while the contralateral limb is not affected by the use of the AFO. However in both cases the increase in affected limb can not be considered statistically significant, as the p-value of the combined factor Condition*Limb is above 0.05 (not significant). A statistical significant difference was observed for these parameters in the comparison between the affected and contralateral limb. In particular both the mean ankle an-

Table 3.3. Data statistics.

		Affected Limb		Contralateral Limb	
		Without AFO	***With AFO***	***Without AFO***	***With AFO***
Ankle	***Mean Angle***	6.00 ± 10	8.50 ± 9.2	10.7 ± 7.4	10.7 ± 7.7
	RoM Angle	29.5 ± 8.1	22.7 ± 5.2	27.1 ± 6.3	26.6 ± 6.0
	Angle at HS	-0.875 ± 12	0.952 ± 10	4.88 ± 7.6	4.39 ± 8.6
Subtalar	***Mean Angle***	3.07 ± 13	4.08 ± 14	7.49 ± 15	8.06 ± 17
	RoM Angle	22.1 ± 11	19.8 ± 9.4	22.9 ± 9.2	20.9 ± 8.7
	Angle at HS	-0.980 ± 16	-0.609 ± 17	4.42 ± 17	4.66 ± 18

All values are expressed in degrees, as mean ± standard deviation.

gle and the angle at HS are increased in the contralateral limb with respect to the affected limb.

The RoM of the ankle angle presents a different behaviour: no statistical difference is registered between the limbs, while a significant change can be observed when the AFO is used. A significant p-value is registered also for the interaction factor Condition*Limb, as it reflects the fact that a relevant change caused by the AFO is only registered on the affected limb (the RoM decreases from 29.5 to 22.7 with the AFO), while the contralateral limb is not affected by this condition.

The kinematic parameters of the subtalar angle do not show statistically significant difference among the two walking conditions, nor considering the combined factor Condition*Limb. However a statistical significant change can be observed in subtalar mean angle over the complete gait cycle and in subtalar angle at HS among the two limbs. The affected limb presents lower values of the subtalar angle for both quantitative parameters with respect to the contralateral limb, in all the walking conditions considered. The use of the AFO produces an increase in these two parameters and a decrease of the RoM of the subtalar angle, but the latter is not statistically significant. None of the factors examined impacts effectively on the RoM of the subtalar angle.

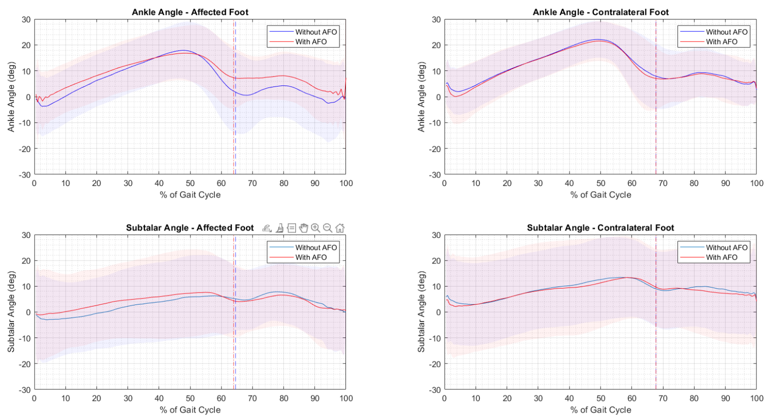

Figure 3.25. Evolution of the joint angles during a gait cycle. Signals were obtained as average of all subjects data. The shaded areas represent the variability around the mean, covering two standard deviations. The dashed vertical lines show the average Toe-Off time during Gait Cycle, for both conditions a. Ankle angle of the foot wearing the AFO (positive values dorsiflexion, negative values plantar flexion). b. Ankle angle of the contralateral foot. c. Subtalar angle of the foot wearing the AFO (positive values inversion, negative values eversion). d. Subtalar angle of the contralateral foot.

3.5.4 Discussion

This application is focused on the kinematics of two essential angles for forward walking propulsion and stability: the dorsi-plantar flexion of the ankle and inversion-eversion of the subtalar joint. The analysis of gait data has been performed integrating data from an optoelectronic gait analysis system with a biomechanical model through the custom MATLAB platform.The use of biomechanical modelling and simulation of gait allows the quantitative evaluation of the effective support provided by the AFO in walking biomechanics and can extend the idea of gait analysis. This working pattern has been employed in a similar analysis by Yamamoto *et al.* [59] and shows potential applications in the area of movement analysis for different purposes.

Results confirmed the initial idea supported by Wiszomirska *et al.* [56] that in the FD the plantar-flexion is prevalent, whereas in the healthy limb

Table 3.4. Results of the statistical ANOVA test.

		Condition	Limb	Condition*Limb
Ankle	***Mean Angle***	*ns*	**	*ns*
	RoM Angle	***	*ns*	**
	Angle at HS	*ns*	**	*ns*
Subtalar	***Mean Angle***	*ns*	*	*ns*
	RoM Angle	*ns*	*ns*	*ns*
	Angle at HS	*ns*	**	*ns*

ns $p > 0.05$, * $p < 0.05$, ** $p < 0.01$, *** $p < 0.001$, **** $p < 0.0001$.

the predominance of dorsiflexion can be observed. The statistical analysis confirms that the mean ankle angle and the ankle flexion registered at foot contact with the ground are significantly higher in the contralateral limb with respect to the affected FD. This findings confirms the results provided by Zollo *et al.* [62] who found higher dorsi-flexion angle at HS in contralateral foot.

The results presented show that the use of the AFO causes the increase of the ankle angle at HS in the affected limb. However it is not statistically significant in the group of analyzed patients, while a relevant change was found in other works [62, 60, 59, 12, 30, 27, 40, 13, 11].

The effect of the use of the AFO are statistically significant in our analysis on the RoM of the ankle angle, which is reduced in the affected foot wearing the orthosis. This parameter is not widely explored in literature, similar findings on RoM of ankle angle are only reported in [62], thus proving that the use of the AFO is effective in correcting the large excursion of the ankle joint in FD.

To the best of our knowledge, the past studies on FD have never focused on subtalar joint, although it is a responsible for the inversion and eversion of the ankle, enabling balanced walking in humans [14]. In the systematic review proposed by Choo and Chang in 2021 [15], none of the reported studies addresses the effects of the use of an AFO on the subtalar angle. In this application the kinematic of this joint was analysed, finding relevant results that show statistically significant differences among the affected and contralateral limb. In particular it is noted in the affected limb a lower value of the subtalar angle, showing a prevalence of eversion. These findings suggest that the FD syndrome affects also the inversion-eversion of the foot during the walking tasks. We can therefore affirm that the subtalar joint should be deeper analyzed in studies regarding FD patient. However, in our analysis, the use of AFO causes an improvement in the angle values, but does not lead to significant changes. We assume that the passive AFO used in this analysis is not specifically recommended for this problem while a different orthosis with two degrees of freedom could improve the kinetic of the joint, as suggested also by Choi *et al.* in [14].

Beyond the specific application, this application has confirmed the potentialities of the workflow of analysis combining motion tracking and biomechanical modelling. Using the biomechanical modelling enables to explore the kinematics and kinetics of all body joints, focusing on the most interesting depending on the application. In this application the focus was on ankle and subtalar angles, however the same approach can be used to explore other joints of the lower limbs that play an active role in the biomechanics of walking, such as knee and hip joint.

Chapter 4

Conclusions

Orthoses are medical devices which are used to support and improve functionalities of body segments affected by musculoskeletal disability. The lower limb orthoses are specifically used on the lower body segments, providing support to the principal function supplied by lower limbs, that is locomotion. Among musculoskeletal disability, locomotor deficits are the most common, and often this conditions can be relieved using orthotics. These devices represent a valid alternative, or a complementary intervention, to the surgical treatments.

The wide variety of available orthoses suggests that the process of choosing the appropriate device for a patient is not simple, requiring consideration of several factors. In addition to that, the new trends introduce the topic of custom orthoses, which allows the production of patient-specific orthotic devices. The novel design, production and material technologies reduce the temporal and economic costs, enabling the diffusion on a larger scale of the processes to produce custom orthosis. However, notwithstanding the patient-specific approach, the standardisation of the design and production process is a relevant aspect to explore, in order to not exclusively rely on the subjective skills of the clinicians, but on objective evaluation of morphological and functional characteristics of the patient.

The present dissertation proposes possible solution to support and improve the design and production of custom AFO, basing on functional assessments of subject performed with well-established systems used in clinical settings. A platform is presented with the general purpose of offering tools for the biomechanical study of gait, in terms of kinematics and dynamics. In addition, specific tools are presented for extracting features which can be used in the design of custom orthoses.

The gait analysis is an established technique particularly used in clinics to evaluate the levels of impairments in gait functionality and also to quantitatively assess the effects of rehabilitation or treatments. Various systems have been developed which provide information about spatio-temporal metrics of gait, kinematics and/or dynamics of the body joints and segments. The platform presented uses data collected with a 3D motion capture system on patient performing static and dynamic trials involving standing and walking. Data are exploited to scale a custom model specifically developed to analyse lower limb biomechanics and to solve inverse kinematics and inverse dynamics problems. The output of the platform is represented by kinematic (velocities and angles) and dynamic (forces and torques) information about the lower limb joints and segments.

In order to exploit these information to improve the process of designing the custom orthosis, a set of specific metrics are extracted regarding the maximum angular displacements registered on joints during the experimental analysis. This represents primarily a measure of the impairment, if compared with the physiological values of the same kinematics in healthy controls, but also an indication about how the orthosis will be stressed during its use on the patient. These values, used as inputs of a FEA, can be used to introduce adjustments to the design of the orthosis and also to validate its static structure before the actual realization. In this perspective the proposed experimental platform presents advantages with respect to the standard approach based on commercial optical systems and associated software. The parameters identified for the customization of the orthosis are not derived in other 'general purpose' systems for gait analysis, while the developed platform provides for their automatic calculation. Moreover raw signals representing the evolution of the angles during movements can be directly exported in the MATLAB environment for further processing. This enables the use of custom and specific algorithms, while the platforms commonly used in clinical environment generally produce reports including synthetic parameters obtained with their own closed software.

In terms of efficacy, it is difficult to measure the effective improvements brought by using this approach. Patients satisfaction may be higher simply because they are influenced by the idea that the orthosis is customised on their needs. However the actual efficacy has to be assessed over the long term, to verify whether the orthosis produces an improvement on gait functionalities and every-day activities, being comfortable and without risk of disruption. Anyway, this dissertation aims to underline the urgency to investigate and introduce innovative and objective approaches for designing and producing patient-specific custom orthosis, also providing a cue represented by a user-friendly application based on the biomechanical study of gait, which can be simply integrated in the production process.

The method introduced to perform the analysis of lower limb biomechanics during gait represent a valid solution not only for the above mentioned purposes, but also to conduct specific analysis regarding kinematics and dynamics of body. In the concluding Section it was described one of the possible application for which the platform has been used. The biomechanical approach allowed the specific study of the single joint (i.e. the ankle joint) with specific insight on the angles of higher interest for the considered area of analysis. The described application, in addition to its clinical and scientific relevance, showed the potentialities of this approach, which is also based on the possibility to develop a custom biomechanical model in order to deeply investigate the part of body of higher interest. As an example, for the purposes presented in this work a biomechanical model was developed which is particularly focused on lower limbs for the study of gait. If necessary, a more specific model can be developed including the description of the upper limbs or of other specific body parts whose experimental movement is desired to be analyzed.

Appendix A

User Manual Biomechanical Platform

This manual shows how the platform can be used, describing, step by step, the functionality and possibilities offered to the user. When the platform is launched, the initial interface in Figure A.1 is presented, which is for introductory and aesthetic purposes only.

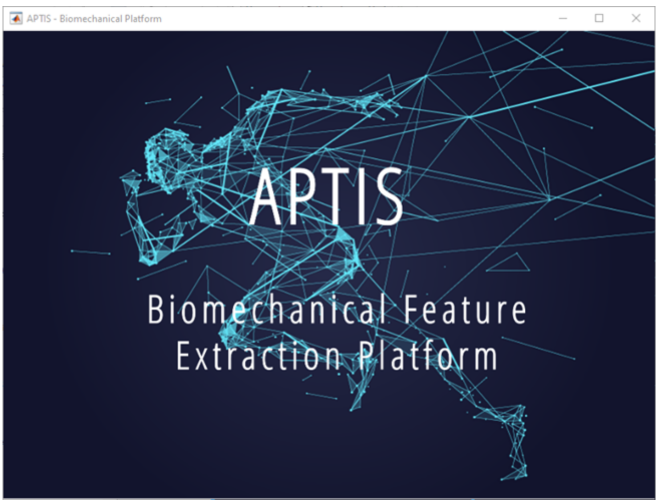

Figure A.1. Opening interface of the biomechanical platform.

After few seconds, the platform is automatically started. At startup, the default database to which the platform points is indicated at the top of the interface. To change it, the user can click the *Edit* button, which opens a dialog box for selecting the folder to be used as new database. To restore the initial path, the *Default* button can be clicked.
Once the reference database has been defined, the user has to select a patient from the first drop-down menu proposed (Figure A.2).

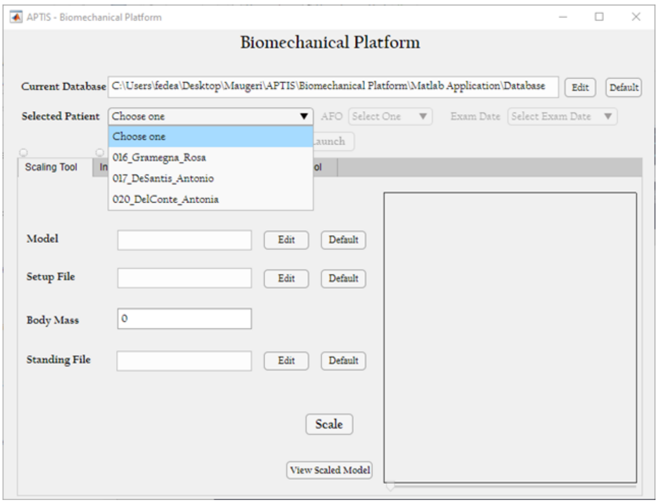

Figure A.2. Drop-down menu for the selection of the patient.

Automatically, the second drop-down menu will be activated for the selection of the walking condition to be considered (without AFO, with a standard AFO or with a custom AFO) (Figure A.3). The platform shows only those conditions for which it is available at least one trial for the selected patient.

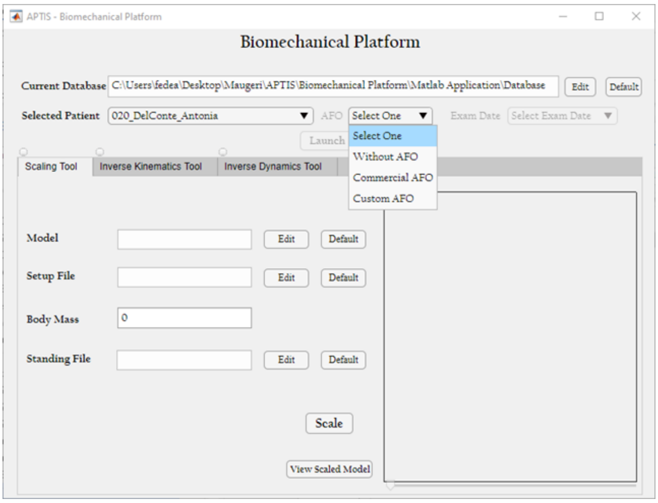

Figure A.3. Drop-down menu for the selection of the walking condition.

Finally, the date of the exam is selected to have unique indication of the measurement session to analyse (Figure A.4). Again, only the sessions for the selected user and walking condition will be visible in the drop-down menu.

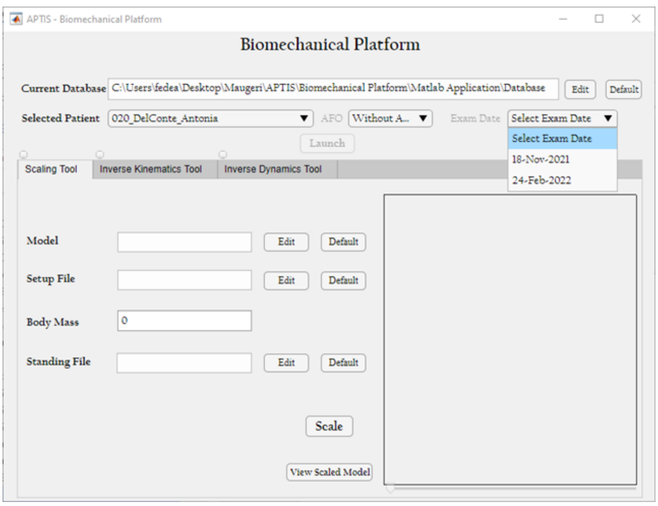

Figure A.4. Drop-down menu for the selection of the session date.

Clicking the *Launch* button, the platform imports the selected measurement session data and prepares the analyses to be performed basing on the available data. A system of light indicators shows which are the available actions above each tool. A green indicator indicates that that analysis has already been performed for that session and the results are already available in the database; a yellow indicator indicates that the analysis has been partially performed on only a subset of the available data in that session; the red indicator indicates that that analysis has not yet been performed; while an inactive (gray) indicator indicates that the analysis cannot be performed because previous preparatory steps must first be completed.

Figure A.5 shows an example of setup for a selected session in which Scaling and Inverse Kinematics processing have already been performed on all the trials in the session, while Inverse Dynamics has been performed on only a part of data. The platform automatically prompts the user to the tab for the analysis that still needs to be performed and suggests which trials need to be processed.

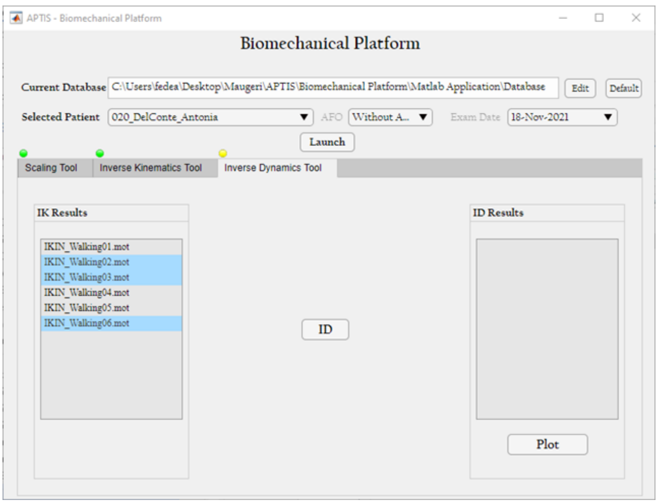

Figure A.5. Setup of the platform based on the data available for the selected experimental session.

Following the same logic, the selection of an experimental session which has not yet been processed through the platform will only activate the Scaling Tool, which is the first step to be taken to continue in the biomechanical analysis. Figure A.6 shows this condition with the platform preparing the user for the Scaling operation in the appropriate tab.

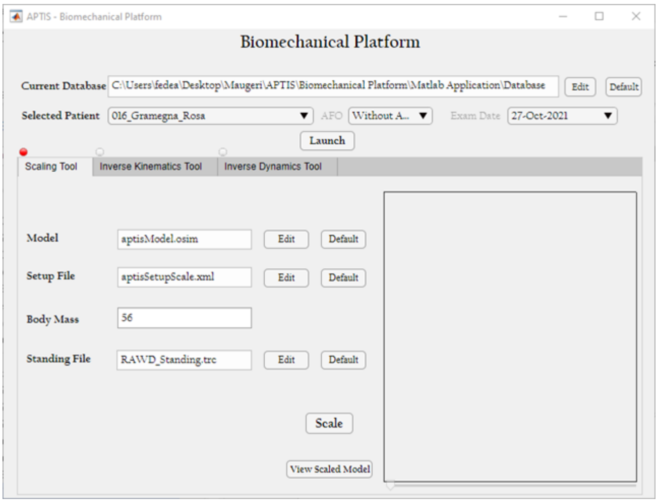

Figure A.6. Start of a new analysis for a patient with unprocessed data.

Data shown on the left side of the interface are loaded directly from the database if available. The user can edit the fields if necessary. The model scaling operation is launched by clicking the *Scale* button which generates the scaled model and saves it within the database according to the default name structure. Moreover, by clicking the *View Scaled Model* button, the model is shown in the panel located on the right side of the interface (Figure A.7). The controls to zoom or move in the spatial view are available, and the user can also use a slider to view the model at the various instants of acquisition of the standing trial.

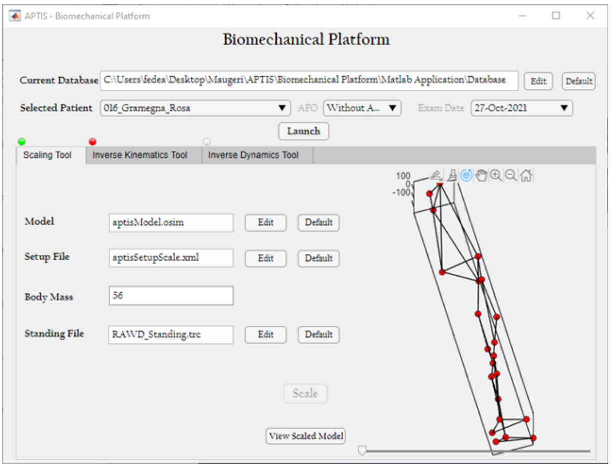

Figure A.7. Model Scaling and visualization.

After scaling, the Inverse Kinematics tool is activated. Automatically, the platform presents the available data, on which the processing can be performed, as well as the name of the model just scaled. The user can select one or more trials and start the Inverse Kinematics analysis clicking the *IK* button (Figure A.8).

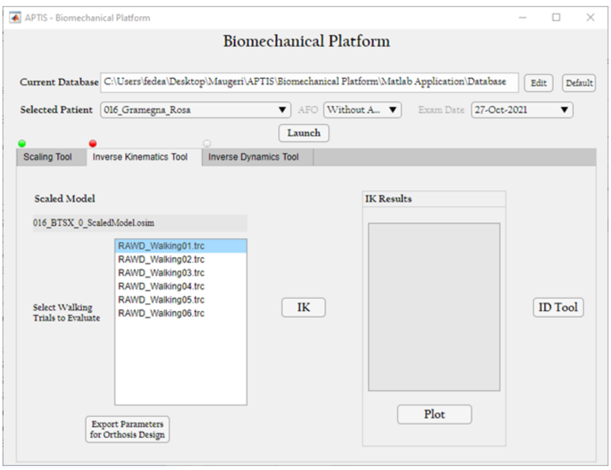

Figure A.8. Inverse Kinematic Tool.

When processing is complete, the results obtained will be visible in the panel on the right of the interface, as shown in Figure A.9.

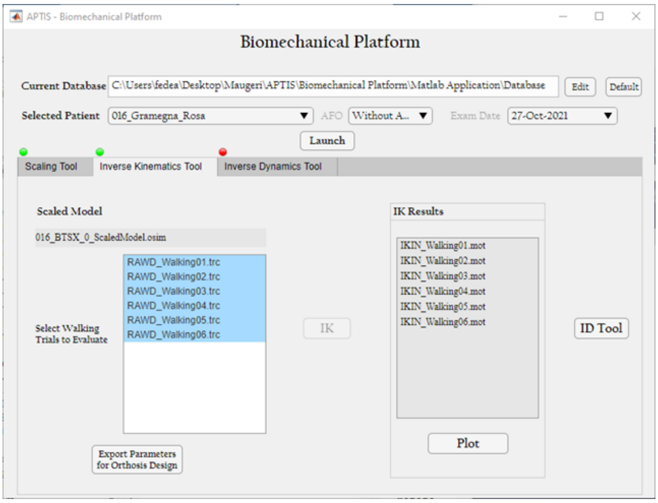

Figure A.9. Inverse Kinematic Tool with the processing results.

The results represent the evolution of the joint angles during the patient walking trials, computed through the inverse kinematics. In order to plot the results of a single trial, the user can click the *Plot* button. The window for plot will open.

One or more joints angles can be plotted at the same time in the chart on the right side of the interface. The user can select the angles of interest and then click the *Show* button. The visualization in Figure A.10 will be activated.

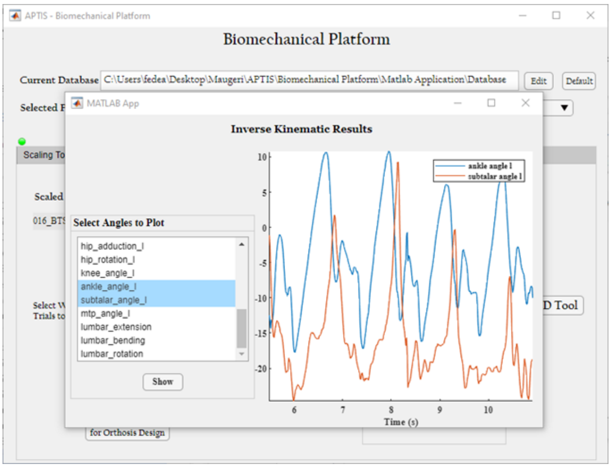

Figure A.10. Plot of the results of Inverse Kinematics.

Returning to the biomechanical analysis, the Inverse Kinematics results can be further processed by Inverse Dynamics elaboration, in order to compute moments and torques acting on the body joints. The tab for this processing is presented as in Figure A.11. Again, the user can select one or more available data on which to launch processing, and then click the *ID* button. The results obtained will be listed in the right panel.

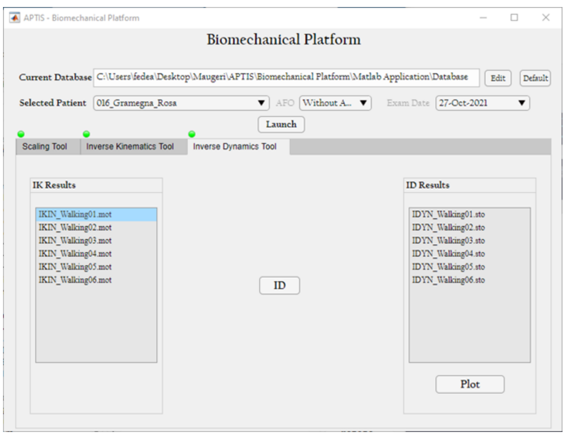

Figure A.11. Inverse Dynamic Tool.

To analyse the moments and torques acting on the joints, the user can select one of the trials and open the visualization window using the *Plot* button. The data visualization window will open. Selecting one or more signals and clicking the *Show* button, they will displayed on the chart, as shown in Figure A.12.

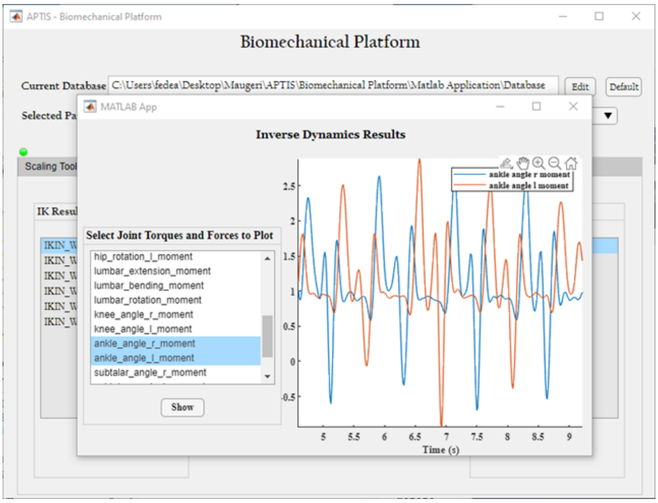

Figure A.12. Plot of the results of Inverse Dynamics.

The last feature offered by the platform regards the export of anthropometric and biomechanical parameters to be used in the orthosis design process. The Export Tool is launched from the Inverse Kinematics tab by clicking the *Export Parameters for Orthosis Design* button. The window that guides the user through the export is shown in Figure A.13.

The user can select the walking trials to be processed to calculate the parameters. If more than one trial is selected, the exported parameter will be the maximum value among those of the individual trials. Clicking on the *Evaluate* button will enable the choice of parameters to be exported, which is done by checking the corresponding boxes on the right part of the interface.

Finally, the *Launch* button activates the export of the parameters to a text file that will be saved within the database, in the folder corresponding to the analyzed acquisition session.

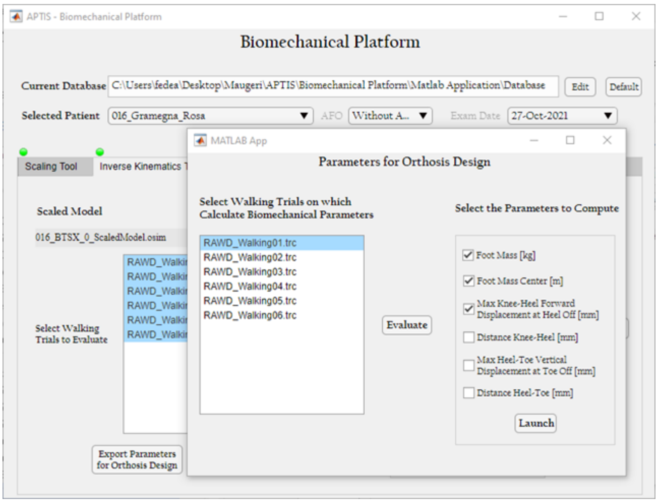

Figure A.13. Export Tool Window.

Bibliography

[1] A. Agrawal, S.K. Banala, S.K. Agrawal, and S.A. Binder-Macleod. Design of a two degree-of-freedom ankle-foot orthosis for robotic rehabilitation. In *9th International Conference on Rehabilitation Robotics, 2005. ICORR 2005.*, pages 41–44, June 2005. ISSN: 1945-7901.

[2] Md. Akhtaruzzaman, Amir Akramin Shafie, and Md. Raisuddin Khan. GAIT ANALYSIS: SYSTEMS, TECHNOLOGIES, AND IMPORTANCE. *Journal of Mechanics in Medicine and Biology*, 16(07):1630003, November 2016.

[3] Morshed Alam, Imtiaz Ahmed Choudhury, and Azuddin Bin Mamat. Mechanism and Design Analysis of Articulated Ankle Foot Orthoses for Drop-Foot. *The Scientific World Journal*, 2014:1–14, 2014.

[4] Frank C. Anderson and Marcus G. Pandy. A Dynamic Optimization Solution for Vertical Jumping in Three Dimensions. *Computer Methods in Biomechanics and Biomedical Engineering*, 2(3):201–231, January 1999.

[5] Hiroyuki Aono, Motoki Iwasaki, Tetsuo Ohwada, Shinya Okuda, Noboru Hosono, Takeshi Fuji, and Hideki Yoshikawa. Surgical Outcome of Drop Foot Caused by Degenerative Lumbar Diseases:. *Spine*, 32(8):E262–E266, April 2007.

[6] Suzanne R Babyar. Gait Analysis: Normal and Pathological Function. *Journal of Physical Therapy Education*, 8(1):47 – 48, 1994.

[7] Joonbum Bae and Masayoshi Tomizuka. A tele-monitoring system for gait rehabilitation with an inertial measurement unit and a shoe-type ground reaction force sensor. *Mechatronics*, 23(6):646–651, September 2013.

[8] Roberta Bardelli, Jaap Harlaar, Giovanni Morone, Patrizia Tomba, Alberto Esquenazi, and Maria Grazia Benedetti. The Codivilla spring: from then to

now and beyond. *European Journal of Physical and Rehabilitation Medicine*, 57(6), December 2021.

[9] A. Baysefer, E. Erdoğan, A. Sali, S. Sirin, and N. Seber. Foot Drop Following Brain Tumors: Case Reports. *min - Minimally Invasive Neurosurgery*, 41(02):97–98, June 1998.

[10] Lauren C. Benson, Christian A. Clermont, Eva Bošnjak, and Reed Ferber. The use of wearable devices for walking and running gait analysis outside of the lab: A systematic review. *Gait & Posture*, 63:124–138, June 2018.

[11] C. Bleyenheuft, G. Caty, T. Lejeune, and C. Detrembleur. Assessment of the Chignon® dynamic ankle–foot orthosis using instrumented gait analysis in hemiparetic adults. *Annales de Réadaptation et de Médecine Physique*, 51(3):154–160, April 2008.

[12] R. G. Burdett, D. Borello-France, C. Blatchly, and C. Potter. Gait comparison of subjects with hemiplegia walking unbraced, with ankle-foot orthosis, and with Air-Stirrup brace. *Physical Therapy*, 68(8):1197–1203, August 1988.

[13] Chih-Chi Chen, Wei-Hsien Hong, Chin-Man Wang, Chih-Kuang Chen, Katie Pei-Hsuan Wu, Chao-Fu Kang, and Simon F. Tang. Kinematic Features of Rear-Foot Motion Using Anterior and Posterior Ankle-Foot Orthoses in Stroke Patients With Hemiplegic Gait. *Archives of Physical Medicine and Rehabilitation*, 91(12):1862–1868, December 2010.

[14] Ho Seon Choi, Chang Hee Lee, and Yoon Su Baek. Design and Validation of a Two-Degree-of-Freedom Powered Ankle-Foot Orthosis with Two Pneumatic Artificial Muscles. *Mechatronics*, 72:102469, December 2020.

[15] Yoo Jin Choo and Min Cheol Chang. Effectiveness of an ankle–foot orthosis on walking in patients with stroke: a systematic review and meta-analysis. *Scientific Reports*, 11(1):15879, December 2021.

[16] Ross A. Clark, Yong-Hao Pua, Adam L. Bryant, and Michael A. Hunt. Validity of the Microsoft Kinect for providing lateral trunk lean feedback during gait retraining. *Gait & Posture*, 38(4):1064–1066, September 2013.

[17] Roy B. Davis, Sylvia Õunpuu, Dennis Tyburski, and James R. Gage. A gait analysis data collection and reduction technique. *Human Movement Science*, 10(5):575–587, October 1991.

[18] Francesco Delitala. *Gli apparecchi ortopedici*. Cappelli, Bologna, 1921.

[19] S. L. Delp, J. P. Loan, M. G. Hoy, F. E. Zajac, E. L. Topp, and J. M. Rosen. An interactive graphics-based model of the lower extremity to study orthopaedic surgical procedures. *IEEE transactions on bio-medical engineering*, 37(8):757–767, August 1990.

[20] Scott L. Delp, Frank C. Anderson, Allison S. Arnold, Peter Loan, Ayman Habib, Chand T. John, Eran Guendelman, and Darryl G. Thelen. OpenSim: open-source software to create and analyze dynamic simulations of movement. *IEEE transactions on bio-medical engineering*, 54(11):1940–1950, November 2007.

[21] Steven Díaz, Jeannie B. Stephenson, and Miguel A. Labrador. Use of Wearable Sensor Technology in Gait, Balance, and Range of Motion Analysis. *Applied Sciences*, 10(1):234, December 2019.

[22] A. Forner Cordero, H.J.F.M. Koopman, and F.C.T. van der Helm. Use of pressure insoles to calculate the complete ground reaction forces. *Journal of Biomechanics*, 37(9):1427–1432, September 2004.

[23] James A. Friederich and Richard A. Brand. Muscle fiber architecture in the human lower limb. *Journal of Biomechanics*, 23(1):91–95, January 1990.

[24] Junji Furusho, Takehito Kikuchi, Miwa Tokuda, Taigo Kakehashi, Kenichi Ikeda, Shouji Morimoto, Yasunori Hashimoto, Hiroki Tomiyama, Akio Nakagawa, and Yasushi Akazawa. Development of Shear Type Compact MR Brake for the Intelligent Ankle-Foot Orthosis and Its Control; Research and Development in NEDO for Practical Application of Human Support Robot. In *2007 IEEE 10th International Conference on Rehabilitation Robotics*, pages 89–94, June 2007. ISSN: 1945-7901.

[25] M. Gabel, R. Gilad-Bachrach, E. Renshaw, and A. Schuster. Full body gait analysis with Kinect. In *2012 Annual International Conference of the IEEE Engineering in Medicine and Biology Society*, pages 1964–1967, San Diego, CA, August 2012. IEEE.

[26] Michela Goffredo, Richard D. Seely, John N. Carter, and Mark S. Nixon. Markerless view independent gait analysis with self-camera calibration. In *2008 8th IEEE International Conference on Automatic Face & Gesture Recognition*, pages 1–6, September 2008.

[27] Haydar Gök, Ayse Küçükdeveci, Haydar Altinkaynak, Günes Yavuzer, and Süreyya Ergin. Effects of ankle-foot orthoses on hemiparetic gait. *Clinical Rehabilitation*, 17(2):137–139, March 2003.

[28] Suzon Al Hasan and Mohammad Zahidul Hoque. Lower limb orthoses: A review. *Journal of Chittagong Medical College Teachers' Association*, 19(1):33–36, 2009.

[29] Rasmus R. Jensen, Rasmus R. Paulsen, and Rasmus Larsen. Analyzing Gait Using a Time-of-Flight Camera. In Arnt-Børre Salberg, Jon Yngve Hardeberg, and Robert Jenssen, editors, *Image Analysis*, volume 5575, pages 21–30. Springer Berlin Heidelberg, Berlin, Heidelberg, 2009.

[30] Serdar Kesikburun. Effect of ankle foot orthosis on gait parameters and functional ambulation in patients with stroke. *Turkish Journal of Physical Medicine and Rehabilitation*, 63(2):143–148, June 2017.

[31] Kevin A. Kirby, Simon K. Spooner, Paul R. Scherer, and John M. Schuberth. Foot Orthoses. *Foot & Ankle Specialist*, 5(5):334–343, October 2012.

[32] Reinhard Klette and Garry Tee. Understanding Human Motion: A Historic Review. In Max Viergever, Bodo Rosenhahn, Reinhard Klette, and Dimitris Metaxas, editors, *Human Motion*, volume 36, pages 1–22. Springer Netherlands, Dordrecht, 2008.

[33] Sridhar Krishnamurthy and Mohamed Ibrahim. Tendon Transfers in Foot Drop. *Indian Journal of Plastic Surgery*, 52(01):100–108, January 2019.

[34] Prashanth R. Kubasad, Somasekhara Rao Todeti, and Yogeesh D. Kamat. A Review on Designs of Various Ankle Foot Orthosis (AFO) Used to Treat Drop Foot Disease. In Dibakar Sen, Santhakumar Mohan, and Gondi Kondaiah Ananthasuresh, editors, *Mechanism and Machine Science*, pages 789–807. Springer Singapore, Singapore, 2021.

[35] Yoshihisa Masakado, Michiyuki Kawakami, Kanjiro Suzuki, Leon Abe, Tetsuo Ota, and Akio Kimura. Clinical Neurophysiology in the Diagnosis of Peroneal Nerve Palsy. *The Keio Journal of Medicine*, 57(2):84–89, 2008.

[36] Emeline Maurice, Thibault Godineau, Diane Pichard, Hanane El Hafci, Gwennhael Autret, Morad Bensidhoum, Véronique Migonney, Mathieu Manassero, and Véronique Viateau. Remnants-preserving ACL reconstruction using direct tendinous graft fixation: a new rat model. *Journal of Orthopaedic Surgery and Research*, 17(1):7, December 2022.

[37] Martine I.V. Mientjes and Martyn Shorten. Contoured cushioning: effects of surface compressibility and curvature on heel pressure distribution. *Footwear Science*, 3(1):23–32, March 2011.

[38] R. v Mises. Mechanik der festen Körper im plastisch- deformablen Zustand. *Nachrichten von der Gesellschaft der Wissenschaften zu Göttingen, Mathematisch-Physikalische Klasse*, 1913:582–592, 1913.

[39] Florent Moissenet and Stéphane Armand. Qualitative And Quantitative Methods Of Assessing Gait Disorders. Nova Science Publishers Inc, 2015.

[40] Sara J. Mulroy, Valerie J. Eberly, Joanne K. Gronely, Walter Weiss, and Craig J. Newsam. Effect of AFO Design on Walking after Stroke: Impact of Ankle Plantar Flexion Contracture. *Prosthetics & Orthotics International*, 34(3):277–292, September 2010.

[41] Alvaro Muro-de-la Herran, Begonya Garcia-Zapirain, and Amaia Mendez-Zorrilla. Gait Analysis Methods: An Overview of Wearable and Non-Wearable Systems, Highlighting Clinical Applications. *Sensors*, 14(2):3362–3394, February 2014.

[42] Ralph Nisell, Gunnar Németh, and Hans Ohlsén. Joint forces in extension of the knee: Analysis of a mechanical model. *Acta Orthopaedica Scandinavica*, 57(1):41–46, January 1986.

[43] Remy Phan Ba, Sébastien Pierard, Gustave Moonen, Marc Van Droogenbroeck, and Shibeshih Belachew. Detection and Quantification of Efficiency and Quality of Gait Impairment in Multiple Sclerosis through Foot Path Analysis. In *Multiple Sclerosis Journal*, volume 18. SAGE Publications, London, United Kingdom, October 2012.

[44] Heather S. Read, M. Elizabeth Hazlewood, Susan J. Hillman, Robin J. Prescott, and James E. Robb. Edinburgh Visual Gait Score for Use in Cerebral Palsy. *Journal of Pediatric Orthopaedics*, 23(3):296–301, June 2003.

[45] L.W. Robinson, N.D. Clement, J. Herman, and M.S. Gaston. The Edinburgh visual gait score – The minimal clinically important difference. *Gait & Posture*, 53:25–28, March 2017.

[46] Fozia Saeed, Soumya Mukherjee, Kausik Chaudhuri, Joel Kerry, Sashin Ahuja, and Debasish Pal. Prognostic indicators of surgical outcome in painful foot drop: a systematic review and meta-analysis. *European Spine Journal*, 30(11):3278–3288, November 2021.

[47] H.H.C.M. Savelberg and A.L.H.de Lange. Assessment of the horizontal, fore-aft component of the ground reaction force from insole pressure patterns by using artificial neural networks. *Clinical Biomechanics*, 14(8):585–592, October 1999.

[48] J. D Stewart. Foot drop: where, why and what to do? *Practical Neurology*, 8(3):158–169, June 2008.

[49] Larry Donald Stredney. *The Representation of Anatomical Structures through Computer Animation for Scientific, Educational and Artistic Applications.* Dissertation Thesis, The Ohio State University, 1982.

[50] Philip Tack, Jan Victor, Paul Gemmel, and Lieven Annemans. 3D-printing techniques in a medical setting: a systematic literature review. *BioMedical Engineering OnLine*, 15(1):115, December 2016.

[51] Gentaro Taga. A model of the neuro-musculo-skeletal system for human locomotion: I. Emergence of basic gait. *Biological Cybernetics*, 73(2):97–111, July 1995.

[52] Weijun Tao, Tao Liu, Rencheng Zheng, and Hutian Feng. Gait Analysis Using Wearable Sensors. *Sensors*, 12(2):2255–2283, February 2012.

[53] Sarah F. Tyson and Ruth M. Kent. Effects of an Ankle-Foot Orthosis on Balance and Walking After Stroke: A Systematic Review and Pooled Meta-Analysis. *Archives of Physical Medicine and Rehabilitation*, 94(7):1377–1385, July 2013.

[54] T. L. Wickiewicz, R. R. Roy, P. L. Powell, and V. R. Edgerton. Muscle architecture of the human lower limb. *Clinical Orthopaedics and Related Research*, (179):275–283, October 1983.

[55] DA Winter. Kinematics. In *Biomechanics and Motor Control of Human Movement*, pages 45 – 81. John Wiley & Sons, Inc.,, 4th edition edition, 2009.

[56] Ida Wiszomirska, Michalina Błażkiewicz, Katarzyna Kaczmarczyk, Grażyna Brzuszkiewicz-Kuźmicka, and Andrzej Wit. Effect of Drop Foot on Spatiotemporal, Kinematic, and Kinetic Parameters during Gait. *Applied Bionics and Biomechanics*, 2017:1–6, April 2017.

[57] Zhaojun Xue, Dong Ming, Wei Song, Baikun Wan, and Shijiu Jin. Infrared gait recognition based on wavelet transform and support vector machine. *Pattern Recognition*, 43(8):2904–2910, August 2010.

[58] Gary T. Yamaguchi and Felix E. Zajac. A planar model of the knee joint to characterize the knee extensor mechanism. *Journal of Biomechanics*, 22(1):1–10, January 1989.

[59] Masataka Yamamoto, Koji Shimatani, Masaki Hasegawa, and Yuichi Kurita. Effect of an ankle–foot orthosis on gait kinematics and kinetics: case study of post-stroke gait using a musculoskeletal model and an orthosis model. *ROBOMECH Journal*, 6(1):9, December 2019.

[60] Sumiko Yamamoto, Souji Tanaka, and Naoyuki Motojima. Comparison of ankle–foot orthoses with plantar flexion stop and plantar flexion resistance in the gait of stroke patients: A randomized controlled trial. *Prosthetics & Orthotics International*, 42(5):544–553, October 2018.

[61] Songning Zhang, Michael Wortley, Qingjian Chen, and Julia Freedman. Efficacy of an Ankle Brace With a Subtalar Locking System in Inversion Control in Dynamic Movements. *Journal of Orthopaedic & Sports Physical Therapy*, 39(12):875–883, December 2009.

[62] L. Zollo, N. Zaccheddu, A. L. Ciancio, M. Morrone, M. Bravi, F. Santacaterina, M. Laineri Milazzo, E. Guglielmelli, and S. Sterzi. Comparative analysis and quantitative evaluation of ankle-foot orthoses for foot drop in chronic hemiparetic patients. *European Journal of Physical and Rehabilitation Medicine*, 51(2):185–196, April 2015.

[63] Natalya Özen, Ece Unlu, Ozgur Zeliha Karaahmet, Eda Gurcay, Ibrahim Gundogdu, and Ebru Umay. Effectiveness of Functional Electrical Stimulation - Cycling Treatment in Children with Cerebral Palsy. *Malawi Medical Journal*, 33(3):144–152, September 2021.

Author's Publications

Donisi, L., D'Addio, G., Pagano, G., **Coccia, A.**, & Cesarelli, M. (2019). Study of Agreement between two Wereable Inertial Systems for Gait Analysis based on a different sensor placement: G-Walk System and Opal System. Gait & Posture, 74, 14. https://doi.org/10.1016/j.gaitpost.2019.07.462

Ricciardi, C., Donisi, L., Cesarelli, G., Pagano, G., **Coccia, A.**, & D'Addio, G. (2020). Feasibility of Machine Learning applied to Poincaré Plot Analysis on Patients with CHF. 2020 11th Conference of the European Study Group on Cardiovascular Oscillations (ESGCO), 1–2. https://doi.org/10.1109/ESGCO49734.2020.9158152

Donisi, L., **Coccia, A.**, Amitrano, F., Mercogliano, L., Cesarelli, G., & D'Addio, G. (2020). Backpack Influence on Kinematic Parameters related to Timed Up and Go (TUG) Test in School Children. 2020 IEEE International Symposium on Medical Measurements and Applications (MeMeA), 1–5. https://doi.org/10.1109/MeMeA49120.2020.9137198

Amitrano, F., Donisi, L., **Coccia, A.**, Biancardi, A., Pagano, G., & D'Addio, G. (2020). Experimental Development and Validation of an E-Textile Sock Prototype. 2020 IEEE International Symposium on Medical Measurements and Applications (MeMeA), 1–5. https://doi.org/10.1109/MeMeA49120.2020.9137302

Coccia, A., Lanzillo, B., Donisi, L., Amitrano, F., Cesarelli, G., & D'Addio, G. (2020). Repeatability of Spatio-Temporal Gait Measurements in Parkinson's Disease. 2020 IEEE International Symposium on Medical Measurements and Applications (MeMeA), 1–6. https://doi.org/10.1109/MeMeA49120.2020.9137357

Lullo, F., **Coccia, A.**, Saltalamacchia, A. M., Cesarelli, M., Lanzillo, B., & D'Addio, G. (2020). Functional Electrical Stimulation for Upper Limbs Flexion-Extension and Prehension Movements in Rehabilitation. Journal of Advanced Health Care. https://doi.org/10.36017/JAHC2009-001

Lullo, F., Donisi, L., Piscosquito, G., Lanzillo, B., **Coccia, A.**, & D'Addio,

G. (2020). Gait analysis: technical notes. Journal of Advanced Health Care, 67–70. https://doi.org/10.36017/JAHC2002-002

Donisi, L., Cesarelli, G., Amitrano, F., **Coccia, A.**, Gargiulo, P., & D'Addio, G. (2020, September 18). An overall agreement evaluation between two measuring systems for gait analysis through a machine learning approach. Nordic Baltic Conference on Biomedical Engineering and Medical Physics 2020 - NBC 2020.

Amitrano, F., **Coccia, A.**, Ricciardi, C., Donisi, L., Cesarelli, G., Capodaglio, E. M., & D'Addio, G. (2020). Design and Validation of an E-Textile-Based Wearable Sock for Remote Gait and Postural Assessment. Sensors, 20(22), 6691. https://doi.org/10.3390/s20226691

Donisi, L., Amitrano, F., **Coccia, A.**, Mercogliano, L., Cesarelli, G., & D'Addio, G. (2021). Influence of the Backpack on School Children's Gait: A Statistical and Machine Learning Approach. In T. Jarm, A. Cvetkoska, S. Mahnič-Kalamiza, & D. Miklavcic (Eds.), 8th European Medical and Biological Engineering Conference (Vol. 80, pp. 682–688). Springer International Publishing. https://doi.org/10.1007/978-3-030-64610-3_76

Donisi, L., **Coccia, A.**, Amitrano, F., Ricciardi, C., Cesarelli, G., & D'Addio, G. (2021, June 9). Benchmarking between a Sensorized E-textile Sock for Remote Monitoring and a Stereophotogrammetric System. Proceedings of the VIII Congress of National Group of Bioengineering – GNB2021.

Donisi, L., Cesarelli, G., Balbi, P., Provitera, V., Lanzillo, B., **Coccia, A.**, D'Addio, G. (2021). Positive impact of short-term gait rehabilitation in Parkinson patients: a combined approach based on statistics and machine learning. Mathematical Biosciences and Engineering, 18(5), 6995–7009. https://doi.org/10.3934/mbe.2021348

Donisi, L., Cesarelli, G., **Coccia, A.**, Panigazzi, M., Capodaglio, E. M., & D'Addio, G. (2021). Work-Related Risk Assessment According to the Revised NIOSH Lifting Equation: A Preliminary Study Using a Wearable Inertial Sensor and Machine Learning. Sensors, 21(8), 2593. https://doi.org/10.3390/s21082593

Donisi, L., Pagano, G., Cesarelli, G., **Coccia, A.**, Amitrano, F., & D'Addio, G. (2021). Benchmarking between two wearable inertial systems for gait analysis based on a different sensor placement using several statistical approaches. Measurement, 173, 108642. https://doi.org/10.1016/j.measurement.2020.108642

Amitrano, F., **Coccia, A.**, Donisi, L., Biancardi, A., Pagano, G., & D'Addio, G. (2021, June 9). Experimental Validation of an E-Textile T-Shirt for ECG Monitoring. Proceedings of the VIII Congress of National Group of Bioengineering – GNB2021.

Donisi, L., Moretta, P., **Coccia, A.**, Amitrano, F., Biancardi, A., & D'Addio, G. (2021). Distinguishing Stroke patients with and without Unilateral Spatial Neglect by means of Clinical Features: a Tree-based Machine Learning Approach.

2021 IEEE International Symposium on Medical Measurements and Applications (MeMeA), 1–5. https://doi.org/10.1109/MeMeA52024.2021.9478727

Amitrano, F., **Coccia, A.**, Donisi, L., Pagano, G., Cesarelli, G., & D'Addio, G. (2021). Gait Analysis using Wearable E-Textile Sock: an Experimental Study of Test-Retest Reliability. 2021 IEEE International Symposium on Medical Measurements and Applications (MeMeA), 1–6. https://doi.org/10.1109/MeMeA52024.2021.9478702

Coccia, A., Amitrano, F., Balbi, P., Donisi, L., Biancardi, A., & D'Addio, G. (2021). Analysis of Test-Retest Repeatability of Gait Analysis Parameters in Hereditary Spastic Paraplegia. 2021 IEEE International Symposium on Medical Measurements and Applications (MeMeA), 1–6. https://doi.org/10.1109/MeMeA52024.2021.9478743

Coccia, A., Amitrano, F., Donisi, L., Cesarelli, G., Pagano, G., Cesarelli, M., & D'Addio, G. (2021). Design and validation of an e-textile-based wearable system for remote health monitoring. Acta IMEKO, 10(2), 220–229. https://doi.org/10.21014/acta_imeko.v10i2.912

Amitrano, F., **Coccia, A.**, Donisi, L., Cesarelli, G., Pagano, G., & D'Addio, G. (2021). Benchmarking of Novel Wearable Smart Socks with Optoelectronic Gait Analysis System in Assessing Walking Cadence. Proceedings XXI Congresso SIAMOC 2021, 85. https://doi.org/10.6092/unibo/amsacta/6846

Coccia, A., Amitrano, F., Pagano, G., Bosco, V., Losavio, E., & D'Addio, G. (2021). Quantitative Outcome Assessment of Ankle Foot Orthosis Using Biomechanical Modelling and Simulation of Gait: a Case Study. Proceedings XXI Congresso SIAMOC 2021, 92. https://doi.org/10.6092/unibo/amsacta/6846

Donisi, L., Cesarelli, G., Capodaglio, E. M., Panigazzi, M., **Coccia, A.**, & D'Addio, G. (2021). Is it possible to discriminate risk classes according to the revised NIOSH lifting equation using machine learning algorithms fed with features extracted from acceleration signals? Proceedings XXI Congresso SIAMOC 2021, 29. https://doi.org/10.6092/unibo/amsacta/6846

D'Addio, G., Donisi, L., Cesarelli, G., Amitrano, F., **Coccia, A.**, La Rovere, M. T., & Ricciardi, C. (2021). Extracting Features from Poincaré Plots to Distinguish Congestive Heart Failure Patients According to NYHA Classes. Bioengineering, 8(10), 138. https://doi.org/10.3390/bioengineering8100138

Cesarelli, G., Donisi, L., **Coccia, A.**, Amitrano, F., D'Addio, G., & Ricciardi, C. (2021). The E-Textile for Biomedical Applications: A Systematic Review of Literature. Diagnostics, 11(12), 2263. https://doi.org/10.3390/diagnostics11122263

Donisi, L., Ricciardi, C., Cesarelli, G., **Coccia, A.**, Amitrano, F., Adamo, S., & D'Addio, G. (2022). Bidimensional and Tridimensional Poincaré Maps in Cardiology: A Multiclass Machine Learning Study. Electronics, 11(3), 448.

https://doi.org/10.3390/electronics11030448

Coccia, A., Amitrano, F., Pagano, G., Dileo, L., Marsico, V., Tombolini, G., & D'Addio, G. (2022a). Biomechanical modelling for quantitative assessment of gait kinematics in drop foot patients with ankle foot orthosis. 2022 IEEE International Symposium on Medical Measurements and Applications (MeMeA), 1–6. https://doi.org/10.1109/MeMeA54994.2022.9856549

Amitrano, F., **Coccia, A.**, Pagano, G., Dileo, L., Losavio, E., Tombolini, G., & D'Addio, G. (2022a). The Impact of Ankle-Foot Orthoses on Spatio-Temporal Gait Parameters in Drop-Foot Patients. 2022 IEEE International Symposium on Medical Measurements and Applications (MeMeA), 1–6. https://doi.org/10.1109/MeMeA54994.2022.9856440

Pagano, G., Aliani, M., Genco, M., **Coccia, A.**, Proscia, V., Cesarelli, M., & D'Addio, G. (2022). Rehabilitation outcome in patients with obstructive sleep apnea syndrome using wearable inertial sensor for gait analysis. 2022 IEEE International Symposium on Medical Measurements and Applications (MeMeA), 1–6. https://doi.org/10.1109/MeMeA54994.2022.9856405

Cesarelli, G., Donisi, L., **Coccia, A.**, Amitrano, F., Biancardi, A., Lanzillo, B., & D'Addio, G. (2022). Ataxia and Parkinson's disease patients classification using tree-based machine learning algorithms fed by spatiotemporal features: a pilot study. 2022 IEEE International Symposium on Medical Measurements and Applications (MeMeA), 1–6. https://doi.org/10.1109/MeMeA54994.2022.9856460

Bisconti, S., Tombolini, G., **Coccia, A.**, Pagano, G., Cesarelli, M., & D'Addio, G. (2022). Movement analysis and medical imaging integrated tools for 3D project and printing of drop foot orthosis. Proceedings XXII Congresso SIAMOC 2022, 57. https://doi.org/10.6092/unibo/amsacta/7027

Amitrano, F., **Coccia, A.**, Pagano, G., Dileo, L., Losavio, E., Tombolini, G., & D'Addio, G. (2022b). Study of Gait and Posture Kinematic Indices for the Evaluation of Ankle-Foot Orthoses. Proceedings XXII Congresso SIAMOC 2022, 38. https://doi.org/10.6092/unibo/amsacta/7027

Pagano, G., Aliani, M., Diasparra, A., Genco, M., **Coccia, A.**, Cesarelli, M., & D'Addio, G. (2022). Gait Analysis for the evaluation of rehabilitation otucome in patients with obstructive sleep apnea syndrome. Proceedings XXII Congresso SIAMOC 2022, 116. https://doi.org/10.6092/unibo/amsacta/7027

Coccia, A., Amitrano, F., Pagano, G., Dileo, L., Marsico, V., Tombolini, G., & D'Addio, G. (2022b). Kinematic analysis of ankle joint during gait in drop foot patients wearing passive Ankle-Foot Orthosis. Proceedings XXII Congresso SIAMOC 2022, 37. https://doi.org/10.6092/unibo/amsacta/7027

Amitrano, F., **Coccia, A.**, Cesarelli, G., Donisi, L., Pagano, G., Cesarelli, M., & D'Addio, G. (2022, October 26). The Impact of Ankle-Foot Orthosis on Walking Features of Drop Foot Patients. Proceedings of the 2022 IEEE International Conference on Metrology for Extended Reality, Artificial Intelligence and Neural Engineering - MetroXRAINE 2022, Rome, Italy.